CONSOLIDATION AND FRICTION MECHANISMS OF WOOD COMPOSITES AND THEIR INFLUENCE ON PULTRUSION PROCESSING

By

KARL RICHARD ENGLUND

A dissertation submitted in partial fulfillment of
the requirements for the degree of

DOCTOR OF PHILOSOPHY

WASHINGTON STATE UNIVERSITY
Department of Civil Engineering

December 2001

To the Faculty of Washington State University:

The members of the Committee appointed to examine the dissertation of KARL RICHARD ENGLUND find it satisfactory and recommend that it be accepted.

_____
Chair

_____

_____

_____

_____

Acknowledgment

I would like to thank my major professor, Dr. Michael P. Wolcott, and my committee members; Dr.'s Donald Bender, Lloyd Smith, Jay Johnson and John Hermanson for their help and guidance. Also, I would like to thank the Office of Naval Research for funding a majority of the research.

Thanks to the staff, both past and present, at the Wood Materials and Engineering Lab for their help and amusement. To all my good friends and fellow colleagues, some of which are the same and too numerous to mention, I extend my gratitude and appreciation for their humor, support and for just being there. To my family, who tried their hardest not to ask the question "When are you going to be finished?" too often, thanks for the love and support. To my road bikes and the WSU cycle team, for providing me with companionship, while I rode off the insurmountable stress associated with a dissertation, on the hills of the Palouse. Most importantly, I thank Vaughn, for being their with me all those nights and weekends, a true testament of man's best friend.

CONSOLIDATION AND FRICTION MECHANISMS OF WOOD COMPOSITES AND THEIR INFLUENCE ON PULTRUSION PROCESSING

Abstract

by
Karl Richard Englund, Ph.D.
Washington State University
December 2001

Chair: Michael P. Wolcott

The polymer processing technique of pultrusion can be utilized to produce wood-based composites, however, limitations occur in the ability of the composite system to flow through the stationary die. The consolidation and frictional response of the wood composite impose the resistance to flow as the material is conveyed through the die through a pulling action. The objectives of this research is to describe the mechanisms that govern the consolidation and frictional behavior of a wood fiber composite, how these mechanisms respond to the pultrusion conditions and composite design, and their influence on application and process engineering of a pultrusion operation. Utilizing a non-woven wood and wood/polypropylene (PP) fiber mat, the uniaxial compression and sliding frictional response was tested and described. The description of consolidation and friction were then incorporated into a pulling force model and compared to experimental pultrusion runs. The description of stress during consolidation was based on

the relative density and instantaneous modulus, while a generalized Maxwell model fit the ensuing relaxation response. The consolidation and friction response was controlled by the viscoelastic nature of the composite, and the mat structure and composition. Through spectral analysis, the mechanisms of the relaxation behavior were found to be interparticle movement and particle deformation. Predicted pulling force at a die temperature of 170°C was found in close agreement with experimental values, however a deviation was observed at higher temperatures. A reduction in pulling load can be obtained with lower densities and higher temperatures with increased PP contents. It was demonstrated that wood and wood/PP composites can be pultruded successfully and with the use of a pulling force model, the mechanisms of pulling resistance can be identified.

Table of Contents

List of Figures

List of Tables

Chapter 1

Project Introduction

Introduction

The wood composites industry has been exposed to a variety of changes not only in the type of products produced, but also in the methods of manufacturing. With the onset of wood/plastic composites, a variety of new processing methods have been introduced. One common method, extrusion, produces lineally constant profiles that are conveyed through a screw-driven process, while batch process injection molding utilizes a screw and/or plunger to convey the heated material into a cold-formed die (Rosen 1993). Another method, which has had limited exposure to the wood industry, is pultrusion, where the composite is pulled through a stationary die formed to the final composite profile.

The commonality between these methods of production lies in the forming of the material around a stationary die, where the flow of the material into or through the die can dictate the feasibility of producing the composite. The traditional use of polymers in these manufacturing methods requires a fluid-based approach to modeling the materials behavior during processing. However, with wood, the flow of the material relies on a solid mechanics approach to process modeling.

With a solid matrix, the compression and frictional behavior of the material are important parameters to consider with these traditional polymer processes. As the

composite is formed into the final profile, a compressive stress is developed. Once the profile has been achieved, an ensuing relaxation of stress occurs. The compressive stress can be influenced by processing and material parameters such as; temperature, flow rate, material geometry and type, density, and moisture content. The frictional properties of the die and material interface have also been found to change with the temperature, time, normal load, and flow rate. For the research involved in this project, the mechanisms of consolidation and friction of a wood fiber composite, and their response to the composite design and exposure to pultrusion conditions, are applied to the process engineering of wood-based pultrusion.

Pultrusion

During pultrusion, material is pulled through a stationary die and formed to a lineally constant profile. The raw material is fed into a tapered entrance section, where the composite is consolidated to the final dimensions. The composite remains at the formed profile in the heated constant geometry section, where the resins are cured, softened, or melted, depending upon the resin utilized. A cooling section is added to the die to harden the thermoplastic resins. A schematic of the wood-based pultrusion system can be seen in Figure 1.1

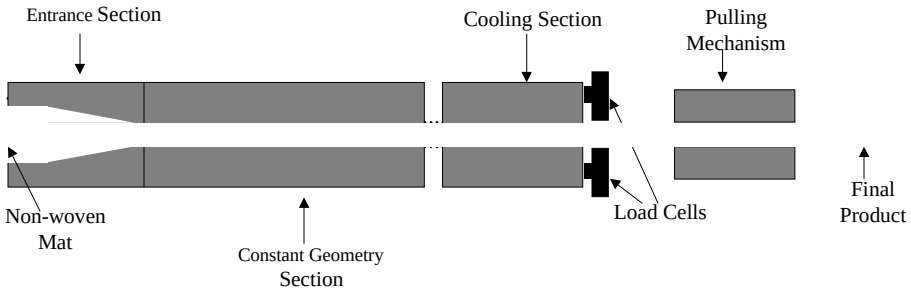

Figure 1.1. Pultrusion die design for wood-based composites.

The feasibility of pultruding any composite system relies upon the ability of the materials to flow through the die. If resistance accumulated within the die exceeds the tensile strength of the composite, product failure will terminate the process. Therefore, it is crucial to understand the mechanisms of resistance during the pultrusion of a wood-based composite. The accumulation of pulling load will result from the consolidation forces contributing to the lineal direction during the tapered section of the die and the frictional resistance throughout the entire die. The materials response to an applied compressive load, the frictional behavior of a wood composite against the die surface, and the geometry of the die all contribute to the pulling force developed in a pultrusion die.

Compression Response of the Fibrous Mat

Consolidation Region (Stress-Strain Response)

The literature on the compression modeling of wood composites has primarily focused on the consolidation of wood strand mats (Dai and Steiner 1993, Wolcott et al. 1994, Lang and Wolcott 1996, and Lenth and Kamke 1996). These consolidation models first simulate a mat structure and then utilize a modified Hookean relationship (Eq.1.1) with a nonlinear strain function ($\psi(\varepsilon)$) to determine the compressive stress (σ_c). Based

$$\sigma_c = E\varepsilon\psi(\varepsilon) \qquad \text{Eq. 1.1}$$

Where:

E = Compression modulus

ε = Compressive strain

upon the accuracy of ($\psi(\varepsilon)$), the models fit the wood-strand mats with reasonable accuracy, however they do not address the large strains associated from elemental movement and bending found in a fibrous mat.

The powder literature has developed models to describe the consolidation behavior of particulates. Early research of consolidation of powders was based on the relative density (ρ_R) and void volume (Konopicky (1948), Heckel (1961), and Cooper and Eaton (1962)). Although these relationships described the linear behavior of σ_c as the powder compacts at higher strains, they do not account for the initial nonlinear stress-strain region.

Based upon ρ_R and the instantaneous modulus ($E(\varepsilon)$), a postulated relationship in Eq.1.2, was developed. The $E(\varepsilon)$ describes the change in stress to the change in strain during the consolidation process. This relationship accounts for the change in material properties with increasing density and provides a good fit of the consolidation stress as observed for fibrous wood composites.

$$\frac{dE(\varepsilon)}{E(\varepsilon)} = m\frac{d\rho_R}{\rho_R} \qquad \text{Eq. 1.2}$$

Relaxation Region (Stress-Time Response)

The relaxation of stress in polymers is a viscoelastic response, which is generally modeled utilizing mechanical analogies. These models can accurately assess the linear viscoelastic response of a material through the use of springs and dashpot elements to represent the elastic and viscous components, respectively. The Maxwell element

incorporates a spring and dashpot in series and is commonly utilized to model stress relaxation at a constant strain (Ferry 1980). The generalized form of the Maxwell model utilizes a discrete number of elements in a parallel fashion to account for the differing relaxation responses, which occur over the monitored time region (Malvern 1969).

Relaxation Spectrum Analysis

The addition of thermoplastics to the fibrous composite, the amorphous components of the wood, and the structural formation of the composite can cause varying responses during relaxation. However, the parameters or relaxation moduli determined with a discrete analysis do not necessarily provide clear insight as to the behavior of the relaxation response. Much of the polymer research in relaxation response analysis utilize continuous forms of mechanical analogies or spectrum analysis to evaluate the relaxation behavior of the material and its structure. The spectrum provides a curve, which displays the concentration of relaxation over the observed time frame (Ferry 1980). With experimental data, numerical and graphical approximations are used to determine the relaxation spectrum.

Friction

The frictional behavior of wood and wood/thermoplastic composites is not well understood. Individually, wood and thermoplastics friction has been extensively researched, with the emphasis on thermoplastics. The most common theory associated with polymeric friction, which includes wood, is the development of adhesive bonds between the polymer and sliding surface (Bowden and Tabor 1964). With adhesion theory, the frictional force results from the bonding of the polymer to the substrate

creating an interface. The shear stress at the interface and the area of contact then determine the magnitude of the frictional force.

The dynamic coefficient of frictional (μ_k) of wood has been found to vary with load, temperature, moisture content, species, orientation, and extractives content (McMillin et al. 1970a, McMillin et al. 1970b, Lemoine et al. 1970, McKenzie and Karpovich 1968), however, there has been minimal research on modeling the response. Many theoretical and semi-empirical molecular models have been developed to describe friction of thermoplastics under varying load, temperature, and sliding velocity (Bowden and Tabor 1964, Spalding et al. 1993, Benabdallah 1993, Benabdallah 1997, Bahadur and Ludema 1971). However, the range over which these models are valid can be restrictive, therefore empirical models are commonly utilized to incorporate a wide variety of treatment variables.

Modeling the Pultrusion of Wood Composites

The accumulated resistance developed during the pultrusion of a wood-based composite system governs the feasibility of producing a pultruded wood composite. The stress developed during pultrusion can not exceed the tensile strength of the composite, as the outputted material is the transfer mechanism for a continuous flow. Handling issues pertaining to the material infeed of the die system can also make pultrusion prohibitive.

To understand the influence the mechanisms of consolidation and friction have on the pultrusion process, a pulling force model was developed. Consolidation stress develops as the composite is pulled through the tapered section of the die, while the relaxation of stress occurs after the composite is compressed to a final profile.

Throughout the entire die, interfacial friction resists forward movement through the die. Based upon the geometry of the entrance section, the pulling direction component of the consolidation stress also contributes to the overall resistance. Contributions of the consolidation and frictional response will vary based upon the engineering of the composite and the design and conditions of the pultrusion process.

Project Objectives

With a wood-based pultrusion process, the resistance to material flow is governed by the compressive and frictional response of the material. Within this report, the main goals are to determine the mechanisms associated with compression and friction of a wood-based composite and to determine the influence composite design and processing conditions impart on the application and engineering of a pultrusion system. The specific objectives within this project are to;

1) Describe the compression (σ_c) and ensuing relaxation of stress (σ_r) for the fibrous mat network exposed to various platen temperatures, strain rates, and PP concentration.
2) Utilize spectrum analysis to discern the mechanisms of relaxation and their response to composite design and processing conditions.
3) Develop a description of the dynamic coefficient of friction (μ_k) of the wood and wood/PP mat along the die interface, with the established composite design and processing conditions.
4) Develop a pulling force model to determine the influence processing parameters impart on the material flow, based upon the consolidation and frictional behavior
5) Compare the pulling force model with an experimental pultrusion operation,.

Rationale and Significance

To improve the exterior performance of wood composites, the trend of the wood and polymer materials research has been to incorporate thermoplastics into a wood

particle or fiber network. With the implementation of polymer processing methods to produce wood-based composites, the fundamental mechanisms of consolidation and material flow are pertinent to provide an engineering approach to process modeling. Although research in wood composites has concentrated on the consolidation of strands, little emphasis has been placed on the of the consolidation and frictional behavior of wood fiber or particle composites.

Research in the consolidation of the wood composites has generally emphasized the influence processing parameters impart on the final product performance. With the use of polymer processing techniques, the stresses developed during consolidation of the composite materials are important not only to the final product properties, but also the ability to produce the composite. With the transfer of material through a stationary die, concern lies with the mechanisms of flow or movement of material. The processing parameters and die design rely upon the mechanism of movement, whether it be solid and/or fluid. Processing temperatures, feed rates, density and composite formulation all play a role in the type of flow mechanisms.

To understand the flow or material movement of a wood-based composite through a polymer processing die, a thorough analysis of the consolidation, relaxation, and friction of the composite is required. The approach of this project is to provide a description of the consolidation and relaxation response of a non-woven wood and wood/thermoplastic mat under the same processing conditions as expected during pultrusion. Utilizing the information developed from consolidation modeling, the frictional response is also to be modeled under similar conditions. Incorporating these models with the geometry of the pultrusion die, a pulling load model can be developed.

A trend has been developed with the onset of wood/thermoplastic composites to utilize polymer processing techniques. Extrusion and injection molding processes were non-existent twenty years ago in the wood products industry, at the present, they are commonplace and their products are becoming accepted throughout traditional dominant wood product markets. Although pultrusion has had limited exposure in the wood products industry, there are many advantages and incentives for future use. Low capital costs are commonly associated with stationary dies due to the minimal moving parts within the die. The ability to use the mechanics of the cross-section and the ease of adding reinforcing fibers provides pultrusion with the advantage of producing engineered wood composites.

References

Bowden, F.P. and D. Tabor. 1964. The friction and lubrication of solids, part II. Oxford University Press. New York, NY.

Bahadur, S. and K.C. Ludema. 1971. The viscoelastic nature of the sliding friction of polyethylene, polypropylene and copolymers. Wear 18:109-128.

Benabdallah, H.S. 1993. The running-in and steady-state coefficient of friction of some engineering thermoplastics. Polymer and Engineering Science. 33(2):70-74.

Benabdallah, H.S. 1997. Reciprocating sliding friction and contact stress of some thermoplastics against steel. Journal of Materials Science 32(19):5069-5083.

Dai, C. and P.R. Steiner 1993. Compression behavior of randomly formed wood flake mats. Wood and Fiber Science. 25(4): 349-358.

Ferry, J.D. 1980. Viscoelastic properties of polymers. John Wiley and Sons, Inc. New York.

Lang, E.M. and M.P. Wolcott. 1996b. A model for viscoelastic consolidation of wood-strand mats. Part II. Static stress-strain behavior of the mat. Wood and Fiber Science 28(3):369-379.

Lenth, C.A. and F.A. Kamke. 1996b. Investigations of flakeboard mat consolidation. Part II. Modeling mat consolidation using theories of cellular materials. Wood and Fiber Science 28(3):309-319.

Lemoine, T.J., McMillin, C.W., and F.G. Manwiller. 1970. Wood variables affecting the friction coefficient of spruce pine on steel. Wood Science 2(3):144-148.

Malvern, L.E. 1969. Introduction to the mechanics of a continuous medium. Prentice-Hall, Inc. Englewood Cliffs, NJ

McKenzie, W.M. and H. Karpovich. 1968. The frictional behavior of wood. Wood Science and Technology 2:138-152.

McMillan, C.W., Lemoine, T.J. and F.G Manwiller. 1970a. Friction coefficient of oven-dry spruce pine on steel, as related to temperature and wood properties. Wood and Fiber 2(1):6-11.

McMillan, C.W., Lemoine, T.J. and F.G Manwiller. 1970b. Friction coefficient of spruce pine on steel - a note on lubricants. Wood Science 3(2):100-101

Rosen, S.L. 1993. Fundamental principles of polymeric materials, 2nd edition. John Wiley and Sons, Inc. New York, NY.

Spalding, M.A., Kirkpatrick, D.E, and K.S. Hyun. 1993. Coefficients of dynamic friction for low density polyethylene. Polymer Engineering and Science 33(7):423-430.

Wolcott, M.P., Kamke, F.A. and D.A. Dillard. 1994. Fundamental aspects of wood deformation pertaining to manufacture of wood-based composites. Wood and Fiber Science 26(4):496-511.

Chapter 2

Modeling the Compression and Relaxation of Wood/Thermoplastic Fiber Mats During Consolidation

Abstract

Secondary processing of non-woven wood and wood/thermoplastic fiber mats is generally performed using compression molding, where heated platens or dies form the final product. Although the study and use of wood-fiber composites is widespread, few research efforts have explicitly described the fundamentals of mat consolidation. In contrast, the wood composite literature has prolifically addressed the compression of wood-strand composites. Models developed for wood-strand composites and powders are reviewed and applied to experimental data for compression of wood and wood/polypropylene (PP) fiber mats. The compression/relaxation response was monitored during consolidation with varying platen temperatures, strain rates, and PP content. The effects of density and percent PP were also analyzed for changes in heat conduction. A model developed from the relationship between the instantaneous modulus and relative density was found to fit the compression of the non-woven fiber mats. The ensuing relaxation was modeled utilizing a linear viscoelastic Maxwell series with good agreement.

Introduction

Non-woven mat technology uses both natural and synthetic fibers to produce a variety of interior use products. The fibrous mats provide the automotive industry with lightweight molded door panels, trunk liners, and dashboards, while other markets include residential door skins, cabinets, and furniture. Recent trends to improve the moisture resistance have included the addition of thermoplastic fibers to the mat network.

Non-woven mats are generally manufactured and sold to producers of auto or residential components. The mat integrity is maintained prior to secondary processing through friction among the interlocking wood and synthetic fibers. In some cases, thermoplastic resins are used as a preliminary adhesive to improve mat strength. A majority of the products manufactured with non-woven mats utilizes some form of compression molding to form and maintain the final profile.

The consolidation mechanisms for wood-based composites have been researched by a variety of authors; Suchsland (1959) and Jones (1963), to name a few. Suchsland (1959) noted that the stress-strain relationship of the mat is a function of the transverse compression of the wood. Jones (1963) found the consolidation mechanism of a wood fiber mat was not only a deformation of the wood fibers, but also due to fiber slippage and bending at contact points.

With the mechanisms of consolidation identified, models developed by Wolcott et al. (1994), Dai and Steiner 1993, Lang and Wolcott (1996a) and Lenth and Kamke (1996), described the stress-strain behavior of a wood-strand mat. All of these models have been useful in identifying the contribution of different consolidation mechanisms in wood-strand composites. In turn, this work has been predicated on describing the

formation and structure of the strand network. Unlike wood fiber systems, void filling by strand shifting does not appear to play a role in strand mats. In addition, the fiber mats formed by blends of wood and thermoplastics differ from a wood-strand mat in both geometry and material type. Combined, these differences make strand-based models somewhat limited in their approach to model a fibrous mat. Therefore, alternative methods and disciplines are needed to describe the consolidation of a fibrous mat.

Research with powder materials has developed models that describe the stress-strain behavior of granulated materials. Konopicky (1948), Heckel (1961), and Cooper and Eaton (1962) established consolidation models for powders based on the relative density and void volume. As in wood-fiber mats, the mechanisms of powder consolidation rely on packing by void filling and particle yielding.

Consolidation models typically describe the stress-strain response of the mat during compression, however they often ignore the ensuing relaxation. For polymeric materials, the relaxation behavior is governed by both processing and material parameters and can influence the final material structure (Wolcott et al 1990, Wang and Winistorfer 2000), which in turn, affects the mechanical and physical properties of the composite.

The goal of this research is to mathematically describe consolidation for a non-woven wood mat blended with varying proportions of polypropylene (PP) fiber. The specific objectives include:

1) Experimentally measure the stress of a non-woven mat in uniaxial compression under varying strain rates, platen temperatures, PP content, and to varying densities.

2) Provide a mathematical model of the compression and relaxation response of a wood and blended wood/thermoplastic mat.

Model Development

The development of a model for the compression/relaxation of a wood/PP fiber mat must consider the response of the constitutive materials to an induced stress and the structure of the composite system. Consolidation of a fibrous composite includes two distinct regions; mat compression and the ensuing relaxation response. The mat compression stage includes the consolidation of the composite through fiber movement and deformation until a final strain is obtained. At the cessation of strain, the stress begins to relax due to further fiber movement and from the viscoelastic behavior of the polymeric materials.

Mat Compression

In an attempt to describe the compression response of a wood/thermoplastic fiber mat, models developed for consolidation of both wood-strand composites and powders are evaluated. Whereas studies addressing powder consolidation identify volume or density ratio to be proportional to the applied compressive stress (σ_c). (Konopicky 1948, Heckel 1961, Shivanand and Sprockel 1992, Cooper and Eaton 1962, Tabil and Sokhansanj 1996, Helle et al. 1985, Walker, 1923), most of the models addressing consolidation of wood-strand mats utilize a Hookean relationship (Eq. 1.1) modified with a non-linear strain function ($\psi(\varepsilon)$) (Wolcott et al. 1994, Dai and Steiner 1993, Lang and Wolcott 1996b, and Lenth and Kamke 1996b).

Dai and Steiner (1993) defined mat structure as a collection of independent strand columns of varying height. A Poisson's distribution was used to numerically describe the number of strands in localized strand columns. The probability ($p(i)$) of an

infinitesimally small column containing *i* number of strands is given by a Poisson distribution is shown in Eq. 2.1. In the mat models, *p(i)* equates to the fractional area of columns containing this number of strands within a mat.

$$p(i) = \frac{e^{-n} n^{i}}{i!} \qquad \text{Eq. 2.1}$$

The mean number of strands (*n*) is estimated for each discrete finite column and is calculated from the strand size, total number of strands allowed in one column, and the mat area. The total compressive stress of the composite during consolidation results from the sum of the discrete columns and can be estimated as:

$$\sigma_c = \sum_{i=1}^{i\,\max} \sigma_i = E \sum_{i=1}^{i\,\max} \psi(\varepsilon_i)\varepsilon_i\, p(i) \qquad \text{Eq. 2.2}$$

The terms σ_i and ε_i denote the stress and strain in columns with *i* number of strands and *E* is Young's modulus of the wood flake. The load resistance increases as the mat continues to be compressed, increasing the total number of strand columns supporting the load. Dai and Steiner neglect any stresses prior to column compression. Lang and Wolcott (1996 a and b) utilized beam theory to augment the column compression approach. Departing from the theoretical approach to describe mat structure, Monte Carlo techniques were used to simulate mat structures obtained from laboratory measurements. Lenth and Kamke (1996a and b) viewed a wood-strand mat as a cellular solid and utilized cellular theories to describe the stress-strain behavior of a wood-strand mat. These models accurately described stresses for strains less than 0.675 where an exponential increase in the stress caused a poor fit to the experimental data.

Many of the compaction studies for powders examine the influence of relative density (ρ_R) on the compressive stress. The ρ_R is a ratio of the density of the powder bed compacted to any given strain to the density of the solid powder particles and is equivalent to the relative density used in foam models. Konopicky (1948) proposed the relationship (Eq. 2.3) between σ_c and ρ_R with metal powders as:

$$\ln\left[\frac{1}{1-\rho_R}\right] = m\sigma_c \qquad \text{Eq. 2.3}$$

Where;

m = Constant of proportionality

Heckel (1961) also examined the compaction of various metal powders with a modified version of Konopicky's relationship (Eq. 2.4). Tabil and Sokhansanj (1996) incorporated Heckel's (1961) method to describe the compression of alfalfa grinds with good agreement. The results of all the preceding work fit the data quite well at higher pressures, however they failed to recognize the initial nonlinear response of the compression curve.

$$\frac{d\rho_R}{d\sigma_c} = m(1-\rho_R) \qquad \text{Eq. 2.4}$$

Other work with powders have incorporated a more rigorous approach to compaction. Jin and Cristescu (1998) utilized a constitutive model, which takes into account the elastic and viscoplastic response of the powder. Ransing et al.(2000) incorporated a discrete and finite element models to emulate the compression of a ductile powder matrix. Although these models provided a more detailed description of the

compaction process, both approaches are cumbersome and require extensive testing to establish many of the parameters involved in the models.

Relaxation Response of the Mat

Viscoelastic mechanical analogies are commonly used to describe the relaxation behavior of polymeric materials. Relaxation behavior is commonly described using Maxwell elements, the general differential equation is given as:

$$\frac{d\sigma_r}{dt} = E\frac{d\varepsilon}{dt} + \frac{\sigma_r}{\lambda} \qquad \text{Eq. 2.5}$$

where λ is the relaxation time (a measure of the rate of decay, (Christensen 1982)), E is the modulus of the spring. At a constant strain (ε_o), a decrease in the compressive stress (σ_r) occurs as the mat begins to relax, where the relaxation modulus ($E(t)$) is defined as σ_r/ε_o. Experimental relaxation data can be more precisely described through a series of the Maxwell elements (Eq. 2.6 and 7). Elements are generally spaced in decade increments when summing the model (Christensen 1982).

$$E(t) = \sum_{i=1}^{n} E_i e^{-t/\lambda_i} \qquad \text{Eq. 2.6}$$

$$\sigma_r = \varepsilon_o \sum_{i=1}^{n} E_i e^{-t/\lambda_i} \qquad \text{Eq. 2.7}$$

Experimental Procedures

Uniaxial Compression Testing

Wood fiber and wood/polypropylene (PP) fiber mats were obtained commercially (Mats Inc.). The mats were made with mechanically refined aspen wood fibers coated with 5% phenol-formaldehyde (PF) resin and needled with 0, 30, 40, and 50% thermoplastic fibers, by weight. An additional 5% of polyolefin coated polyester fibers (Celbond ®) were also blended with the mat. The mat was passed through an oven to melt the polyester fibers and provide integrity during handling.

Square test specimens (2.5 x 2.5 in.), were cut from the mats for uniaxial consolidation. The mats were compressed to a density of 60, 65 and 70 lb/ft^3 at platen temperatures of 170, 180 and 190°C. These platen temperatures were chosen to prevent thermal degradation of the wood <200°C (Goldstein 1973)) and to exceed the melt temperature (T_m) of the polypropylene ($T_m \approx 162°C$).

A final thickness of 0.25 in. was targeted, therefore, mats were layered upon each other to obtain the final density. A servo-hydraulic universal test apparatus with heated aluminum platens was used to compress the non-woven mat at a strain rate of 0.006 in/in-s. A thermocouple was inserted in the center of the layered mats to monitor the core temperature.

Once the composite reached a final thickness, the platens were held constant for 4 minutes, while the relaxation load response was recorded. A time frame of 4 minutes at final density was found to be sufficient at the mentioned platen temperatures to ensure melt of the PP and cure of the PF resin. A sample size of three per test group was utilized

and the behavior of the stress-strain and stress-time curves were found to be quite similar. A representative curve was chosen from each group for analysis.

Results and Discussion

Compression Model

The compression curves for a wood/PP fiber mat were modeled with the same methods as Dai and Steiner (1993). The wood element in this case was considered to be an average wood fiber or fiber bundle for aspen species. In Figure 2.1, an element thickness of 10 $x10^{-3}$, 10 x 10^{-4}, and 5 x 10^{-5} in. was used to represent a fiber bundle, single, and half fiber diameters, respectively. In all cases, the experimental data failed to be represented by the model. The strains, at which stress begins to accumulate in the wood fiber mats, is approximately at 0.9, substantially greater than that predicted by any of the wood-strand models.

One of the underlying assumptions of a Poisson distribution is that the likelihood of an event to occur is independent and cannot influence any other event (Ang and Tang 1975). In reality, the structure of a randomly oriented mat has overlapping and intertwining wood elements. In this case, the finite columns that comprise the mat structure do not necessarily behave as independent elements. Fibers that share columns may influence the stress-strain relationship of the neighboring columns. This assumption was recognized by Dai and Steiner (1983), and was not found to strongly influence wood-strand mats. The influence of fiber bending and repositioning may render a consolidation model utilizing a Poisson's distribution inadequate for a fibrous network.

The cellular model utilized by Lenth and Kamke (1996b) failed to fit their experimental data at the higher strains. The same was true for the wood/PP fiber mats as an exponential increase in the data was observed at a lower strain of 0.65-0.75, depending upon the constants utilized in their cellular model. Lenth and Kamke (1996b) surmised their model did not consider the changing density of the cellular material, in this case, the wood strands. The same effect holds true for a wood/PP fiber mat.

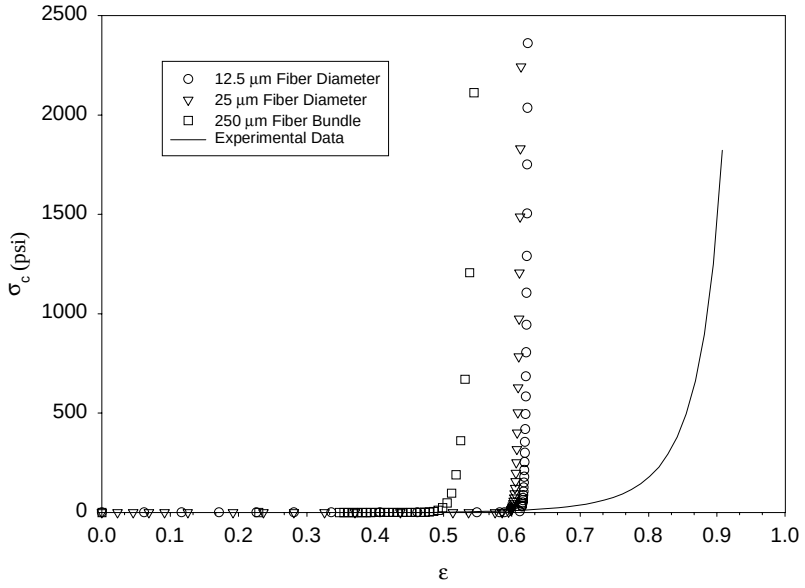

Figure 2.1 Poisson's distribution with differing element diameters compared to a non-woven mat with 0%PP compressed to a 65 lb/ft^3 density at 180°C.

The poor prediction of strand mat consolidation models for wood/PP fiber mats is due to the large strains that occur during consolidation of fiber mats. In a loosely formed mat, a substantial amount of deformation occurs before stress begins to accumulate (Figure 2.1). This would indicate a large amount of fiber movement, presumably through repositioning and bending. During fiber movement, voids are filled and the density continues to change until the cessation of strain. As the density increases, so do the mechanical properties of the composite. Mechanical testing of the compressed wood

composite exhibits a parabolic relationship between the density and modulus (E) of the composite (Wong et al. 1997). Shivan and Sprockel (1992) found similar increases in tensile strength with highly compacted cellulose powders.

Many of the powder compaction studies examine the influence the relative density (ρ_R) has on the compressive stress. However, the curve-fitting models utilized in the powder research did not address the low stress, non-linear region of the curve. This was also found to be true when the models of powder compression were utilized with the wood/PP fiber composites. The lack of fit with Konopicky (1948) and Heckel's (1961) models can be attributed to the linear relationship assumed between σ_c and ρ_R. In powder compacts, this assumption of linearity can provide an accurate representation of the stress-strain response, however, with wood/PP fiber composites, the initial nonlinear behavior of the compression curve is too substantial to overlook.

For the linear section of the stress-strain curve, the instantaneous modulus $E(\varepsilon)$ ($d\sigma_c/d\varepsilon$) remains constant. However, $E(\varepsilon)$ is continuously increasing with an increase in ρ_R during the consolidation at strains between 0.7 and 0.9. Based upon the powder compaction literature, the following correlation between the change in modulus and relative density is postulated:

$$\frac{dE(\varepsilon)}{E(\varepsilon)} = m\frac{d\rho_R}{\rho_R} \qquad \text{Eq. 2.8}$$

During consolidation, the ρ_R is related to engineering strain (ε) as:

$$\rho_R = \frac{C_1}{1-\varepsilon} \qquad \text{Eq. 2.9}$$

$$d\rho_R = \frac{C_1}{(1-\varepsilon)^2} d\varepsilon \qquad \text{Eq. 2.10}$$

where;

C_1 = Initial ρ_R at ε=0

Substituting Eqs. 2.9 and 2.10 into 2.8 yields:

$$\int \frac{dE(\varepsilon)}{E(\varepsilon)} = m \int \frac{d\varepsilon}{1-\varepsilon} \qquad \text{Eq. 2.11}$$

Integrating Eq. 2.11 with respect to *E(ε)* and *ε*, the natural logarithm of *E(ε)* becomes proportional to the compressive true strain (ε_T) of the composite mat. Linearizing this relation for the entire pressing schedule (Figure 2.2) yields:

$$\ln E(\varepsilon) = B + A\ln(1-\varepsilon) \quad or \quad E(\varepsilon) = (1-\varepsilon)^A e^B \qquad \text{Eq. 2.12}$$

where;

ln(1-ε) = True strain(ε_t)

To determine σ_c, *E(ε)* must be defined as $d\sigma_c/d\varepsilon$ during consolidation.

Separating the variables and taking the exponent of each side (Eq. 2.13), yields A and B as coefficients of the linear approximation of ln E_t vs ln (ε_T)

$$d\sigma_c = (1-\varepsilon)^A e^B d\varepsilon \qquad \text{Eq. 2.13}$$

Integrating both sides with respect to σ_c and *ε*, the following estimate of the positive compressive stress is given by Eq. 2.14. A comparison of experimental data and the stress predicted in Eq. 2.14 is presented in Figure 2.3. The compression curves for all treatments can be seen in Appendix A. The coefficients *A* and *B* for varying PP content, density, and platen temperature were determined graphically. An average value of the coefficients are provided in Table 2.1. The slope (*A*) of the relationship between ln(E(ε))

and ε_T increases with an increase in PP content. This corresponds to the similar behavior with the ultimate compressive stress, as the composite with PP required a higher stress to achieve the target density.

$$\sigma_c(\varepsilon) = -\frac{e^B}{(A+1)}\left[(1-\varepsilon)^{A+1} - 1\right] \qquad \text{Eq. 2.14}$$

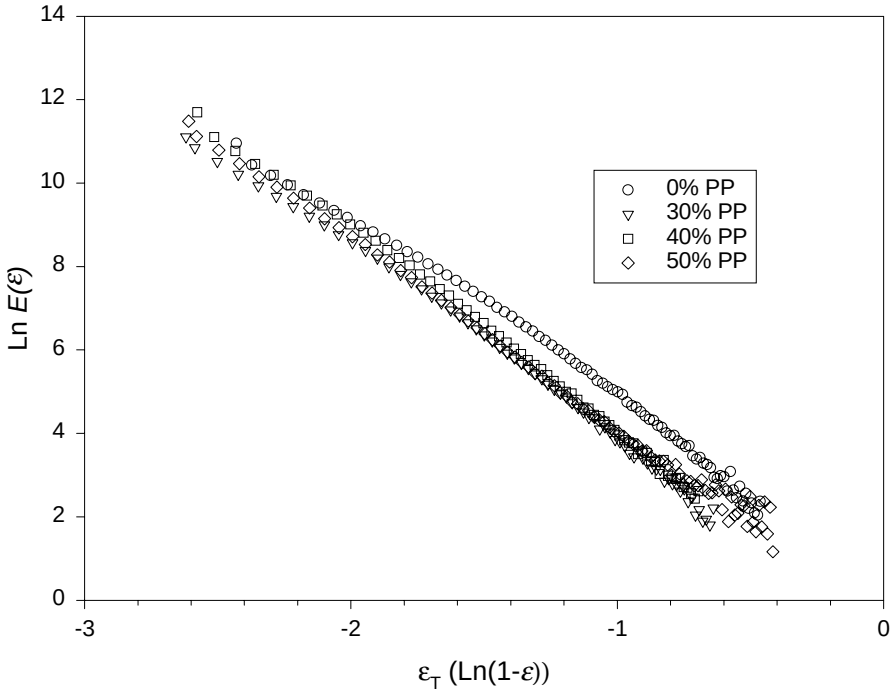

Figure 2.2. Relationship between E(ε) and ε_T for various percentage levels of PP at 180°C platen temperature and 65 lb/ft^3 density.

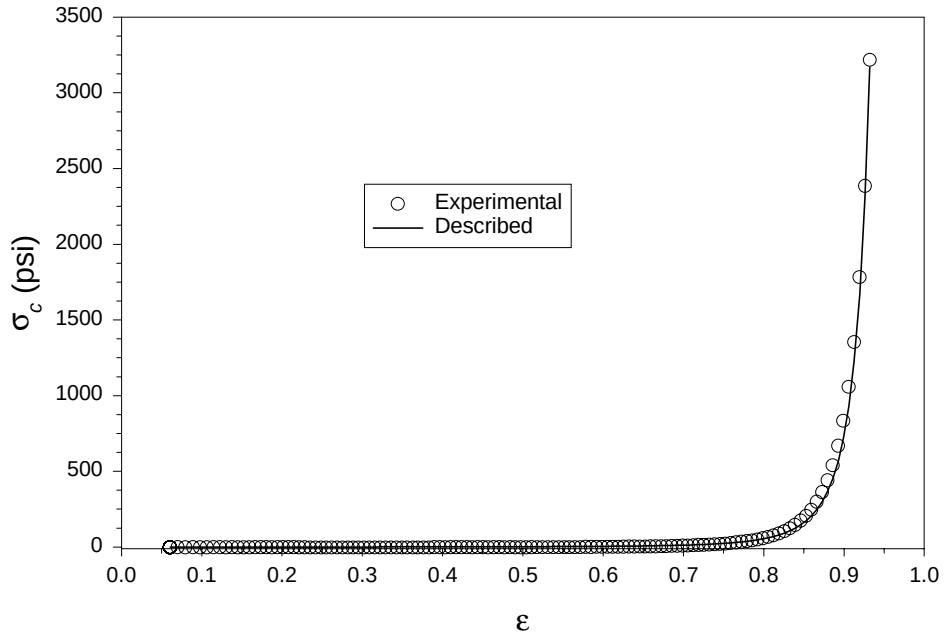

Figure 2.3. Comparison of the modeled and experimental stress during the compression of a 50%PP wood fiber mat at 180°C and 65 lb/ft^3 density.

Table 2.1. Linear coefficients, *A* and *B* for the ln *E(ε)* vs true strain plot.

		0% PP		**30% PP**		**40% PP**		**50% PP**	
	Density (lb/ft^3)	***A***	***B***	***A***	***B***	***A***	***B***	***A***	***B***
170°C	**60**	-4.091	0.805	-4.494	-0.451	-4.602	-0.010	-4.660	-0.805
	65	-4.097	1.057	-4.444	-0.377	-4.600	-0.071	-4.611	-0.468
	70	-4.064	1.245	-4.439	-0.350	-4.538	0.151	-4.581	-0.390
180°C	**60**	-4.094	1.011	-4.456	-0.532	-4.739	-0.553	-4.712	-0.927
	65	-4.069	1.188	-4.456	-0.277	-4.664	-0.344	-4.718	-0.717
	70	-4.074	1.091	-4.398	-0293	-4.615	-0.112	-4.571	-0.403
190°C	**60**	3.905	1.648	-4.493	-0.711	-4.711	-0.552	-4.726	-1.135
	65	-3.944	1.378	-4.454	-0.321	-4.708	-0.508	-4.750	-1.085
	70	-3.999	1.296	-4.545	-0.347	-4.615	-0.253	-4.666	-0.673

Relaxation Model

The stress relaxation of the composite was described using a 4-parameter Generalized Maxwell model (Eq. 2.15) shown in Figures 2.5 and 2.6. The relaxation times (λ) were chosen as increments of the natural exponent (e^1, e^3, e^5, e^7). Using non-

linear regression techniques (Marquardt-Levenberg method) with the experimental data, $E(t)$ values were found for each composite type and treatment (Table 2.2).

$$\sigma_r(t) = \varepsilon_o \sum_{i=1}^{4} E_i e^{-t/\lambda_i} \qquad \text{Eq. 2.15}$$

Table 2.2. Relaxation modulus parameters for the prediction of the compressive stress response. Where $E_{1\text{-}4}$ correspond to λ's of e^1, e^3, e^5, and e^7.

PP Content		**0% PP**			**30% PP**			**40% PP**			**50% PP**		
Density (lb/ft^3)		**60**	**65**	**70**	**60**	**65**	**70**	**60**	**65**	**70**	**60**	**65**	**70**
170°C	**E_1**	227	470	325	409	186	443	246	184	271	230	299	209
	E_2	859	1430	1712	816	1198	1391	1112	1536	1882	849	1155	1695
	E_3	45.6	258	296	791	745	771	963	1231	1576	1027	1137	1592
	E_4	400	447	640	14.5	298	749	201	569	893	58.0	726	947
180°C	**E_1**	358	380	630	41.0	246	302	207	116	124	0.00	297	0.00
	E_2	808	1225	1550	992	1178	1387	1179	1576	1931	1217	1376	1984
	E_3	53.4	272	339	531	800	1152	1063	1590	2301	822	1762	2262
	E_4	381	340	518	0.00	0.00	318	0.00	0.00	0.00	0.00	0.00	0.00
190°C	**E_1**	311	627	736	10.3	128	168	0.00	0.00	0.00	0.00	0.00	0.00
	E_2	730	1104	1366	1117	1303	1675	1500	2112	2814	1484	2078	2335
	E_3	102	295	451	264	583	1380	730	1049	1358	706	956	1309
	E_4	278	291	350	0.00	0.00	2.53	0.00	0.00	0.00	0.00	0.00	0.00

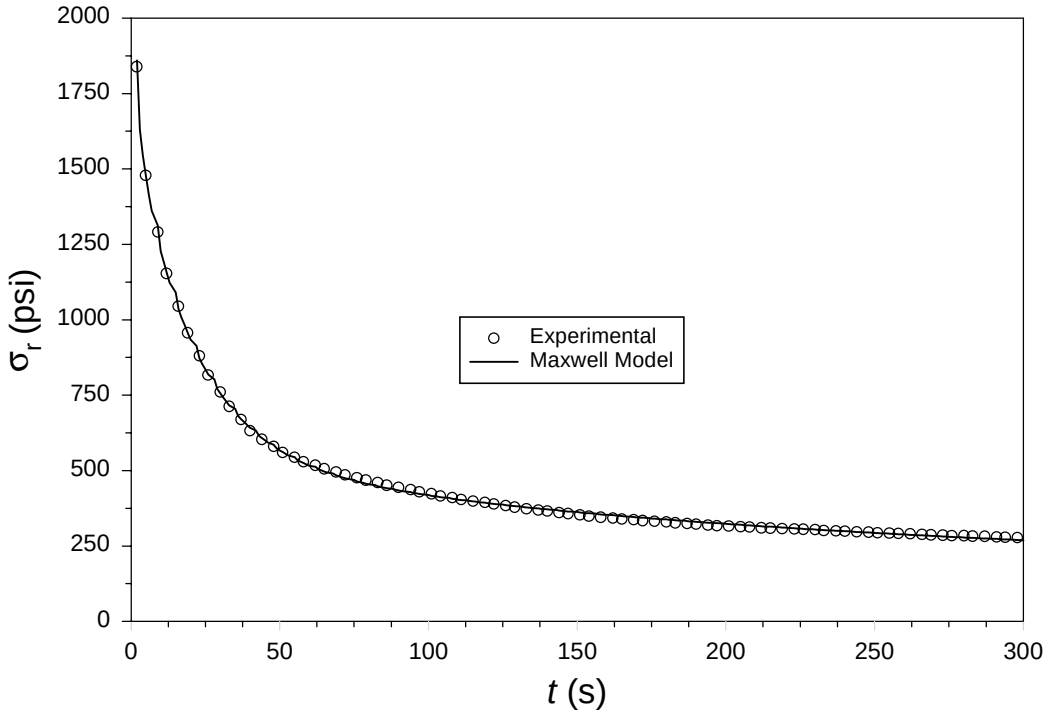

Figure 2.4. Fit of the 4 parameter Maxwell model for 0%PP mat compressed to a 65 lb/ft3 density at 180°C.

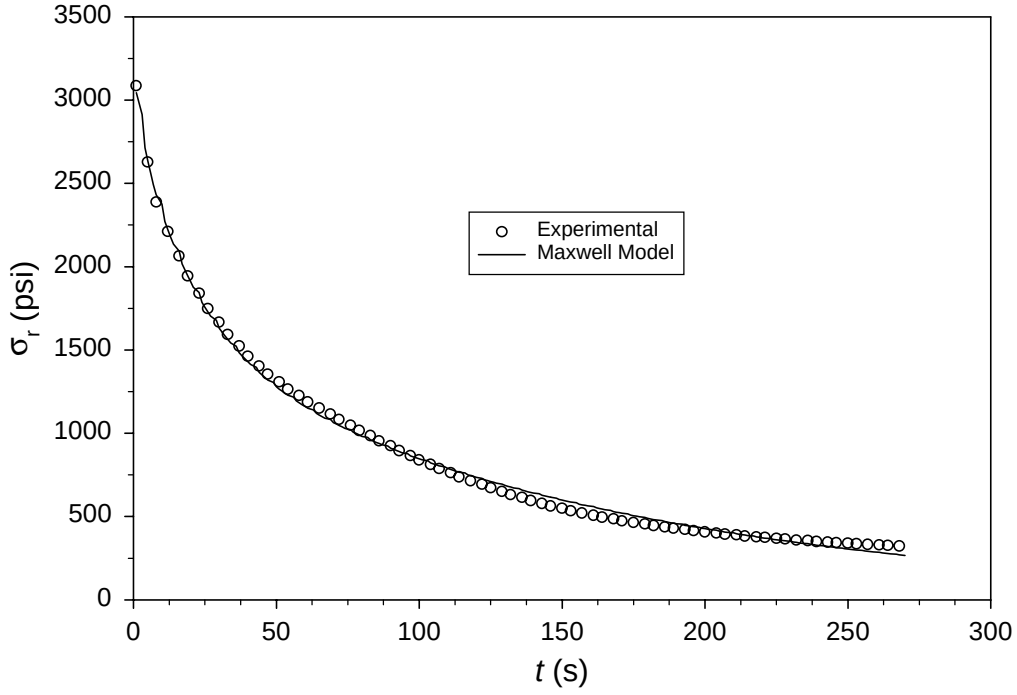

Figure 2.5. Fit of the 4 parameter Maxwell model for 50%PP mat compressed to a 65 lb/ft3 density at 180°C.

The Maxwell model provided an accurate estimate of the relaxation response of a fibrous WPC. The composite with no PP showed the closest agreement with the model (Fig 2.4), while the higher PP levels showed some deviation from the model (Fig. 2.5). The melt transition of the PP causes a non-linear viscoelastic behavior to occur during relaxation. The Maxwell model identified in Eq. 2.15 is based on the assumptions of linear viscoelasticity. However, the deviation between the data in Figure 2.4 and 2.5 was slight, with an R^2 of 0.999 and 0.997, respectively. Relaxation curves for all treatments can be seen in Appendix B.

Conclusion

When forming a wood fiber composite through compression molding, heated platens apply stress to the mat until the final profile is established. The amount of stress required to compress the mat and the duration of the processing time are function of the consolidation mechanisms and the heat/mass transfer of the composite. Modeling the compressive stress with established methods in the wood-strand literature did not fit the experimental data. The poor fit can be attributed to the high strains developed in a wood fiber mat and neglecting the contribution of fiber bending in the models.

The models developed in the powder literature fit the wood/PP fiber mat in the higher stress regions of the stress-strain curve, but failed to fit the initial non-linear region. Utilizing the concept of the mechanical property relationship with relative density (ρ_R) in the powder models, a proportionality was established between the $E(\varepsilon)$ and ρ_R. With this relationship, a model was developed to predict the compressive stress during closure with close agreement with the experimental data. The viscoelastic

relaxation response of the compressive stress was modeled utilizing a four parameter

Maxwell model and also provided a good fit with the wood/PP fiber compression data.

References

Ang, A.H. and W.H. Tang. 1975. Probability concepts in engineering planning and design. John Wiley and Sons, Inc. New York.

Bolton, A.J., Humphrey, P.E. and P.K. Kavvouras. 1989. The hot pressing of dry-formed wood –based composites. Part IV The importance of stresses in the pressed mattress and their relevance to the minimization of pressing time, and the variability of board properties. Holzforschung 43:406-410.

Boodig, J and J.R. Goodman. 1973. Prediction of elastic parameters for wood. Wood Science 5(4):249-264.

Christensen, R.M. 1982. Theory of viscoelasticity, an introduction. Academic Press. New York.

Cooper, A.R. and L.E. Eaton. 1962. Compaction behavior of several ceramic powders. Journal of the American Ceramic Society. 45(3):97-101.

Dai, C. and P.R. Steiner 1993. Compression behavior of randomly formed wood flake mats. Wood and Fiber Science. 25(4): 349-358.

Ferry, J.D. 1980. Viscoelastic properties of polymers. John Wiley and Sons, Inc. New York.

Findley, W.N., Lai, J.S and K. Onaran. Creep and relaxation of nonlinear viscoelastic materials; with an introduction to linear viscoelasticity. Dover Publications New York, NY

Gibson, L.J. and M.F. Ashby. 1988. Cellular solids: structure and properties. Pergamon Press. New York, NY.

Goldstein, I.S. 1973. Degradation and protection of wood from thermal attack. *In*: Wood deterioration and its prevention by preservative treatments. Vol 1 Degradation and protection of wood. D.D. Nicholas ed. Syracuse University Press. New York.

Heckel, R.W. 1961. An analysis of powder compaction phenomena. Transactions of the Metallurgical Society of AIME. 221:1001-1008.

Jones, R.L. 1963. The effect of fiber structural properties on compression response of fiber beds. Tappi 46(1):20-27.

Jin, J and N.D. Cristescu. 1998. A constitutive model for powder materials. Journal of Engineering Materials and Technology. 120:97-104.

Kamke, F.A. and L.J. Casey. 1988. Fundamentals of flakeboard manufacture: internal-mat conditions. Forest Products Journal 38(6):38-44.

Konopicky, K. 1948. see R. Kieffer and W.Hotop. Sintereisen and Sinteristabl. Springer-Verlag, Wein.

Lang, E.M. and M.P. Wolcott. 1996a. A model for viscoelastic consolidation of wood-strand mats. Part 1. Structural characterization of the mat via monte carlo simulation. Wood and Fiber Science 28(1):100-109.

Lang, E.M. and M.P. Wolcott. 1996b. A model for viscoelastic consolidation of wood-strand mats. Part II. Static stress-strain behavior of the mat. Wood and Fiber Science 28(3):369-379.

Lenth, C.A. and F.A. Kamke. 1996a. Investigations of flakeboard mat consolidation. Part I. Characterizing the cellular structure. Wood and Fiber Science 28(2):153-167.

Lenth, C.A. and F.A. Kamke. 1996b. Investigations of flakeboard mat consolidation. Part II. Modeling mat consolidation using theories of cellular materials. Wood and Fiber Science 28(3):309-319.

Mark, R.E. 1967. Cell wall mechanics of tracheids. Yale University Press. New Haven, CT.

Panshin, A.J. and C. DeZeeuw. 1980. Textbook of wood technology. McGraw-Hill Book Company. New York.

Ransing, R.S., Gethin, D.T., Khoei, A.R., Mosbah,P., and R.W. Lewis. 2000. Powder compaction modeling via the discrete and finite element method. Materials and Design. 21:263-269.

Suchsland, O. 1959. An analysis of the particleboard process. Michigan Quarterly Bulletin 42(2):350-372.

Suchsland, O. 1967. Behavior of a particleboard mat during the press cycle. Forest Products Journal 17(2):51-57.

Shivanand, P. and O.L. Sprockel. 1992. Compaction behavior of cellulose polymers. Powder Technology. 69:177-184.

Tabil Jr., L.G. and S.Sokhansanj. 1996. Compression and compaction behavior of alfalfa grinds. part 1: compression behavior. Powder Handling and Processing. 8(1):17-23.

Tschoegl, N.M. 1989. The phenomenological theory of linear viscoelastic behavior. Springer-Verlag. New York.

Wolcott, M.P., Kamke, F.A. and D.A. Dillard. 1990. Fundamentals of flakeboard manufacture: viscoelastic behavior of the wood component. Wood and Fiber Science 22(4):345-361.

Wolcott, M.P., Kamke, F.A. and D.A. Dillard. 1994. Fundamental aspects of wood deformation pertaining to manufacture of wood-based composites. Wood and Fiber Science 26(4):496-511.

Wang, S. and P.M. Winistorfer. 2000. Fundamentals of vertical density profile formation in wood composites. part II. methodology of vertical density formation under dynamic conditions. Wood and Fiber Science 32(2):220-238.

Wong, E.D. Zhang, M. Wang, Q. and S. Kawai. 1999. Formation of the density profile and its effects on the properties of particleboard. Wood Science and Technology 33:327-340.

Chapter 3

Compression and Relaxation Behavior of Wood/Thermoplastic Fiber Mat During Consolidation

Abstract

Wood-fiber mats are hot-pressed to form flat and molded panels for the building construction and automotive industries. After reaching final thickness, the compression stress in the mat decreases with time in a classical relaxation phenomenon. This stress relaxation data can be used to approximate continuous relaxation spectra ($H(\lambda)$) for discerning mechanisms of the overall consolidation process. The compression response of wood and blended wood/polypropylene (PP) fiber mats was monitored to determine the influence of material and processing parameters on consolidation. Machine formed non-woven fiber mats were produced with varying PP levels and compressed with different platen temperatures and strain rates. The maximum consolidation stress developed varied with strain rate and PP content, however, temperature did not affect the consolidation behavior. The relaxation response of the composite was described through a relaxation spectrum analysis. A numerical approximation of the spectra showed variations in the transient relaxation response due primarily to fiber slippage within the network. The relaxation concentration within the asymptotic region of the spectrum was attributed to the softening of the amorphous wood constituents and the melting of the PP resin. A positive correlation was also observed with the platen temperature and the

relaxation behavior of the mats with PP fibers. Use of computed relaxation spectra during hot-pressing provides a means to monitor the internal stresses developed within the wood composite.

Introduction

The uniaxial stress, which occurs during wood-based fiber composite processing, can be divided into two separate time domains; stress-strain and stress-time. During the stress-strain region, stress is accumulated as the composite is compressed to a target thickness or density. The ensuing stress-time response occurs as the composite is held at a constant strain and a relaxation in stress is observed. The consolidation stress develops a nonlinear response to both strain and time, which can be attributed to the viscoelastic behavior of the material and structure.

The stress resulting from consolidation is a function of both material and processing parameters. The strain rate and processing temperature can alter the compression response as well as the moisture content (MC) and geometry of the composite materials (Suchsland 1967). The addition of thermoplastics to the wood matrix to improve the exterior performance of wood composites, will undoubtedly result in changes to the stress-strain and stress-time response of the mat during processing.

The goal of this work is to provide an analysis of the compressive response of wood and blended wood/polypropylene (PP) fiber composites. The specific objectives within this work include:

1) To obtain the stress-strain and stress-time response of a wood/PP fiber mat during consolidation through uniaxial compression tests.

2) Provide calorimetric and thermal mechanical data on the composite materials for use in evaluation of the compression and relaxation response of the mats during consolidation.

3) Use spectrum analysis to evaluate the influence of processing and material parameters on the relaxation behavior.

Stress-Strain Response

The nonlinear behavior of the stress-strain response during consolidation is a result of the cellular structure of both the mat and wood fibers, and the viscoelastic response of the amorphous wood components and thermoplastic elements. During consolidation of a wood-fiber mat, large strains occur as the mat undergoes fiber bending and large void filling through repositioning. The last stage of consolidation is dominated by fiber compression, often resulting in cellular collapse (Jones 1963).

The initial stress in fibrous mat compression develops as fibers slide past one another to fill the voids within the mat resulting in a non-recoverable deformation (Jones 1963). The contribution of resistance during packing is influenced by inter-fiber friction. Further non-recoverable and recoverable deformation is then caused by the bending of the fibers (Jones 1963). Separating bending and packing into distinct regions of the consolidation curve can be difficult due to the overlap of their contributions.

As the mat is consolidated further , a majority of the wood and thermoplastic fibers experience transverse compression. As the wood material is compressed, the viscoelastic behavior and the cellular structure contribute to the stress-strain response of the mat. The molecular viscoelastic behavior of wood can be attributed primarily to the amorphous constituents, hemicelluloses and lignin, whereas damage development is manifested through fracture and plastic hinge development associated with cellular

collapse (Gibson and Ashby 1988). Gibson and Ashby (1988) found similar nonlinear behaviors with synthetic foam and honeycomb structures made with elastic materials. Cowin and Nunziato (1983), described the nonlinear stress-strain behavior of elastic materials with voids incorporating mechanical analogies commonly used for viscoelastic materials. The heterogeneity of the voids within the material causes a deviation from the elastic stress-strain response.

The response of the amorphous wood components and thermoplastic fibers to an applied stress is based upon their viscoelastic behavior. Time, temperature, and diluent concentration (ie MC) can influence a viscoelastic material and cause a deviation from a linear stress - strain Hookean relationship. This rheological behavior can be influenced by the material and processing parameters associated with consolidation processing.

Stress-Time Response

Once the composite reaches a constant strain, stress decreases as the composite begins to relax. This relaxation is a function of both the viscoelastic nature and movement of the fibers. The thermodynamic conditions in the mat contribute to relaxation through thermal transitions of the polymers. These transitions are manifested in molecular relaxations leading to softening or melting. For powders and fibers, a contribution to the stress relaxation may also occur with inter-fiber slippage. In aggregate, all of these mechanisms define the stress relaxation and will influence the composite relaxation modulus ($E(t)$) during consolidation.

In solid polymers, relaxation mechanisms are primarily governed by movement and/or relaxation of molecular bonds, resulting in chain reptation and molecular degradation (Sperling 1992). These mechanisms are also influenced by the viscoelastic

effects of time, temperature, and diluent content. In addition to these molecular parameters, the relaxation of a wood-based composites is influenced by the structure of the wood elements, mechanics of the fiber network, and the development of microstructural damage (Wang and Winistorfer 2000).

The stress relaxation that occurs in a wood-based composite is complicated by the unsteady state developed from the pressing environment. Wolcott (1989) concluded that the density profile continued to form during the relaxation period of a wood flake mat. Wang and Winistorfer (2000) measured the vertical density profile of wood-strand panels during consolidation and found experimental evidence for density profile formation resulting from differential relaxation. The authors separated the relaxation into two separate stages. The initial stage included relaxation of the viscoelastic materials and further microstructural damage under pressure of the surface layers of the panel. The second stage was comprised of a core densification as the temperature and MC increased, while the surface density slightly decreases. Their work concluded relaxation behaviors vary throughout the thickness of the compressed panel, due to the mechanisms of heat and mass transfer, where the amount of variation can be altered through process parameters.

To understand the mechanisms of the relaxation response of polymeric material, a relaxation spectrum (*H*) can be developed from experimentally determined mechanical properties of the material (Ferry 1980 and Tschoegl 1989). Utilizing the relaxation modulus (*E(t)*), the *H* can be represented over a continuous interval as:

$$E(t) = E_{\infty} + \int_0^{\infty} H e^{-t/\lambda_i} d \ln \lambda \qquad \text{Eq. 3.1}$$

where λ represents the relaxation time and E_∞ is the modulus of the material once the stress has converged at an infinite time frame. The relaxation time spectrum can be derived indirectly from linear viscoelastic data generally through numerical approximation (Ferry 1980).

The spectrum is a valuable tool, which provides a representation of concentrations in the relaxation process (Ferry 1980). A maxima in the spectrum can be associated with a high level of relaxation occurring within the material. As *H* approaches zero, the relaxation ceases and can be considered perfectly elastic at short times and an uncrosslinked viscous liquid at longer times (Ferry 1980)

Analytical Background

The relaxation spectrum can be computed from stress relaxation data using different methods. From Equation 3.1, we can see that relaxation spectrum can be evaluated by directly differentiating the stress relaxation data using numerical approximations. While this method may be the most straightforward, it is prone to errors from noise in the collected stress data. Often it is best to represent the relaxation data using a numerical function, which is subsequently used to evaluate the relaxation spectrum.

The stress relaxation response of a polymer can be modeled through mechanical analogies such as the Maxwell model:

$$E(t) = E_\infty + \sum E_i e^{-t/\lambda_i} \qquad \text{Eq. 3.2}$$

where *t* represents the elapsed time from constant strain. In practice, the modulus parameters (E_i) can be estimated from the experimental data using nonlinear regression techniques. To provide a more detailed description of the viscoelastic properties, the number of model parameters can be increased. However, numerical methods of nonlinear systems are subject to over-parameterization and may cause a convergence to zero for many of the parameters. The amount of elements within a well-defined model can be determined through stepwise regression techniques. Most stepwise techniques utilize a F statistic to select variables based upon a predetermined level of significance (Neter et al. 1990).

Plotting the E_i values from the Maxwell model provides a characterization of the relaxation process, however, a more rigorous and informative method for interpretation of polymer mechanics is to describe the relaxation over a continuous interval via the relaxation spectrum (H) (Eq. 3.1). In essence, the spectrum is an alternative form of the relaxation moduli relating a discrete function to a continuous spectrum (Christensen 1982). A viscoelastic material response to an imposed stress is a function of time; the spectrum describes the material function on a basis that is independent of time (Tschoegl 1989). The relaxation spectrum can be simply approximated as the change of E(t) with respect to time. Therefore, any maxima developed in the spectrum, indicates a concentration of relaxation during the corresponding time frame (Ferry 1980).

Applying the closed form solution of the integral in Eq. 3.2 with experimental data can be a tedious task, which is only performed when very small transitions are evaluated on a molecular level. Rather, $H(\lambda)$ is commonly approximated through numerical or graphical techniques (Ferry 1980). Ferry (1980) suggests a numerical

approximation developed by Tshoegl (1981), which provides an estimate of $H(\lambda)$ through numerical derivatives:

$$H(\lambda) = -\frac{dE(t)}{d\ln t} + \frac{1}{3}\frac{d^2E(t)}{d(\ln t)^2};\ \textit{where}\ t = \frac{\lambda}{\sqrt{2}} \qquad \text{Eq. 3.3}$$

Many approximations of $H(\lambda)$ have been proposed throughout the literature, however, care must be taken if higher order methods are utilized. With third derivative methods, the experimental data must be inordinately precise so that the inferences made can be correlated with phenomenological events and not that of a mathematically ill-posed problem (Ferry 1980). The approximation in Eq. 3.3 is considered a conservative approach where the role of the second derivative is minimal (Ferry 1980). This method was chosen here as a reasonable compromise between numerical simplicity and mathematical rigor, recalling that the goal of this study is to infer mechanisms for mat relaxation.

Experimental Procedures

Uniaxial Compression

The data from the uniaxial compression tests on the non-woven wood fiber and wood/polypropylene (PP) fiber mats pressed to a 65 lb/ft^3 density in Chapter 2 was used for the compression and relaxation information in the following results. Additional compression tests were also run to determine the influence fiber surface friction and moisture has on the stress-strain relationship. Wood fibers, identical to those used in the non-woven mats, were hand-laid into mats (12 x 15 in.). Prior to forming, the fibers were blended with either 3 weight percent zinc stearate (Synpro DLG20B by Ferro Chemical), a common lubricant in the wood plastics industry or 5% powdered PF. The moisture

content of the non-lubricated fibers was increased by spraying enough water to elevate the 6% initial MC to 9% and 12%. The fibers were allowed to equilibrate in sealed plastic bags for 5 days. The actual MC were calculated to be 5.67, 9.17 and 11.98%.The hand-laid mat was held together between two sheets of veneer and cut to a 2.5 inch square specimen. The specimens were compressed to a 65 lb/ft3 density using a 180°C platen temperature.

A servo-hydraulic, universal test machine fitted with heated aluminum platens was used to compress the non-woven and hand laid mats at a strain rate of 0.006 in/in-s. A thermocouple was inserted in the center of the layered mats to monitor the core temperature. Once the composite reached a final thickness, the platens were held constant for 4 minutes, while the relaxation load response was recorded. A time frame of 4 minutes at final density was found sufficient at the applied platen temperatures to ensure melt of the PP and cure of the PF resin. A sample size of three per test group was utilized and the behavior of the stress-strain and stress-time curves were similar. A representative curve from the spectrum analysis was chosen from each group for analysis.

Relaxation Spectrum Determination

The spectral response of a material can be directly obtained from molecular theory, however, only approximations to an actual response can be developed from experimental data (Emri and Tschoegl 1995). Emri and Tschoegl (1995) developed an algorithm that utilizes experimental data to determine the spectral response of a material. However, to encompass the entire stress-strain and stress-time response of the fibrous composite, a large (55 kips) load cell was utilized for the compression tests. The small fluctuations inherent in acquiring the load signal on a reduced scale made direct use of

the experimental data difficult. Therefore, a continuous mathematical description of this data was provided through a power series (Eq. 3.4). The β and α coefficients, which can be associated with E and λ of the Maxwell model, were estimated by the Marquardt-Levenberg nonlinear regression technique. The values for E_i were normalized by the value obtained at the initial time step (i.e. time attaining final strain) for the purpose of behavioral comparative analysis. From the data generated in the power series in Eq. 3.4, a forward-difference method was used to solve Eq. 3.3 for estimating $H(\lambda)$.

$$E(t) = \beta_o + \sum_{i=1}^{3} \beta_i e^{-\alpha_i t} \qquad \text{Eq. 3.4}$$

The coefficients for the power series in Eq. 3.4 are shown in Tables 3.1 and 3.2 for the data represented. The Maxwell model in Eq. 3.2 is a power series function, in which λ values are generally spaced at decade increments. In this power series, λ is equal to $1/\alpha$, while the β coefficients are the same as E_i's.

Table 3.1. Power series coefficients for the hand laid wood fiber mats.

Power Series Coefficients	**Hand Laid Fiber Mats**				
	6% MC	**9%MC**	**12%MC**	**w/Zinc Stearate**	**w/PF Resin**
E_o	121.615	165.4842	90.0081	155.0351	166.538
E_1	404.409	570.2656	418.8226	371.6126	386.2092
λ_1	3.799392	3.904725	3.025719	3.111388	2.922268
E_2	530.8715	649.8271	296.7238	372.0396	415.6513
λ_2	36.63004	47.61905	49.50495	24.57002	22.98851
E_3	100.8485	210.0829	379.2074	108.8702	206.606
λ_3	511.5875	175.7253	49.50495	271.0027	213.4608
r^2	0.999326	0.999354	0.998284	0.998969	0.999312

Table 3.2. Power series coefficients for the non-woven wood and wood/PP fiber mats.

Power Series Coef.s	Non-Woven Fiber Mats							
	0% PP 170°C	0% PP 180°C	0% PP 190°C	30% PP 180°C	40% PP 180°C	50% PP 170°C	50% PP 180°C	50% PP 190°C
E_o	294.72	264.83	231.96	105.47	232.26	562.98	239.05	123.08
E_1	508.22	676.51	711.88	817.39	801.74	493.66	904.78	636.45
λ_1	1.8570	1.0312	1.0936	10.204	7.2723	1.4132	8.3403	4.9261
E_2	1300.4	1031.2	1042.2	472.82	1008.7	937.94	980.01	1136.2
λ_2	19.455	15.432	14.881	72.993	71.429	16.155	81.301	57.471
E_3	383.44	440.2	442.15	616.92	1048.0	1493.6	1035.8	1143.2
λ_3	153.84	107.53	97.087	72.993	71.429	102.04	81.301	57.471
r^2	0.9995	0.9998	0.9997	0.9994	0.9996	0.9999	0.9996	0.9994

Differential Scanning Calorimetry (DSC)

A sample of the uncompressed wood/PP fiber mats were Wiley® milled and passed through a 40 mesh screen. Approximately 5 mg of the screened material was weighed to the nearest 0.1mg and encapsulated in a hermetically sealed pan. Utilizing a ramp rate of 10°C/min, the specimen was heated from 40 to 200°C. Data acquired from the DSC testing were the heat flow and the heat capacity of the material.

Dynamic Mechanical Analysis (DMA)

Dynamic mechanical analysis (DMA) was performed through the use of a three-point bending test procedure. Specimens were obtained from compression test specimens, which were processed at 190°C with 0 and 30% PP and compressed to a 65lb/ft^3 density. The 0.5 x 0.125 x 2 in. specimens were flexed with a 1 Hz frequency, while exposed to a thermal ramp of 5°C/min from ambient to 220°C. The storage (*E'*) and loss (*E"*) modulus were recorded during the temperature ramp.

Results and Discussion

Compression to Final Strain

The initial compression region of the wood/PP fiber mat was influenced by the strain rate and PP content. However, the platen temperature had little or no effect on the compressive stress behavior of the wood/PP mats (Figure 3.1). The lack of a temperature effect is likely due to the core temperatures remaining between ambient and 80°C for the compression zone in all conditions. As evident in the DSC spectra for the 0% and 50% PP mats (Figure 3.2), no material transitions occur within the major components of the composite between ambient and 80°C.

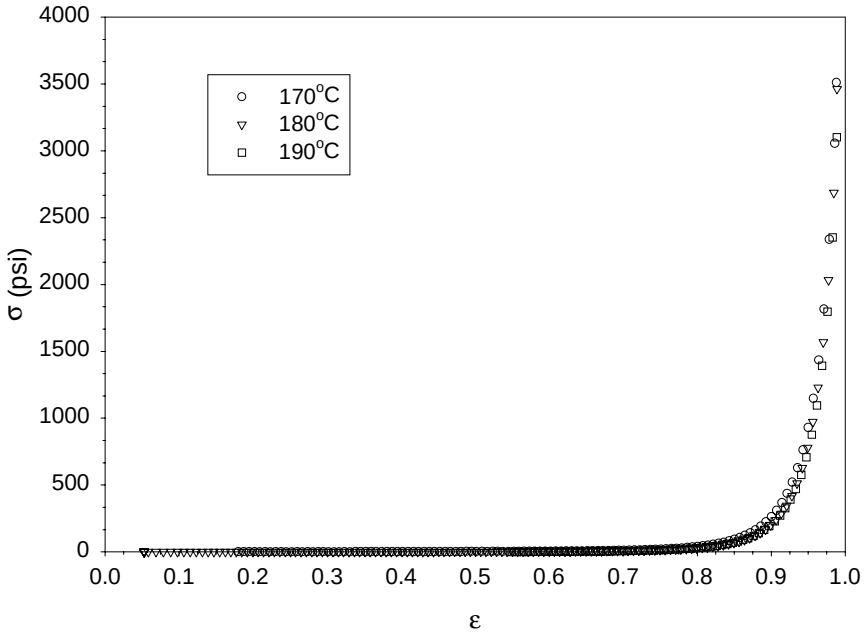

Figure 3.1. Compression curve for non-woven mats with 40% PP pressed to 65 lb/ft^3.

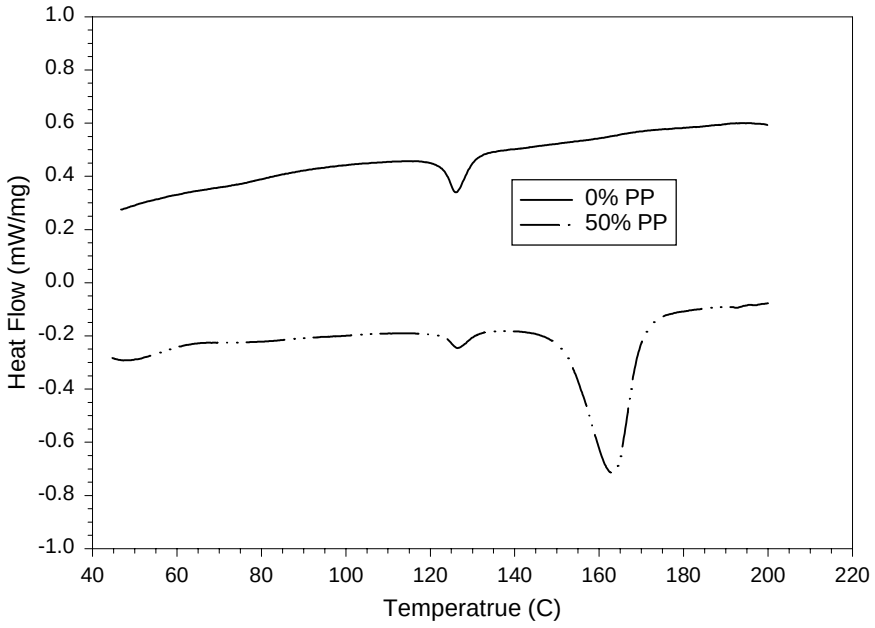

Figure 3.2. DSC plot of 0 and 50% PP mats scanned at 10°C/min using 40 mesh Wiley milled samples.

Increasing PP content in the fiber network resulted in increased final compressive stress. This effect was accentuated with an increase in the strain rate (Figure 3.3a and 3.3b). The compressive stress of the composites with no PP exhibited an increase in stress at a lower strain than with the mats containing PP, however, the ultimate compressive stress at the final thickness was lower. Figures 3.4a and 3.4b represent the relative stress-strain behavior of mats with varying amounts of PP and indicates an increased stress accumulation with the 0% PP mat. Since the final strains were different for each specimen, a normalized strain was used to compare when the accumulation of stress occurred. The σ and ε data was normalized by dividing by the ultimate stress (σ_o) or final strain (ε_o), respectively.

Suchsland (1967) pressed wood particleboard with a range of strain rates and found a lower final compressive stress with the longer closing times. The strain rates used for the non-woven mats may have been too slow to see any time-dependent effects on the wood fibers. The mechanical behavior of wood is not completely governed by viscoelasticity. The cellulose component is a highly-crystalline material, which exhibits many elastic attributes (Mark 1967). The behavior of PP can be classified primarily as a viscoelastic material and would, therefore, be more susceptible to a time rate change than the mats with only wood fiber.

Jones (1963) states that the initial stages of fiber mat compression are dominated by fiber bending and relocation. The same conclusion for wood-strand composites was found by Dai and Steiner (1993) and Lang and Wolcott (1996b). Since the bending modulus of wood is nearly four times higher than PP, the observation of Jones (1963) holds true (Figure 3.4a). Jones also states the final stage of mat compression is dominated by fiber compression. Assuming a majority of the fibers lie within the plane of the platen, the properties of the fiber in the transverse direction would govern the stress behavior. The transverse compression moduli of aspen (Bodig and Goodman 1973) is approximately one-tenth of PP, resulting in a lower final compressive stress for the high wood fiber mats.

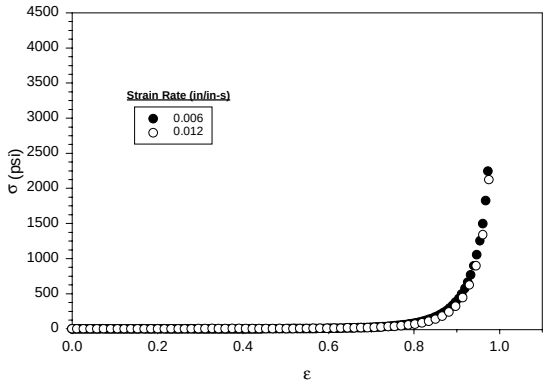

Figure 3.3a. Comparison of the compressive stress at varying strain rates for 0% PP mats pressed to a 65 lb/ft^3 density at 180°C.

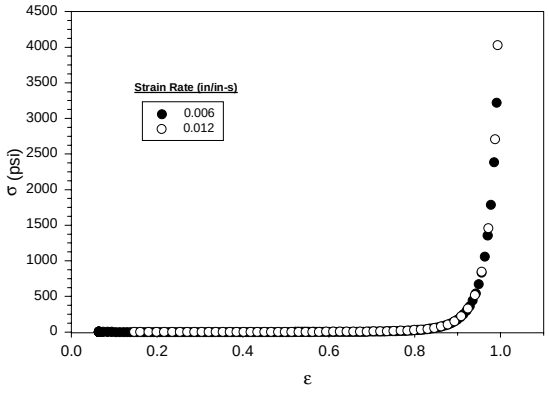

Figure 3.3b. Comparison of the compressive stress at varying strain rates for 50% PP mats pressed to a 65 lb/ft^3 density at 180°C.

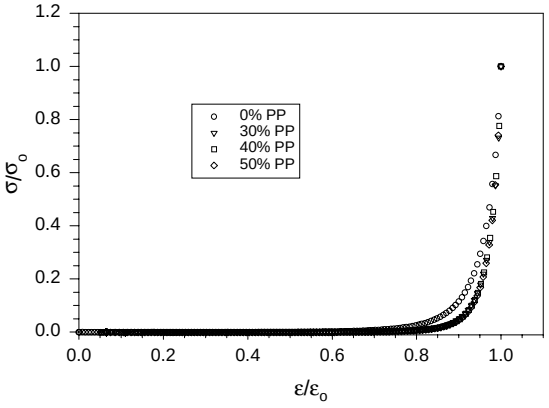

Figure 3.4a. Normalized compressive stress for varying PP levels pressed to 65 lb/ft^3 density with a platen temperature of 180°C.

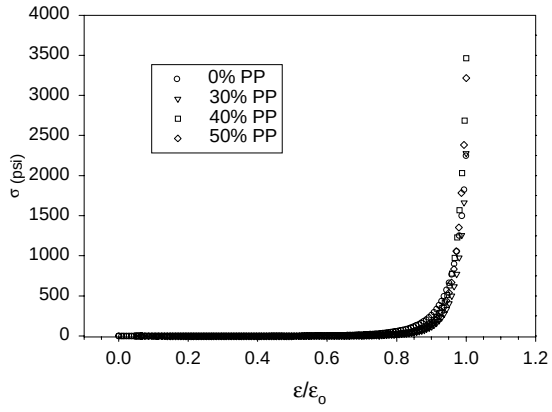

Figure 3.4b. Compressive stress for varying PP levels pressed to 65 lb/ft^3 density with a platen temperature of 180°C.

With the addition of the zinc stearate lubricant on the wood fiber surface, a lower final compressive stress occurred as seen in Figure 3.5. The zinc stearate provided a reduction of the frictional contribution to the compressive load, by decreasing the final

compressive stress by 12%. The lubricant increased the packing efficiency of the mat structure by allowing more fiber movement with less frictional resistance

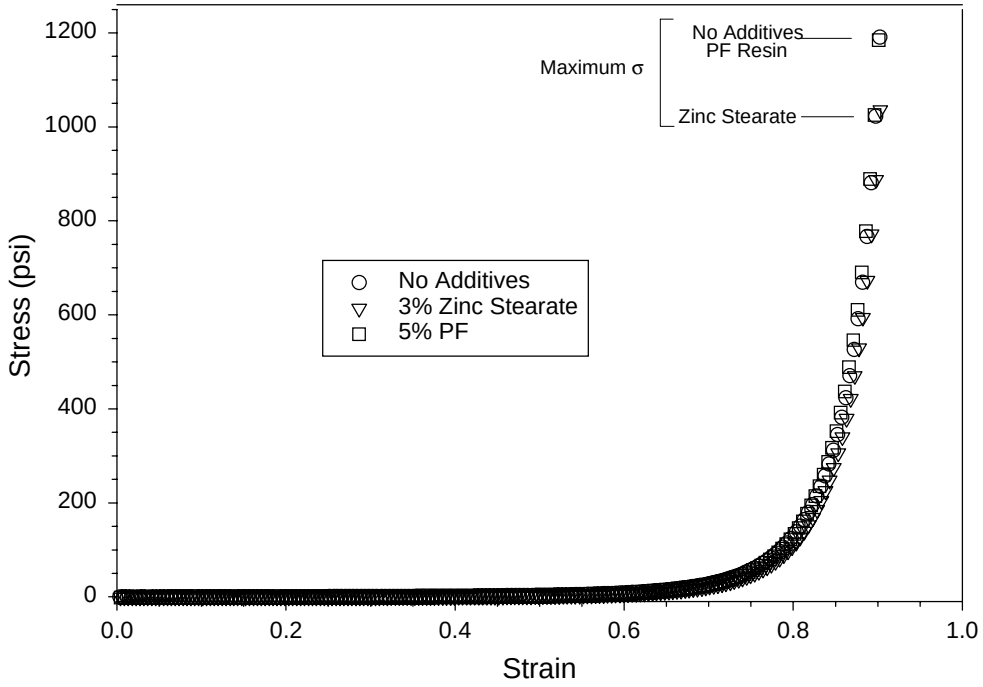

Figure 3.5. Compressive stress-strain curve for PF and zinc stearate additives to the hand-laid mat. Panels pressed to 65 lb/ft^3 density with a platen temperature of 180°C.

Stress Relaxation

The relaxation behavior of the wood/PP composites was influenced by the platen temperature, lubricant level, and PP level. To evaluate and compare the effect these parameters impart on the relaxation behavior, a stress-time plot can be utilized to denote differences in the material and test parameters, however, the relaxation spectrum provides more insight into the mechanisms of relaxation in the composite. In the following graphs, the relaxation time (*t*), begins when compression strain is constant (i.e. press closure).

Two distinct mechanisms of stress relaxation, interparticle movement and material deformation, were associated with the consolidation of the fibrous wood/PP

mats. During the initial stages of relaxation, the fibers reposition themselves by sliding past one another. Further relaxation occurs as heat and moisture transfer towards the core of the panel. The moisture and temperature effects alter the mechanical properties of the wood and PP constituents. The amorphous wood components exhibit a modulus reduction as the composite temperature approaches the T_g of lignin and hemicellulose. Once the temperature profile reaches the melt of PP, a continued relaxation is observed and, at present, assigned to the thermoplastic flow.

Interparticle Movement

In Chapter 2, the compression behavior of the non-woven mats was found to be similar to that of powders. Umeya and Hara (1978) studied the consolidation of polystyrene (PS) particles and determined the consolidation mechanisms to be the deformation of the particles and the inter-particulate surface friction. In further work, Umeya and Hara (1980) determined a majority of the relaxation was due to the viscoelastic nature of the PS. However, the initial stages of relaxation was strongly influenced by the inter-particle friction. An addition of lubricants to the particles reduced the sliding friction between the PS particles.

An analogous behavior was noted when the wood fiber mats were blended with the zinc stearate lubricant. The stearate coated fibers had a slightly higher spectral concentration in the initial stages of relaxation (Figure 3.6). Similar to the influence of lubricant on the ultimate compressive stress, the lubricant could also allow for more fiber movement decreasing the contribution of stress. The absence of an initial spectral concentration in the non-woven mats with added PP fibers, may also indicate the presence of fiber movement or slippage (Figure 3.7). During the stress-strain region of

the consolidation process, the core temperature of the composite is below the melt of the PP (≈162°C). However, the outer surfaces are above the T_m of PP and remainder of the cross-sectional profile is beginning to softening, which may impede the movement of fibers.

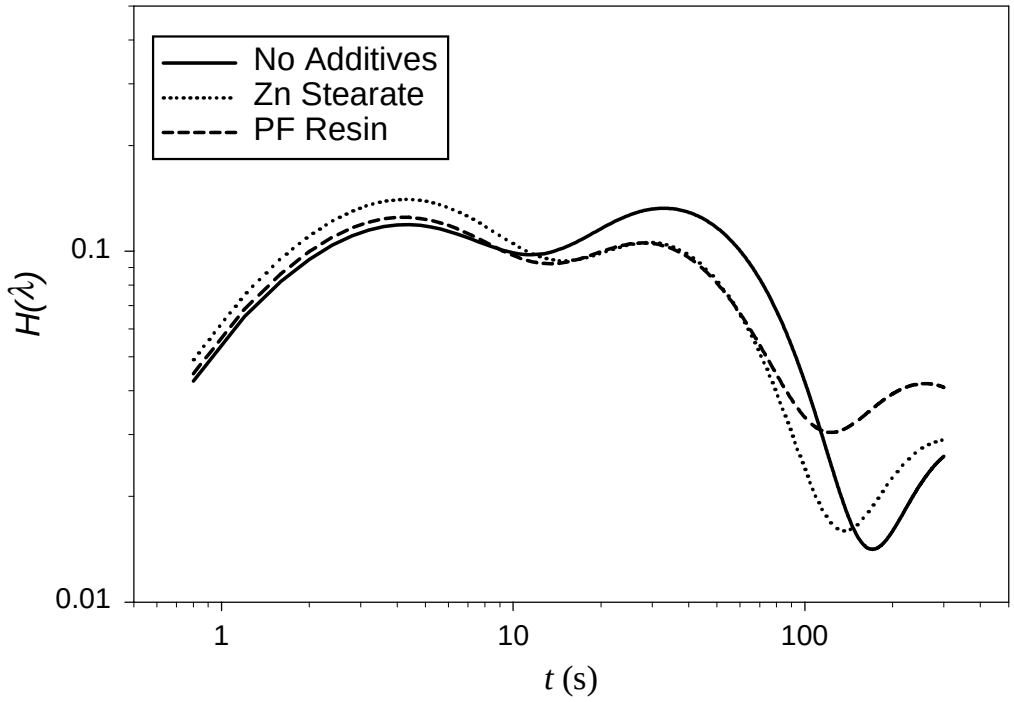

Figure 3.6. Relaxation spectra of hand laid wood fibers with additives at a platen temperature of 180°C pressed to a 65 lb/ft^3 density.

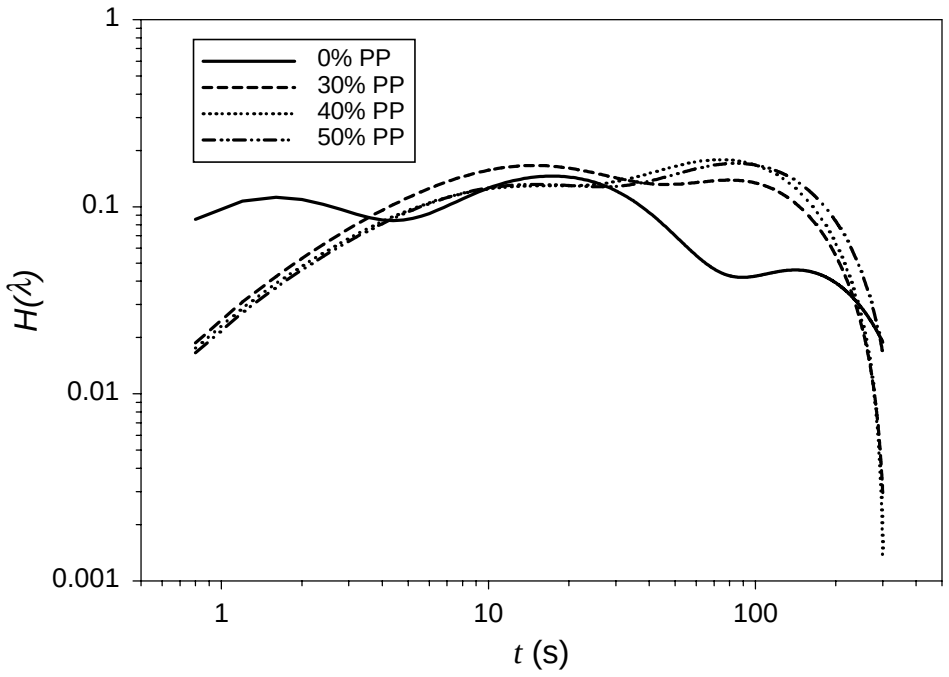

Figure 3.7. Relaxation spectra of non-woven mats with various amount of PP at 180°C pressed to a 65 lb/ft^3 density.

Material Deformation

Wood Element

The mechanical properties of the amorphous constituents of wood, lignin and hemicellulose, are greatly influenced by their glass transition temperature (T_g). As the polymer changes from a glassy to a rubbery phase, the modulus of amorphous components can decrease by three orders of magnitude (Sperling 1992). The effect of T_g on the modulus of solid wood is somewhat diminished by the reinforcing contribution of cellulose (Wolcott et al.1990).

Determining the T_g of wood during panel manufacturing is complicated by the MC. Kelly et al. (1987) found that T_g decreased non-linearly with wood MC between 0-30%. The authors utilized the Kwei model to predict the T_g for wood and found close agreement to their experimental data. In a study by Wolcott et al. (1990), the Kwei

model was used to identify the change in T_g throughout the manufacture of a wood-strand panel. For the wood-strand panels made at a 6% MC, the authors identified a sharp increase in the T_g during the relaxation period of the press cycle due to the changes in the panel environment.

The second peak associated with the spectrum curves of the wood fibers in Figure 3.6 can be attributed to the T_g of the wood components. The relaxation concentration is increased as the lignin and/or hemicellulose exhibits a softening effect and the modulus of the wood element is reduced. In Figure 3.8, the normalized stress of the higher MC mat incurs a greater amount of relaxation from the plasticizing effect of water on wood. The spectrum in Figure 3.9 indicates a higher relaxation concentration with the increased MC mats. Once the softening of lignin occurs, a reduction in the relaxation can be observed by a downward trend in the spectrum curve.

As water was added to the fibers to increase the MC, a decrease in T_g would be expected. However, the results of the varying MC's show no distinct trend associated with the T_g (Figure 3.10). The temperature curves in Figure 3.9 display a shoulder effect around 125-130°C, which indicates a rise in internal gas pressure (Strickler 1959 and Bolton et al. 1989). The saturated steam environment, which may have developed in the higher MC panels, may have influenced the lignin and hemicellulose T_g.

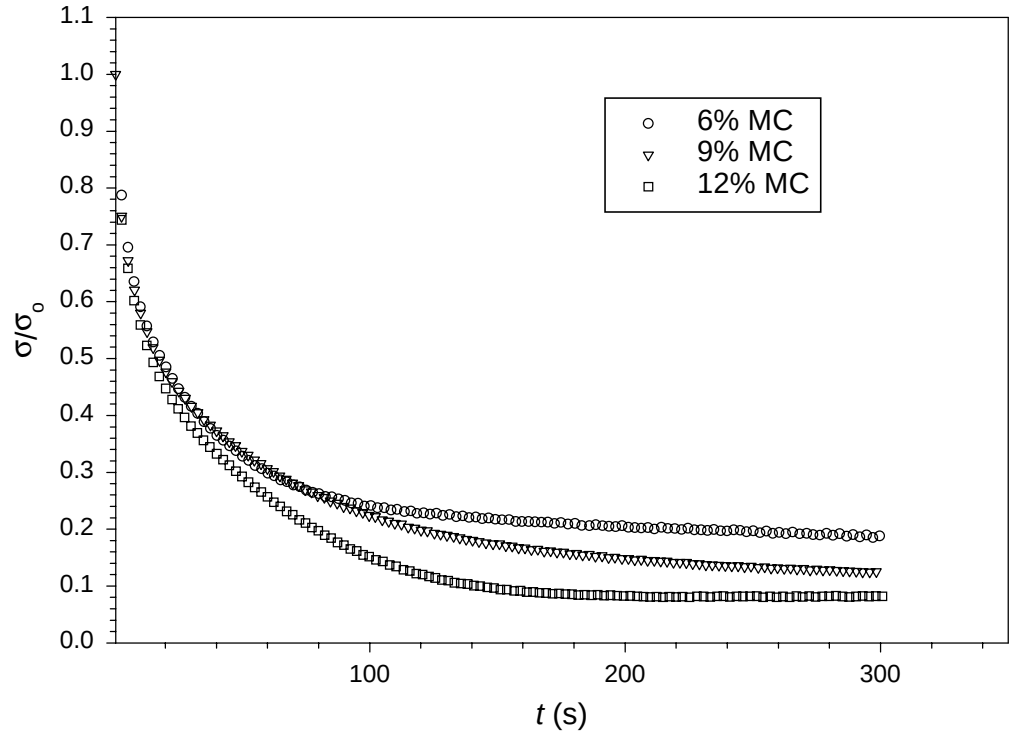

Figure 3.8. Stress-time plot for MC's of 6, 9, and 12% at a platen temperature of 180°C pressed to a 65 lb/ft^3 density.

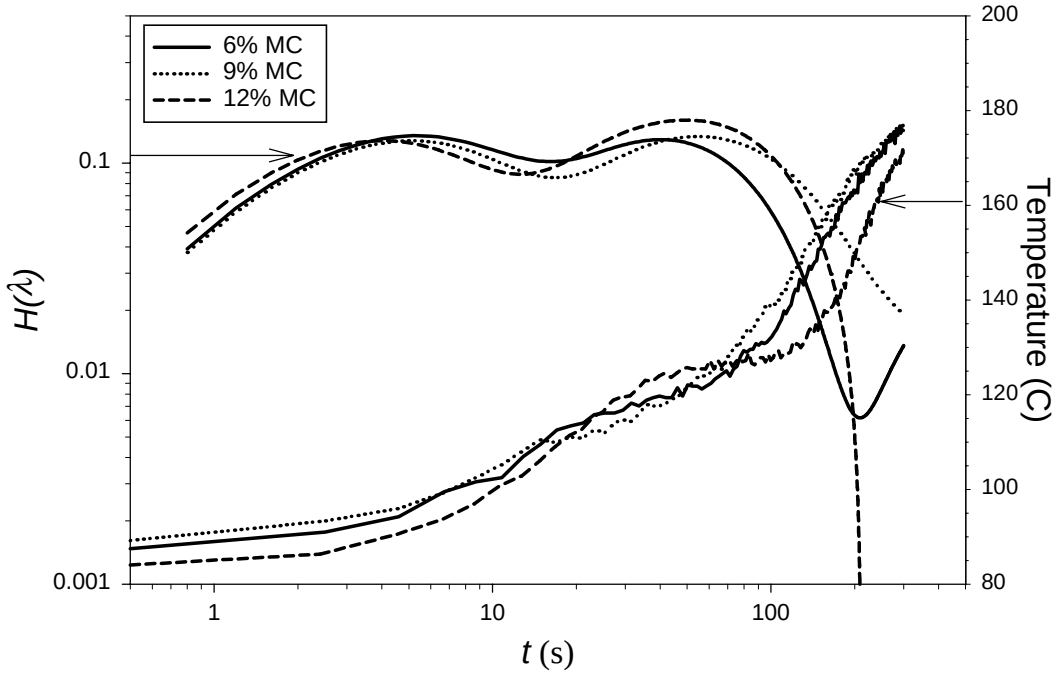

Figure 3.9. Relaxation spectra of wood fiber mats at varying initial MC's based on a logarithmic time scale.

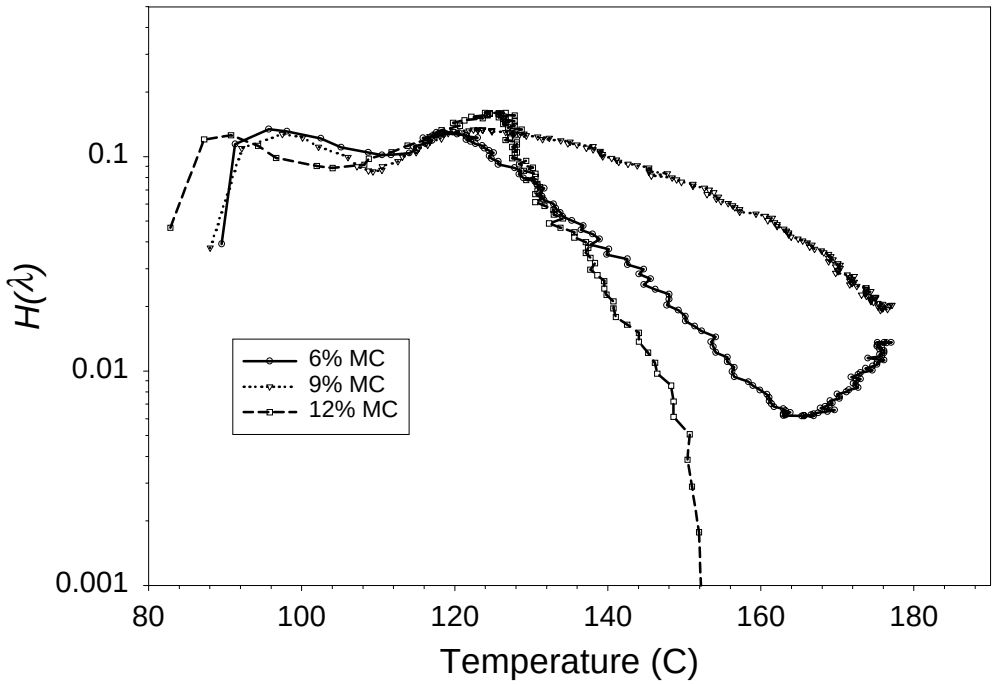

Figure 3.10. Relaxation spectra of wood fiber mats at varying initial MC's based upon the temperature of the composite

PP Influence

The stress-time plot in Figure 3.11 provides a linearly scaled representation of relaxation occurring with different levels of PP percentages. The 0 and 30% PP curves exhibit a more rapid transient relaxation to an asymptotic behavior than the panels with 40 and 50% PP. A higher amount of relaxation occurs with the wood/PP mats within the time frame of this test, while the 0% PP panels appear to converge to an asymptotic behavior more quickly.

The influence of temperature on the composite relaxation was enhanced with increased levels of PP. The plots in Figure 3.12a and 3.12b clearly display the influence temperature has on the stress relaxation of mats with 0 and 50% PP. As the temperature increases the relaxation of the panels with 50%PP became asymptotic more quickly,

which can be attributed to the increased melting rate of PP at a higher platen temperature.

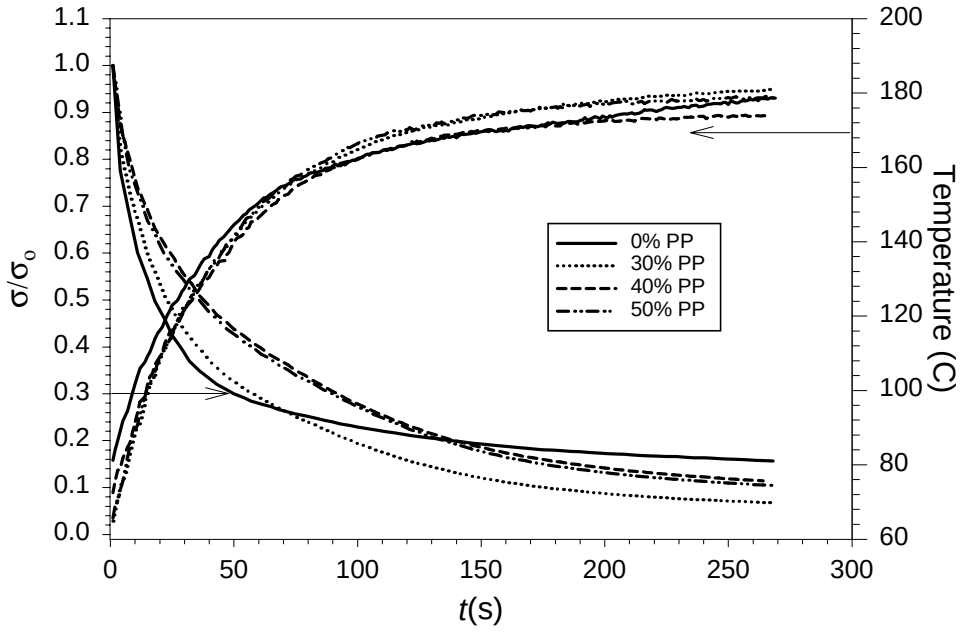

Figure 3.11. Stress-time plot for varying PP levels at a platen temperature of 180°C pressed to a 65 lb/ft^3 density.

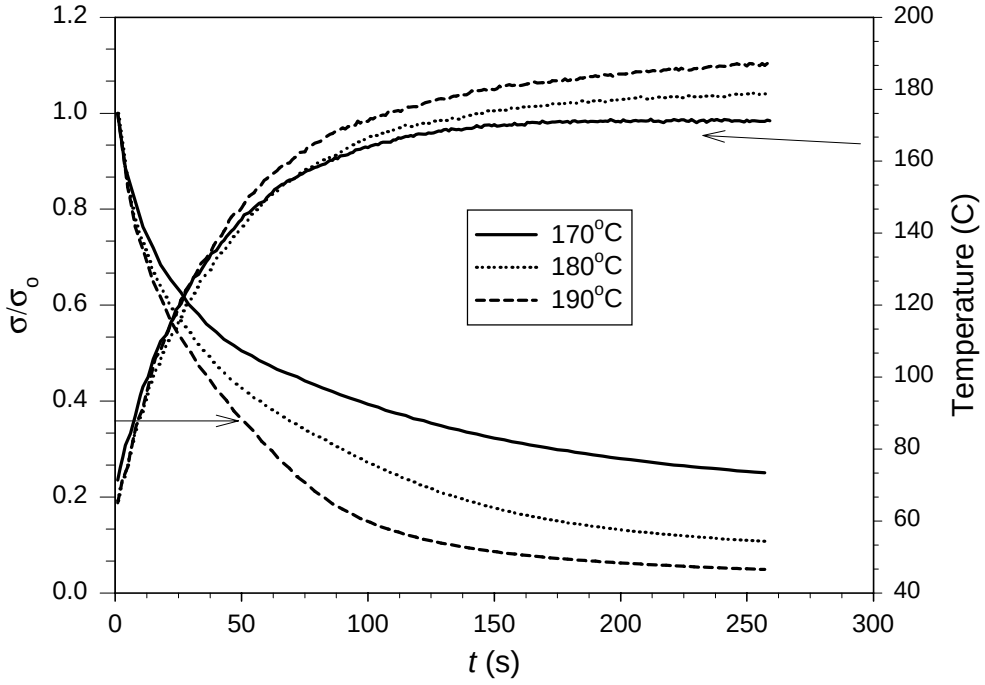

Figure 3.12a. Comparison of the stress relaxation response of varying platen temperatures for 50% PP panels pressed to a 65 lb/ft^3 density.

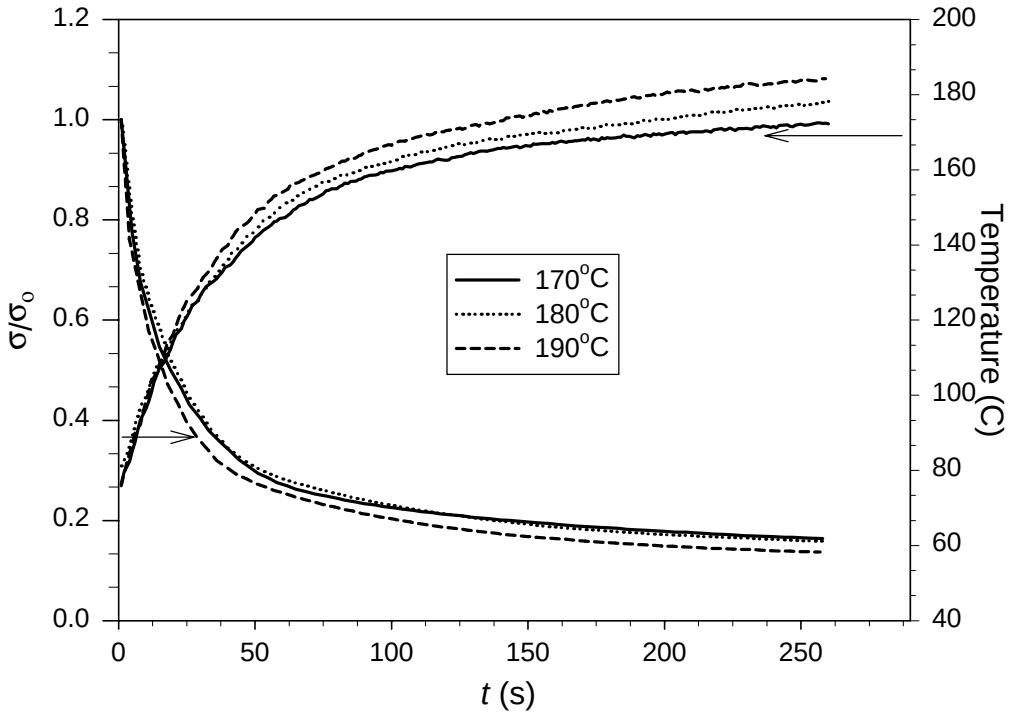

Figure 3.12a. Comparison of the stress relaxation response of varying platen temperatures for 0% PP panels pressed to a 65 lb/ft^3 density.

The spectral analysis indicated a higher concentration of relaxation behavior with an increase in temperature, which was also enhanced with a higher level of PP (Figure 3.13). Wang and Winistorfer (2000) noted that the relaxation behavior had varying degrees of concentration throughout the vertical profile of a wood-strand mat during panel processing. In our mats, a profile is developed when the temperature is sufficient to cause a melt of the PP. Interpretation of DSC spectra indicate the melt for the PP component was found to be approximately 162°C, however the DMA results in Figure 3.14 show a rapid decrease in *E'* as temperatures exceed 120°C. This reduction in the modulus would cause the gradual increase in the relaxation spectrum prior to T_m.

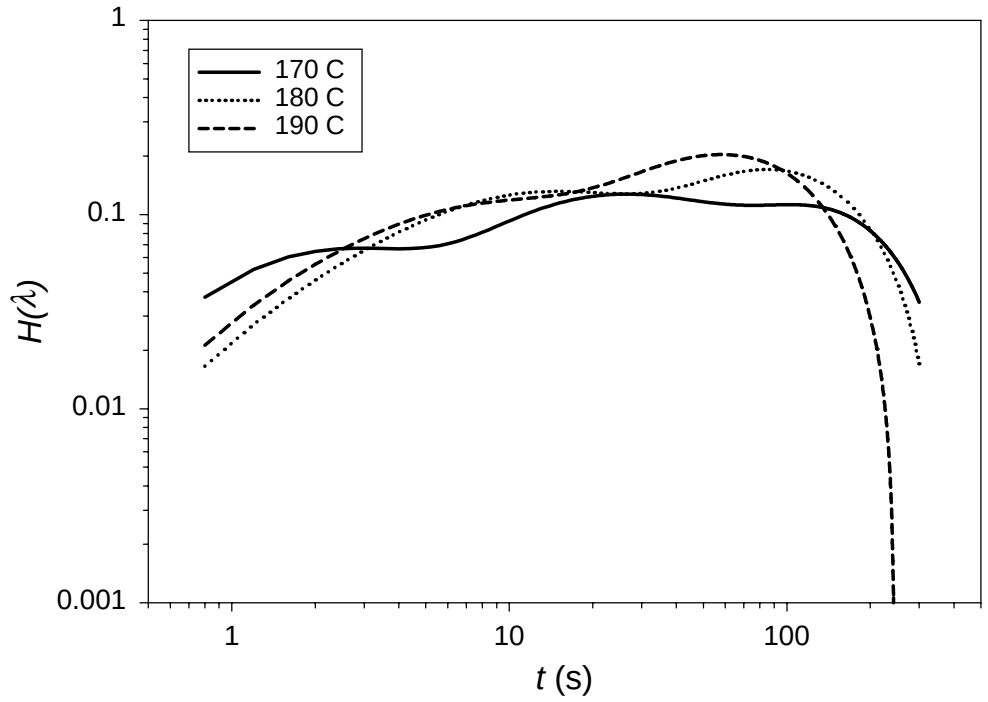

Figure 3.13. Relaxation spectra of 50%PP non-woven mats at varying platen temperatures pressed to a 65 lb/ft^3 density.

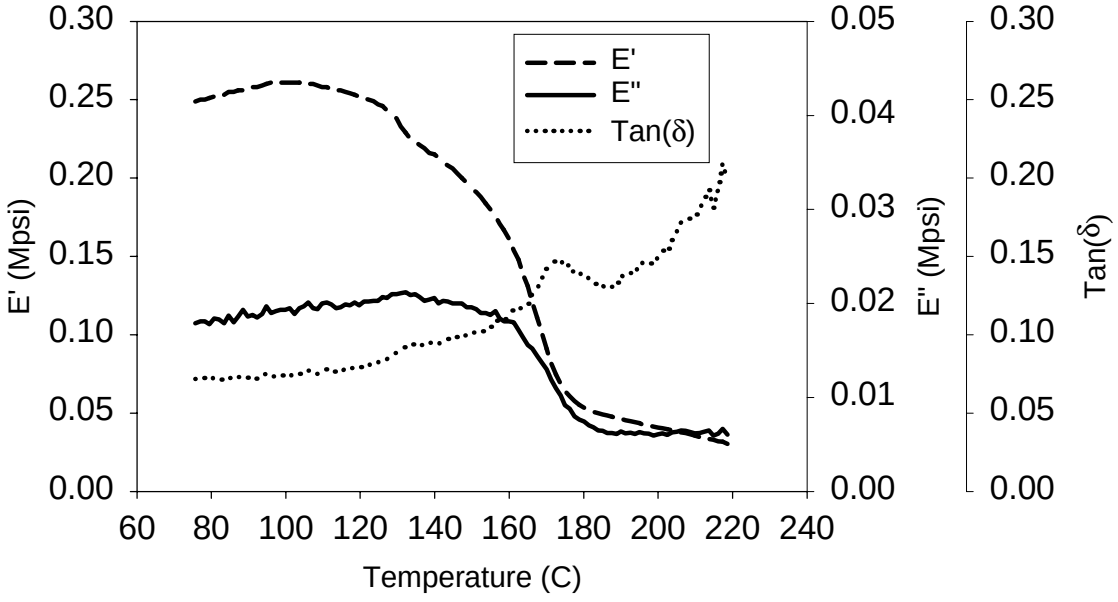

Figure 3.14. DMA plot for the 30%PP panel pressed to a 65 lb/ft^3 density.

Conclusion

The uniaxial stress response of a wood/PP fiber mat has been shown to vary with fluctuations in the material and processing variables. During compression to a final strain, the closing rate and the percentage level of PP influenced the stress-strain response. Higher strain rates resulted in increased compressive loads on panels made with PP fiber caused by the time-dependent behavior of the polymer. The mats with no PP developed higher initial loads at lower strains primarily from the higher bending modulus exhibited by wood fibers. Changes in the platen temperature did not influence the stress-strain response of any test material.

A spectrum analysis was utilized to describe the composite relaxation. The initial transient relaxation proved to be a function of the fiber network structure. Lubricated wood fibers showed a higher concentration of relaxation in the initial relaxation period. The latter stages of relaxation were dominated by the thermal transitions occurring within the viscoelastic components of the panel. The lignin and hemicelluloses within the wood exhibited a T_g, while the melt of PP was found to dominate the panels with higher PP levels.

Monitoring the relaxation of stress during processing can be beneficial to the quality of the final product. Suchsland (1967) and Adcock and Irle (1997) noted that the relaxation of wood composites is necessary to minimize expansion of the product after pressing. The relaxation spectrum can provide a method to monitor the stress-time response of wood-based composites and determine preferred pressing schedules.

References

Adcock, T. and M. Irle. 1997. The effect of compaction ratio on the dimensional recovery of wood particles pressed perpendicular to the grain. Proceedings from the 1st European Panel Products Symposium. 1:10-20.

Bolton, A.J., Humphrey, P.E. and P.K. Kavvouras. 1989. The hot pressing of dry-formed wood-based composites. part III. predicted vapor pressure and temperature variation with time, compared with experimental data for laboratory boards. Holzforschung 43:265-274.

Bodig, J and J.R. Goodman. 1973. Prediction of elastic parameters for wood. Wood Science 5(4):249-264.

Christensen, R.M. 1982. Theory of viscoelasticity, an introduction. Academic Press. New York.

Cowin, S.C. and J.W. Nunziato. 1983. Linear elastic materials with voids. Journal of Elasticity. 13:125-147.

Dai, C. and P.R. Steiner 1993. Compression behavior of randomly formed wood flake mats. Wood and Fiber Science. 25(4): 349-358.

Emri, I. and N.W. Tschoegl. 1995. Determination of mechanical spectra from experimental respnses. International Journal of Solid Structures. 32(6/7):817-826.

Gibson, L.J. and M.F. Ashby. 1988. Cellular solids: structure and properties. Pergamon Press. New York, NY.

Goldstein, I.S. 1973. Degradation and protection of wood from thermal attack. *In*: Wood deterioration and its prevention by preservative treatments. Vol 1 Degradation and protection of wood. D.D. Nicholas ed. Syracuse University Press. New York.

Ferry, J.D. 1980. Viscoelastic properties of polymers. John Wiley and Sons, Inc. New York.

Humphrey, P.E. 1991. Pressing issues in panel manufacture: internal behavior during pressing and its impact on time minimization, properties and profit. Proceedings of the 25th International Particleboard/Composite Materials Symposium. Washington State University. Pullman, WA. 25:99-108.

Jones, R.L. 1963. The effect of fiber structural properties on compression response of fiber beds. Tappi 46(1):20-27.

Kamke, F.A. and L.J. Casey. 1988a. Gas pressure and temperature in the mat during flakeboard manufacture. Forest Products Journal 38(3):41-43.

Kamke, F.A. and L.J. Casey. 1988b. Fundamentals of flakeboard manufacture: internal-mat conditions. Forest Products Journal 38(6):38-44.

Lang, E.M. and M.P. Wolcott. 1996a. A model for viscoelastic consolidation of wood-strand mats. Part 1. Structural characterization of the mat via monte carlo simulation. Wood and Fiber Science 28(1):100-109.

Lang, E.M. and M.P. Wolcott. 1996b. A model for viscoelastic consolidation of wood-strand mats. Part II. Static stress-strain behavior of the mat. Wood and Fiber Science 28(3):369-379.

Mark, R.E. 1967. Cell wall mechanics of tracheids. Yale University Press. New Haven, CT.

Neter, J., Wasserman, W. and M.H. Kutner. 1990. Applied linear statistical models – regression, analysis of variance, and experimental designs 3rd ed. Irwin, Homewood, IL.

Sperling, L.H. 1992. Introduction to physical polymer science, 2nd edition. John Wiley and Sons. New York, NY.

Suchsland, O. 1967. Behavior of a particleboard mat during the press cycle. Forest Products Journal 17(2):51-57.

Suo, S. and J.L Bowyer. 1994. Simulation modeling of particleboard density profile. Wood and Fiber Science 26(3):397-411.

Strickler, M.D. 1959. Effect of press cycles and moisture content on properties of douglas-fir flakeboard. Forest Products Journal 9(7):203-215.

Thömen, H. 2000. Modeling the physical processes in natural fiber composites during batch and continuous pressing. Ph.D. Dissertation, Oregon State University, Corvallis, OR.

Tschoegl, N.M. 1981. The theory of linear viscoelastic behavior. Academic Press. New York

Tschoegl, N.M. 1989. The phenomenological theory of linear viscoelastic behavior. Springer-Verlag. New York.

Umeya, K. and R. Hara. 1978. Rheological studies of compaction for polystyrene powder. Polymer Engineering and Science 18(5):366-371.

Umeya, K. and R. Hara. 1980. On the rheology of packed polymer powders. Polymer Engineering and Science 20(12):778-782.

Wang, S. and P.M. Winistorfer. 2000. Fundamentals of vertical density profile formation in wood composites. part II. methodology of vertical density formation under dynamic conditions. Wood and Fiber Science 32(2):220-238.

Wolcott, M.P. 1989. Modeling viscoelastic cellular materials for the pressing of wood composites. Ph.D. Dissertation, Virginia Polytechnic Institute and State University, Blacksburg, VA.

Wolcott, M.P., Kamke, F.A. and D.A. Dillard. 1990. Fundamentals of flakeboard manufacture: viscoelastic behavior of the wood component. Wood and Fiber Science 22(4):345-361.

Chapter 4

The Friction of Wood-Based Composites

Abstract

The manufacture of wood/thermoplastic composites utilizing continuous techniques, requires knowledge of the composites frictional properties. The frictional properties of polymers are found to be influenced by many processing variables such as; normal stress, temperature, sliding velocity and moisture. The coefficient of dynamic friction (μ_k) was determined for wood/polypropylene (PP) fibrous composites at varying amounts of wood, applied normal stresses, temperatures, and dwell times. The results found that the μ_k was decreased when the applied normal stress and dwell time were increased. An increase in μ_k was observed when the wood content and temperature were increased. The normal stress appeared to have the greatest influence and had a semi-logarithmic relationship with μ_k. The mechanism of friction was assumed to be through adhesion. Therefore, the area of contact and the interfacial shear stress played an important role in the frictional properties. Utilizing the independent variables, a multiple linear regression was developed through stepwise procedures to estimate the μ_k exposed to the various processing parameters.

Introduction

Wood plastic composites (WPC's) can be manufactured in continuous processes such as; extrusion and pultrusion, where the material is pushed or pulled through a

stationary die. During these processes, the material frictional properties play an important role in the conveyance of the composite through the die. In extrusion, friction is a primary mechanism for the transport of material through the die, while in a pultrusion process, friction creates resistance to the applied pulling load.

Much of the research with thermoplastic polymers has found that the frictional properties will be influenced by temperature, applied normal force, and sliding velocity (Bowden and Tabor 1964, Bahadur and Ludema 1971, Spalding et al. 1993, Benabdallah 1993, Benabdallah 1997). When dealing with wood, the moisture content, extractives, grain orientation, and applied normal load have been found to alter the frictional properties (McKenzie and Karpovich 1968, McMillin et al. 1970a, McMillin et al. 1970b, Lemoine et al. 1970, and Bejo and Lang 2000). Although research has been performed on wood and thermoplastics individually, little or no literature has addressed the frictional properties of a wood/thermoplastic composite during a continuous manufacturing process.

Friction of most materials can be classified into two categories; dry (Couulomb) or fluid. In fluid friction the two contacting surfaces are separated by a fluid layer, while dry friction results in the absence of any lubricating layer (Hibbeler 1998). The most common description of a materials frictional properties is through the coefficient of friction (μ_k). Theμ_k is the ratio of the frictional force (F_f) to the applied normal load (N) (Eq. 4.1). Throughout this paper, the μ_k will be considered dynamic to represent the movement of material against the contact surface during processing.

$$\mu_k = \frac{F_f}{N} \qquad \text{Eq. 4.1}$$

The mechanisms of polymer friction, including wood, can be attributed to the adhesion of the polymer to the contact surface (Bowden and Tabor 1964). In adhesion theory, the material creates a bonding layer to the contact surface, where a tangential frictional force (F_f) develops from the shear stress (τ) of the bond interface over the area of contact ($A\phi$) (Eq. 4.2), where A is the area and ϕ is the fractional area in contact with the surface, which is related to the surface roughness (Hwang and McKelvey 1989). The normal applied load (N) is simply the product of the compressive stress (σ) and apparent area of the material (A) (Eq. 4.3). Inserting Eq.'s 4.2 and 4.3 into Eq.4.1 yields the following relationship in Eq. 4.4.

$$F_f = \tau A \phi \qquad \text{Eq. 4.2}$$

$$N = \sigma A \qquad \text{Eq. 4.3}$$

$$\mu_k = \frac{\tau \phi}{\sigma} \qquad \text{Eq. 4.4}$$

With polymers, the classification of friction is complicated by the viscoelastic nature of the material. Barteneve and El'kin (1967) divided the friction of polymer-metal interface into three regions based upon temperature; 1) below the glass transition temperature (T_g), 2) above T_g, and 3) beyond the melt temperature (T_m) of the polymer. At temperatures below T_g, the polymer behaves similar to metal-metal friction where temperature has little influence on μ_k. As the temperature exceeds T_g to a rubbery phase, the μ_k is increased based on its ability to conform with the minute structure of the metal surface. At this temperature range, the shear stress of the polymer is greater than the interfacial bond between the polymer and metal. As the temperature begins to increase,

the shear stress of the polymer weakens and becomes lower than the adhesive interfacial stress. Above the melt of a crystalline polymer (T_m), the viscous drag instead of friction may be governing the lateral resistance of the solid material (Hwang and McKelvey 1989).

An underlying problem in calculating the μ_k of a contact system results from the inability to accurately determine ϕ. Measuring the actual area of contact is difficult because of the inherent surface roughness and asperities of the two contacting surfaces. Further complications arise from the rheological properties of a polymer, which alters the value of ϕ when the polymer is exposed to changes in the temperature and/or normal load (Bowden and Tabor 1964). In an extrusion or pultrusion operation, the barrel temperatures are high enough to melt the thermoplastic and therefore any friction analysis of a wood/thermoplastic system must take into consideration the viscous state of the polymer.

The effect temperature plays on the frictional properties of polymers during an extrusion process was examined by Hwang and McKelvey (1989). Adhesive bonds form, break and reform as the polymer slides across the contacting surface. As the temperature increases, the bonds can reform more quickly and the area of contact increase, resulting in a higher μ_k. However, the temperature can also reduce τ causing a cohesive failure and a decrease in μ_k. Of the solid polymers tested by Hwang and McKelvey (1989), a general decrease in μ_k was found with an increasing temperature. Similar results were found when Spalding et al. (1993) determined the frictional properties of low density polyethylene.

The role of temperature on the frictional properties of wood has had little research exposure . McMillan et al. (1970a.) noted a decreasing μ_k for spruce pine when the temperature of the contacting, polished steel plate increased from 24 - 108°C. This temperature range falls short of the temperatures utilized in most wood-based composite processing. Although there has been minimal research on the frictional properties of wood, another similar area of interest in the wood composites field is the adhesion abilities of wood. Surface inactivation has been determined to be the reason for poor glue bonds of wood dried at elevated temperatures (Troughton and Chow 1971, Chow 1971, Chow 1971). The oxidation and/or pyrolysis of the wood components resulted in poor glue bonds that were accentuated by increased temperatures and exposure times (Chow 1971). Since the friction of polymers can be explained through adhesion theory, one could surmise a change in μ_k would result due to higher temperatures and exposure dwell time.

The effect N on the frictional properties of thermoplastics has been investigated extensively (Bowden and Tabor 1964, Bartenev and Larentev 1981, Spalding et al. 1993, Hwang and McKelvey 1989, Benabdallah 1993, Benabdallah 1997, Schelling et al. 1991), and to a limited extent with wood (McKenzie and Karpovich 1968 and Bejo et al 2000). The general trend seen by a majority of the research with both thermoplastics and wood identifies a decrease in μ_k as N increases. The justification for the influence of load can be based upon the nonlinear relationship that must occur with τ,ϕ, and N. In Eq. 4.4, an increase in μ_k would occur if the contact area and/or τ increased. As more pressure is applied to the specimen, a higher contact are will result from deformation and ϕ will eventually converge to unity. Bowden and Tabor (1964) noted that τ will also increase to

some degree as the applied load is increased. However, a nonlinear relationship must exist within the $\tau\phi$ and N in order for load to influence μ_k.

Theoretical models have been developed to describe polymer friction and are usually based on molecular attributes. Application of these models can be cumbersome and are generally specific to one underlying condition (Bartenev and Lavrentev 1981), therefore, empirical models are commonly used to estimate the μ_k of a contact system where many variables are considered.

Objectives

The goal of this paper is to characterize the influence of processing parameters on the frictional properties of a wood/thermoplastic fiber composite. The specific objectives are:

1) Determine the coefficient of dynamic friction (μ_k) of a wood/polypropylene(PP) fiber composite exposed to varying platen temperatures, applied normal loads and dwell times.
2) Apply a multiple linear regression analysis to empirically determine the μ_k at the various processing conditions.

Experimental Procedures

The frictional force of a wood/PP fiber mat was determined using the testing protocol found in ASTM D 2394, with some additions and modifications. Two test specimens, measuring 2.5 x 4 in., were compressed between 3 x 6 in. heated steel platens and the 2.5 x 4 in. pulling block (Figure 4.1). The pulling block was adhered with 3/16 in. thick virgin grade leather on both sides to create a non-slip surface. The block was

pulled with a screw driven universal testing apparatus at a constant rate of 3 in./min. The heated platens were mounted in a servo-hydraulic universal testing apparatus.

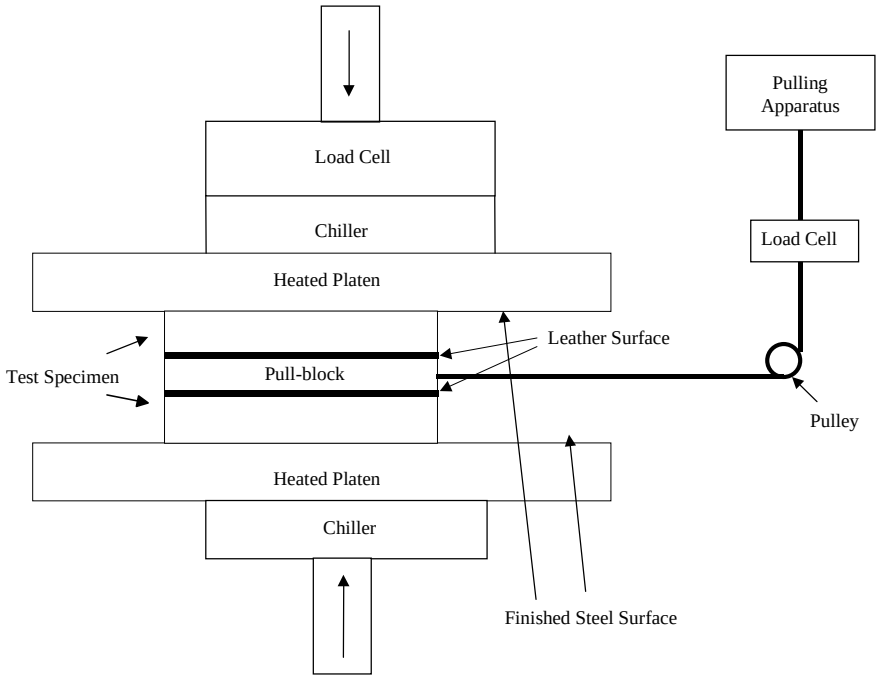

Figure 4.1. Friction test diagram for the double-sided specimen.

The normal load applied by the hydraulic test apparatus was operated in load control to account for the relaxation of the material. As the specimen was pulled across the platen surface, the frictional force was measured by a load cell placed in series with the screw-driven test apparatus. The load required to pull the specimen at a constant velocity divided by the applied normal load was recorded as μ_k.

The test specimens were exposed to various platen temperatures, normal loads, and dwell times. Normal loads were 440, 1,100 and 1760 psi for the wood/PP fiber mats. Platen temperatures were 170, 180, and 190°C and the dwell time, or the time under

which the specimen was exposed to the normal stress before pulling, was 1, 60 and 180 seconds. A sample size of 5 specimens were tested for each group.

Results and Discussion

All of the test parameters were found to have a significant effect on the μ_k of the wood/PP fiber mat. Using SAS® statistical software, an ANOVA procedure identified significance among the μ_k for all independent variables and their interactions. Over all test levels, a general decrease in μ_k was found when the stress, dwell time, and PP level increased, while an increase in μ_k was observed at higher temperatures. The influence temperature and dwell time on the friction was observed to be less dramatic as with the change in PP level and with stress.

The applied normal stress greatly influenced the behavior of μ_k. The graph in Figure 4.2 displays the substantial decrease in μ_k as the stress is increased from 440 to 1,760 psi. As the level of wood in the mat decreased, a more logarithmic relationship developed as seen in Figure 4.3, similar to the results with wood (Bejo et al. 2000) and thermoplastics.

Much of the polymer friction literature attributes the change in μ_k with increasing stress to the nonlinear relationship between τA and normal stress. Hwang and McKelvey (1989) found this nonlinear relationship with PP as they increased normal stress from 123 to 1852 psi. At similar temperatures the μ_k dropped from a range of 0.10-0.14 to 0.06-0.08 with an increase in pressure. The lower μ_k values found with the wood/PP fiber mats could be attributed to the surface roughness.

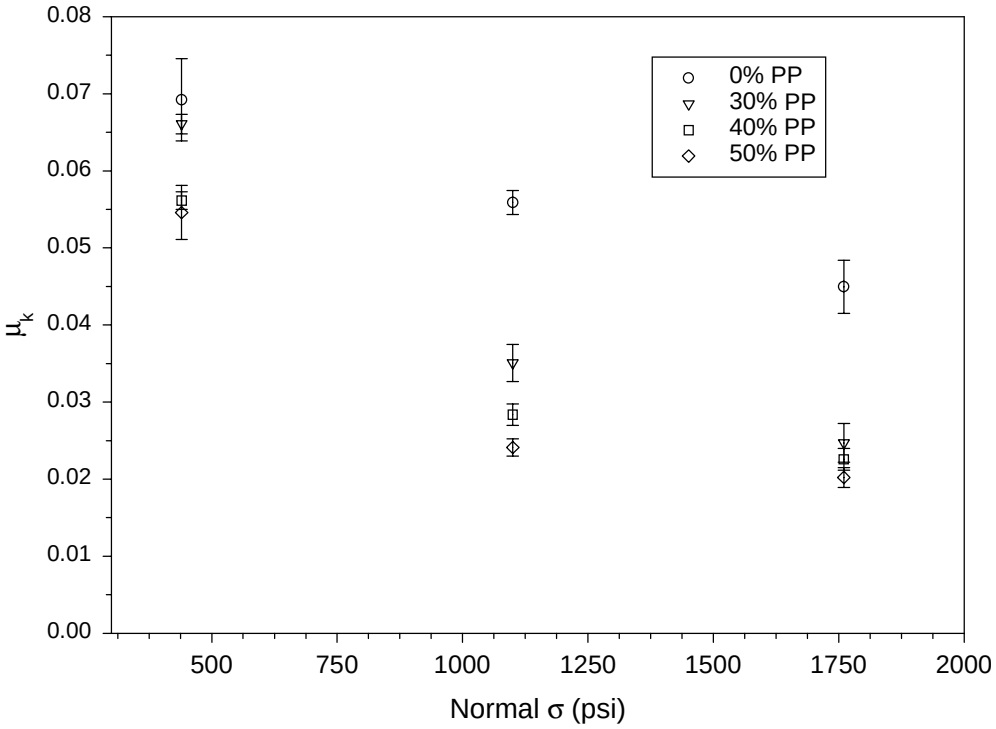

Figure 4.2. Influence of normal load on the μ_k of non-woven mats at a platen temperature of 190°C and a 60 s dwell time.

The influence of temperature on PP will generally cause a decrease in μ_k as noted by the work by Hwang and McKelvey (1989). However, a slight increase in μ_k with increasing temperature was found with the wood/PP fiber composites. This increase in μ_k results because of the increase in contact area. At higher temperatures the PP will melt and the wood will soften more extensively. This would allow the constituent materials to fill the voids on the surface of the composite, thus increasing the contact area and causing a higher μ_k. The effect of temperature was found to be more pronounced in the specimens exposed to the lower normal stress of 440 psi (Figure 4.4), however at higher stress levels of 1,100 and 1,760 psi the influence of temperature was very limited.

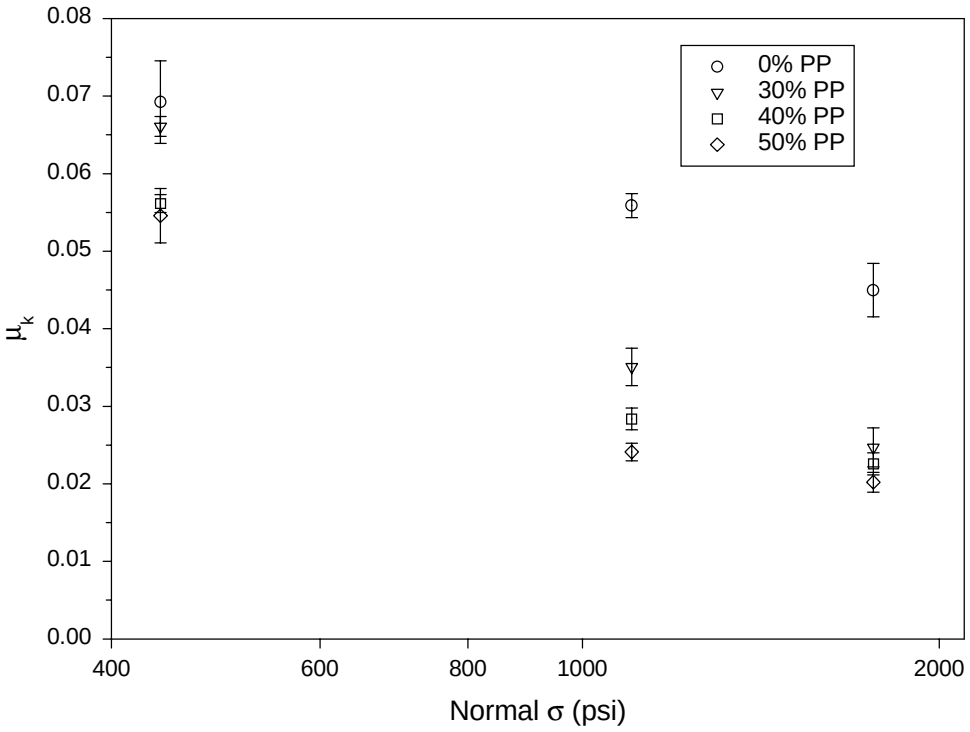

Figure 4.3. Semi-logarithmic relationship of normal load and μ_k for non-woven mats at a platen temperature of 190°C and a 60 s dwell time.

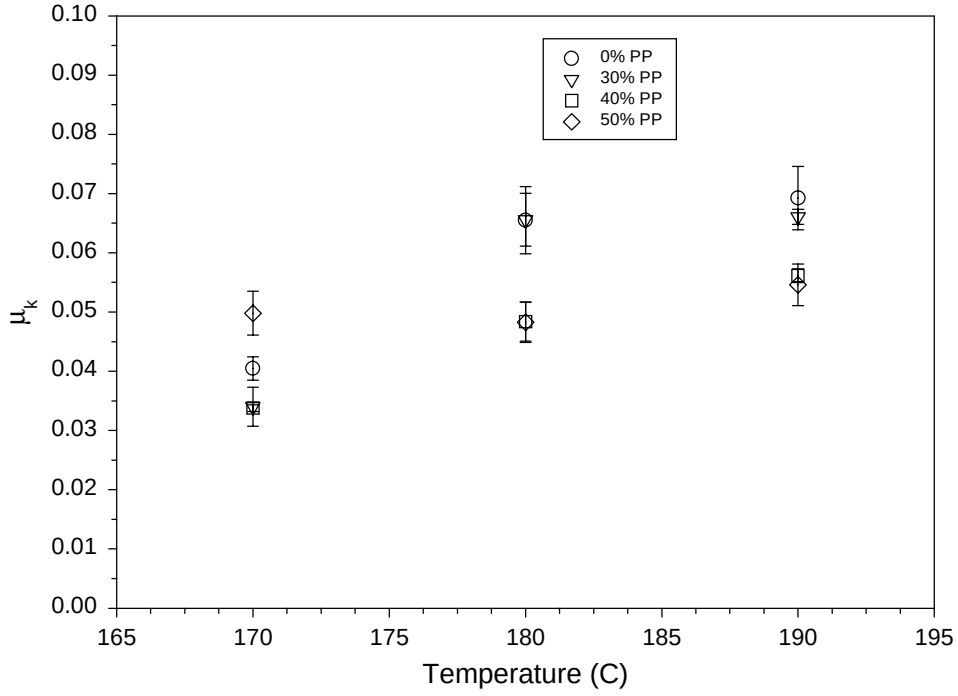

Figure 4.4. Relationship between temperature and μ_k for non-woven mats under 440 psi at a 60 s dwell time.

As the percentage of PP increased in the fiber composite mat, a decrease in the μ_k observed (Figure 4.5). This is in part due to the lower μ_k for PP when compared to that of wood. Hwang and McKelvey (1989) plotted the μ_k for PP between 0.06 and 0.08 over the same temperature range and pressures. Gang et al. (1995) observed a lower μ_k for melted PP in the range of 0.01 to 0.03. McMillin et al. (1970a) tested spruce pine on a steel plate at 107°C and observed a μ_k between 0.099 and 0.131, varying with grain orientation at minimal pressure. Further graphical plots of the influence normal σ, dwell time and temperature have on the varying PP mats can be seen in Appendices C, D, and E.

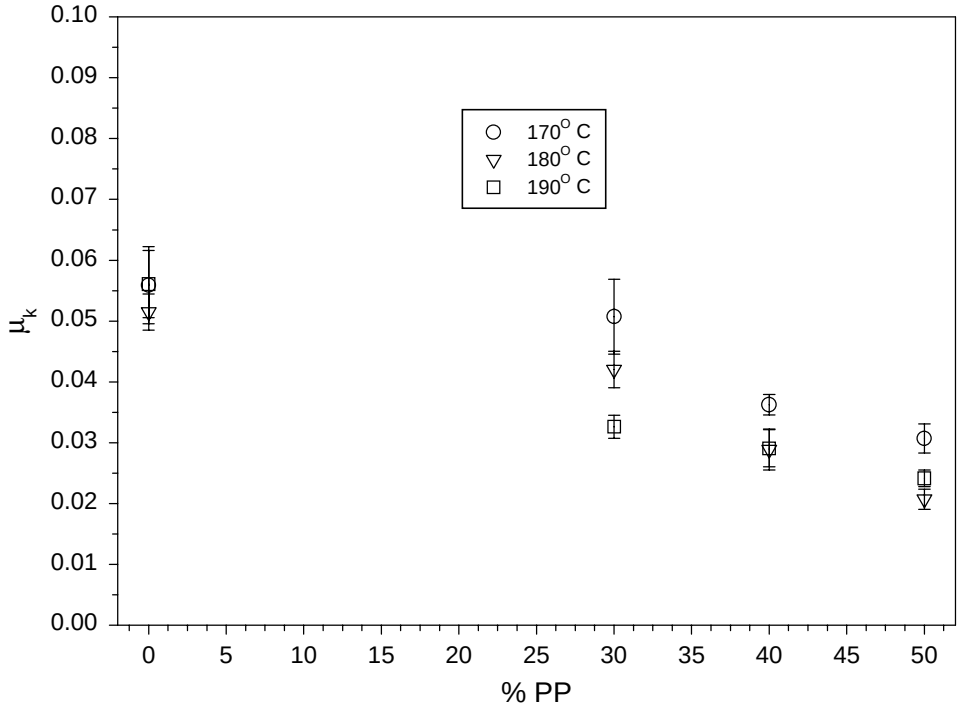

Figure 4.5. Relationship between percentage of PP and μ_k for non-woven mats under 1,100 psi at a 180 s dwell time at varying temperatures.

Estimate of μ_k

A multiple semi-logarithmic regression model was utilized to estimate the dynamic friction of the wood/PP mat under the four test conditions; wood percentage (wood), platen temperature (temp), normal stress (stress), and exposure or dwell time (dwell). The model for the non-interactive regression analysis is shown in Eq.4.5, where the β_i's are the parameters to be estimated and ε is the error term. The logarithmic value of stress was utilized. base upon the better fit to μ_k.

$$\mu_k = \beta_o + \beta_1 wood + \beta_2 temp + \beta_3 \log(stress) + \beta_4 dwell + \varepsilon \qquad \text{Eq. 4.5}$$

The fit of the regression model had a coefficient of determination (r^2) of 0.67, utilizing the four parameters (Figure 4.6). Parameter estimates are given in Table 4.1. A Stepwise (SAS®) procedure was utilized to determine the best fit for the regression model. The Stepwise procedure determines the addition of an independent variable to the model through the significance of the F statistic. If the independent variable is above the predetermined acceptance level, than the variable is included in the model. For the determination of μ_k, all the independent variables were added to the model at a significance level of 0.15.

Conclusion

The frictional properties of a wood plastic composite are subject to change when exposed to the various conditions found in an extrusion or pultrusion process. The μ_k of a wood/PP composite can be influenced by temperature, normal stress, dwell time, and the level of PP. The effect these parameters have on the composite, dictate the conveyance of the material through the processing die.

Table 4.1. Parameter estimates for the multiple regression model to determine the μ_k for a wood/PP fiber mat.

Independent Variable	Parameter Estimate	Standard Error
B_1 – *Wood* (100,70,60, & 50%)	0.000348	0.0000200
B_2 – *Temp* (190, 180, & 170°C)	0.000182	0.0000458
B_3 – *Stress* (1760, 1100, & 440 psi)	-.0414	.00150
B_4 – *Dwell* (180, 60, & 1 s)	-.0000264	0.00000502
B_0 - Intercept	0.108	0.00949

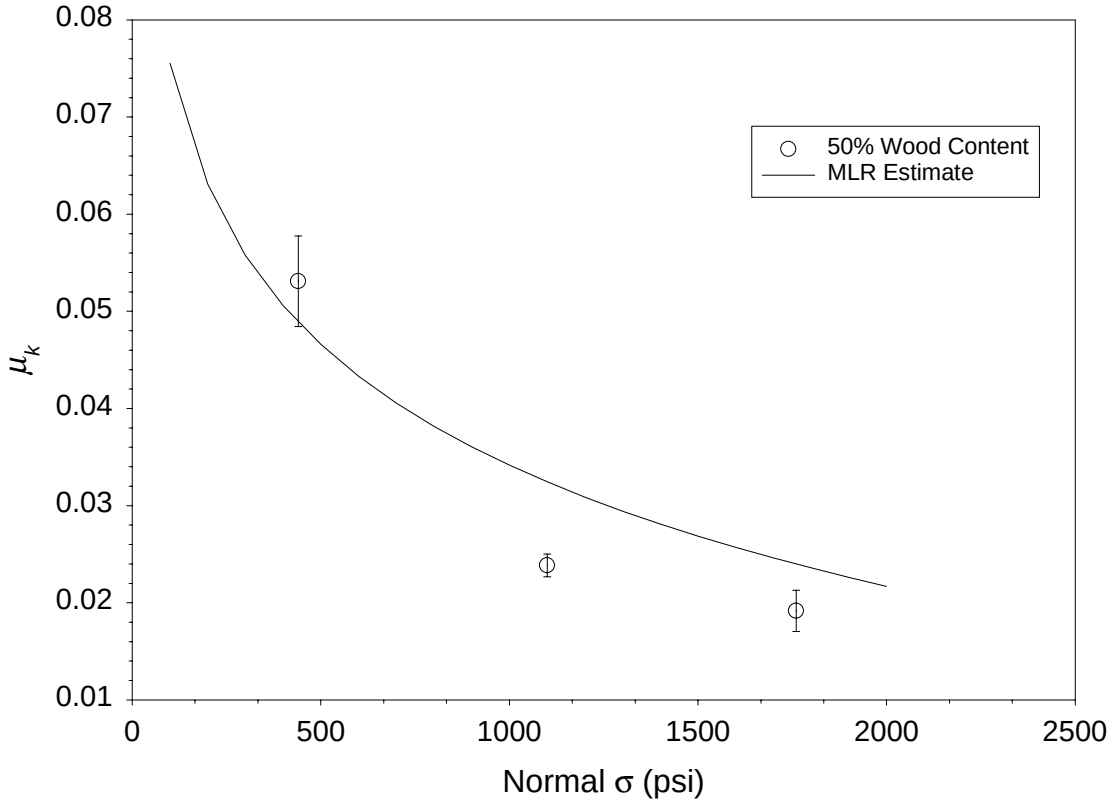

Figure 4.6. Estimate of μ_k for 50% wood non-woven mats at a platen temperature of 180°C and a dwell time of 1s.

The normal stress and μ_k relationship exhibited a decreasing semi-logarithmic behavior and had the greatest effect on the frictional properties of the wood/PP composite. This behavior may have been a result of nonlinear relationship between interfacial shear stress and the applied normal load. As the dwell time increased, a decrease in the μ_k was also observed, but at a smaller degree. An increase in μ_k was found when the amount of wood fiber and temperature was increased. The increase in friction with increasing wood, can be associated with the slightly higher μ_k of wood compared to that of PP. Temperature normally decreases μ_k for solid polymers, however as the polymer melts in a wood/PP system the flow of PP to the surface increases the contact area of surfaces.

Utilizing multiple linear regression techniques, the μ_k or a wood/PP fibrous composite exposed to the change in processing variables can be estimated. The regression showed a reasonable fit with the experimental data having a $r^2 = 0.67$ with all of the parameters included. Although empirical, the multiple linear regression technique can aid in modeling a continuous process system.

References

Bartenev, G.M. and A.I. El'kin. 1967. Nature and mechanism of friction of rubberlike polymers in different physical states. Polymer Mechanics 3(1):123-135.

Bahadur, S. and K.C. Ludema. 1971. The viscoelastic nature of the sliding friction of polyethylene, polypropylene and copolymers. Wear 18:109-128.

Bejo, L., Lang, E.M. 2000. Friction coefficients of wood-based structural composites. Forest Products Journal 50(3):39-43.

Benabdallah, H.S. 1993. The running-in and steady-state coefficient of friction of some engineering thermoplastics. Polymer and Engineering Science. 33(2):70-74.

Benabdallah, H.S. 1997. Reciprocating sliding friction and contact stress of some thermoplastics against steel. Journal of Materials Science 32(19):5069-5083.

Bowden, F.P. and D. Tabor. 1964. The friction and lubrication of solids, part II. Oxford University Press. New York, NY.

Chow, C.Z. 1970. Infared spectral characteristics and surface inactivation of wood at high temperatures. Wood Science and Technology. 5:27-30.

Gang, H.G., Cuculo, J.A., Nam, S., and D.H. Crater. 1995. Frictional properties of polyolefins treated with fluoroelastomer processing aids. Journal of Applied Polymer Science. 55:1465-1476.

Hibbeler, R.C. 1998. Engineering mechanics – statics. Prentice –Hall, Inc. Upper Saddle River, NJ.

Hwang, C.G. and J.M McKelvey. 1989. Solid bed compaction and frictional drag during melting in a simulated plasticating extruder. Advances in Polymer Technology 9(3):227-251.

Lemoine, T.J., McMillin, C.W., and F.G. Manwiller. 1970. Wood variables affecting the friction coefficient of spruce pine on steel. Wood Science 2(3):144-148.

McKenzie, W.M. and H. Karpovich. 1968. The frictional behavior of wood. Wood Science and Technology 2:138-152.

McMillan, C.W., Lemoine, T.J. and F.G Manwiller. 1970a. Friction coefficient of oven-dry spruce pine on steel, as related to temperature and wood properties. Wood and Fiber 2(1):6-11.

McMillan, C.W., Lemoine, T.J. and F.G Manwiller. 1970b. Friction coefficient of spruce pine on steel - a note on lubricants. Wood Science 3(2):100-101

Nelson, S. 1997a Structural composite lumber. *In:* Engineered Wood Products: A Guide for Specifiers, Designers and Users. Smulski, S. ed. PFS Research Foundation. pp 147-172.

Spalding, M.A., Kirkpatrick, D.E, and K.S. Hyun. 1993. Coefficients of dynamic friction for low density polyethylene. Polymer Engineering and Science 33(7):423-430.

Troughton, G.E. and S.Z. Chow. 1971. Migration of fatty acids to white spruce veneer surface during drying: relevance to theories of inactivation. Wood Science 3(3):129-133.

Chapter 5

Pultrusion Of Wood-Based Composites

Abstract

The onset of wood/thermoplastic composites has initiated new methods of manufacturing in the wood composites industry. Polymer manufacturing techniques such as; extrusion, injection molding, and pultrusion differ from traditional wood composite process in that they require an understanding of the materials ability to flow through a stationary die. The pultrusion process is commonly utilized in the polymer industry to produce high strength, unique profiles, and a continuous geometry, however the wood industry has had little exposure to this process. The high loads associated with pulling a solid wood matrix through a stationary die may cause failure with the composite during manufacture, therefore, a model was developed to estimate the pulling load for a wood-based composite system. The model accumulates the pulling resistance resulting from the consolidation within the entrance section of the die and through the friction developed throughout the entire die. A lab-scaled pultrusion operation provided experimental data on a non-woven wood and wood/polypropylene(PP) mats at various die temperatures and PP content. The model and experimental results showed good agreement with all PP levels processed at the lowest temperature of 170°C. However, as the processing temperature increased, the model over-predicted the total pulling load. The deviation from the model results may have developed from the ductile “necking” of the composite,

which reduced the cross-sectional area and minimized the effect of friction, thus reducing the experimental load.

Introduction

The recent interest in wood/thermoplastic composites has brought about change in the type of production methods. The most common method of manufacture the wood thermoplastic composites is through extrusion and to a limited extent, injection molding. Both of these methods utilize a screw or plunger to push the composite material through a stationary die. Wood particles and flours are commingled with thermoplastics to produce many exterior use products utilizing these methods.

Another method, which pulls the material through a profiled die, is pultrusion. Pultrusion has had minimal exposure in the wood industry, however, it is commonly used in the polymer industry to produce high stiffness composites with continuous profiles. Products manufactured using polymer pultrusion are generally comprised of synthetic fiber tows, mats or weaves, which are impregnated with thermosetting adhesives. A wood-based pultrusion system varies from traditional methods in that the initial state of the composite material is solid, rather than a viscous liquid..

With the fluid matrix and high strength of traditional pultrusion products, pulling force models have had minimal exposure when utilizing thermoset resins. A model by Moschiar et al. (1996), neglected the consolidation effects to the pulling load and considered only the friction and viscous drag to influence the resistance. While Kim et al. (1997) and Batch and Macosko (1987) estimated the pulling load through fluid flow pressure developed at the infeed and through viscous and frictional resistance. The

neglect of consolidation by Moschiar et al. (1996), is due primarily to the relatively small tapered section commonly associated with the use of low viscosity resins in pultrusion.

Recent work with thermoplastic pultrusion has begun to address the pulling load associated with higher viscosity resins (Tso et al. 1993, Astrom and Pipes 1993a, Lee et al. 1991, and Blaurock and Mitchell 1997). For thermoplastic pultrusion, the entrance or tapered region is significantly larger than with thermoset pultrusion (Astrom et al. 1991). Their models address the consolidation, friction and viscous resistance within a thermoplastic pultrusion die. Similar to thermoset matrices, the consolidation of a thermoplastic system during the tapered die region was based upon pressure gradients developed with the fluid flow of a melted resin.

Incorporating a wood-based system into a pultrusion process can be achieved by the use of non-woven fibrous mats. The non-woven mat industry utilizes a wide range of natural and synthetic fibers, which are incorporated into a variety of products. , The invention developed by Beall (1991) describes a pultrusion method utilizing a cellulosic non-woven fiber mat, which is enveloped within a resin matrix. The primary purpose of the fiber mat was to assist in the even distribution of resin throughout the profile of the composite.

For the wood-based pultrusion system, a non-woven wood and wood/thermoplastic fiber mat is utilized as the primary matrix component. The pultrusion die is similar to the die geometry that is commonly utilized with a thermoplastic matrix, where a large tapered entrance and a cooling section are present (Figure 1.1). During the infeed process the mats maintain integrity, however, the use of

continuous synthetic reinforcement is required due to the high loads developed with a solid matrix.

The high loads developed within this process can be attributed to the solid mechanics behavior of the material system, where the consolidation and frictional forces are present. Consolidation and or frictional behavior of a non-woven wood and wood/thermoplastic fiber mat can be greatly influenced by many pultrusion processing parameters. In the second Chapter, the consolidation and ensuing relaxation of a wood and wood/thermoplastics fiber mat were modeled at varying thermoplastic levels (polypropylene (PP)), temperatures and densities. The same non-woven mat material was also subjected to friction tests and the coefficient of dynamic friction (μ_k) was found to change with temperature, normal pressure and exposure or dwell time (Chapter 4).

Objectives

The goals of this chapter are to establish a model based upon a solid mechanics approach, and to determine the pulling loads developed during a wood-based pultrusion system. Specific objectives are to;

1) To develop a pulling force model based upon the consolidation and frictional behavior of wood and wood/PP non-woven mats.

2) Compare the pulling force model results to experimental data obtained in a lab-scaled pultrusion process.

3) Utilize the model and experimental results to assess the important mechanisms, which influence the pulling resistance.

Model Development

The model incorporates a rectangular cross-section of a wood-based material, which is pultruded through a forming die with a linear entrance taper. The die is comprised of two sections, an entrance section where the material is consolidated to a final profile and a constant geometry section where the profile of the composite is held constant as the resins are cured (Figure 5.1). A cooling section is added on to the die to harden the thermoplastic, however, due to thermal contraction and a slightly increased cross-sectional dimension, little resistance is developed.

The forces in the entrance section develop from the consolidation (Px_{con}), Eq.5.1, and friction (Px_{frict}), Eq. 5.2, that result from the compressive stress (σ_c) developed as the composite is pulled through the tapered section (Figure 5.2). The total resistance (P_{ent}) in the entrance section will be a summation of the two components (Eq. 5.3). The load is doubled based on the contact between the top and bottom surfaces and the *x* is the direction in which the composite is pulled. An assumption for this model is that the edges of the composite along the die surface results in a minimal load accumulation and are neglected within the model.

$$Px_{con} = w\int_0^{L_e} \sigma_c \tan\theta \, dx \qquad \text{Eq. 5.1}$$

$$Px_{frict} = w\int_0^{L_e} \sigma_c \, \mu_k \, dx \qquad \text{Eq. 5.2}$$

where:

w - width of the composite
μ_k - dynamic coefficient of friction
θ - entrance angle

$$P_{ent} = 2(Px_{con} + Px_{frict}) \quad \text{Eq. 5.3}$$

As the composite enters the constant geometry (CG) section, the normal force will begin to decay as the compressive stress begins to relax (σ_r) at a constant strain. The total force for this section is due to friction along the die surface (Eq. 5.4). The total resistance to the applied load (P_{tot}) then becomes a summation of the forces developed in the entrance and constant geometry sections (Eq 5.5).

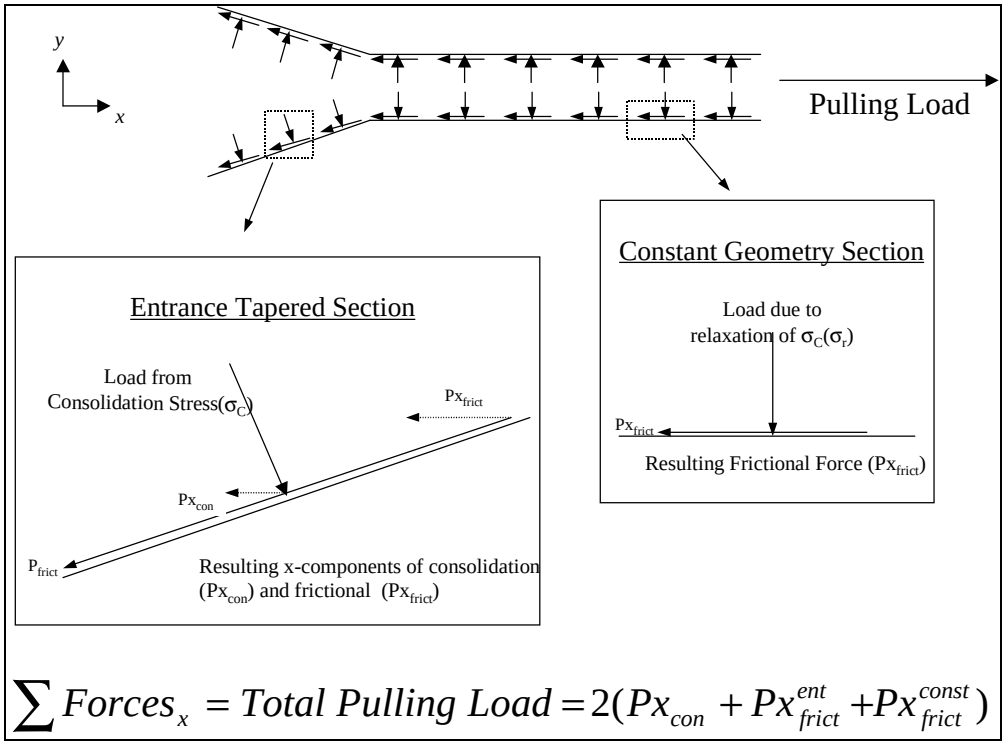

Figure 5.2. Schematic of forces in a pultrusion die design.

$$P_{const} = 2P_{frict} = w\int_0^L \sigma_r \mu_k dx \quad \text{Eq. 5.4}$$

$$P_{tot} = P_{ent} + P_{const} \quad \text{Eq. 5.5}$$

The stress developed during the uni-axial consolidation of a non-woven wood and wood/PP mat can be used to describe the mechanical response during the entrance and CG sections of the die. The descriptive equations to emulate the behavior of σ_c and σ_r are shown in Eqs. 5.6 and 5.7 , which were developed in Chapter 2. The σ_c can be described either with the strain (ε) or the relative density (ρ_R) of the composite mat. The ρ_R provides a more convenient method of determining the compressive stress.

$$\sigma_c = -\frac{e^B}{(A+1)}\left[\left(\frac{C_1}{\rho_R}\right)^{A+1} - 1\right] \qquad \text{Eq. 5.6}$$

$$\sigma_r(t) = \varepsilon_o \sum_{i=1}^{4} E(t)_i e^{-t/\lambda_i} \qquad \text{Eq. 5.7}$$

where:

C_1 – initial relative density

A,B – linear coefficients

ε_o – strain at final profile

$E(t)$ – relaxation modulus parameter

λ – relaxation time

The frictional response of a fibrous wood composite was found to vary with the changing conditions within a pultrusion process as shown in Chapter 4. An increase in the applied stress and exposure time decreased the coefficient of dynamic friction (μ_k), while an increase in temperature from 170 to 190°C caused a slight increase in μ_k. The authors utilized the following multiple linear regression to estimate the μ_k during the change of process parameters;

$$\mu_k = \beta_o + \beta_1 w + \beta_2 T + \beta_3 Log(\sigma) + \beta_4 dt$$ Eq. 5.8

where:

w – amount of wood fiber

T – die temperature

σ – either σ_c or σ_r, depending upon die location

dt – time exposed in die

β_i's – regression coefficients

Experimental Procedures

Pultrusion

A pultrusion die was fabricated with a linear entrance taper, a rectangular cross-section opening with a roller pulling mechanism (Figure 5.1). The entrance section of the die compresses the product to a 2.5 x 0.25 in. cross-section with a taper of 5° over a length of 8 in. The constant geometry section maintains the cross-sectional profile over a 12 in. length where the composite enters the cooling section. During cooling, the die opening increases to a 2.5 x 0.5 in. profile to eliminate any contribution of frictional resistance to the pulling load. The die surface was machined to a ground #32 finish. The pulling mechanism utilized consisted of a series of ten polyurethane covered rollers. The rollers were compressed on the top and bottom surface of the composite exiting the die. A variable speed motor developed the required torque to pull the composite through the die.

The materials utilized in the pultrusion process were non-woven wood and wood/PP mats and PP pre-impregnated carbon fiber (CFPP) tape (Baycomp® Uni Tape). The non-woven mats were cut into 2.5 in. strips and the CFPP tape remained the original width of 1.75 in. Two CFPP tapes and 3-5 non-woven mats, depending upon the mat

thickness, were used during pultrusion. Mats with 0, 30, 40 and 50% PP were transferred through the die with the CFPP tape. The mats were positioned within the profile so that the die surface was only in contact with the mats and not the CFPP. A target final mat density of 60-65 lb/ft^3 was maintained throughout all pultrusion runs. The mat density was determined by a weighted percentage of the non-woven mat and CFPP.

The pultrusion die rested upon rollers while the load was acquired in real time. Compression load cells were positioned at the end of the die (Figure 5.1) equally spaced above and below the exiting pultrudate. The total pulling resistance was recorded as a summation of the load from each load cell.

Model Calculation

The pulling forces in Eqs. 5.1,2, and 4 were integrated numerically. At discrete time intervals, the load was calculated from the contribution of friction and consolidation forces. The elements were then summed to determine the total pulling load.

An average composite density was calculated over the range of measured load and entered into the model. The density of the composite was based upon the die thickness at the out-feed to eliminate die swell effects commonly associated with thermoplastic processing. The change in density throughout the tapered section of the die was determined from the die geometry and pulling speed. As seen in Chapter 2, temperature was found to be have little influence on the stress-strain behavior of the various mat types, the linear coefficients *A* and *B*, were averaged for each PP level.

Density Adjustment

The stress developed during consolidation is dependent upon the density of the composite. In Chapter 2, the consolidation stress behavior of the the wood/PP mats was reported for 60, 65, and 70 lb/ft^3 densities. The predicted value of σ_c in Eq. 5.6 is based upon the density of the composite and no further adjustment is required if the density varies from the experimental data. However, the relaxation moduli (*E(t)*) in Eq. 5.7 are distinct to one density. Due to the inherent variability within the initial mat density of the non-woven mats, an adjustment of *E(t)* to varying densities is required.

In the log-log plot of the E(t) vs. relaxation time (λ), a similar trend is exhibited between the various densities of the wood and wood/PP composites during the relaxation of stress (Figures 5.3 and 5.4). Since the relaxation behavior appears to be offset only in magnitude between the densities, the following relationship is proposed in Eq 5.9.

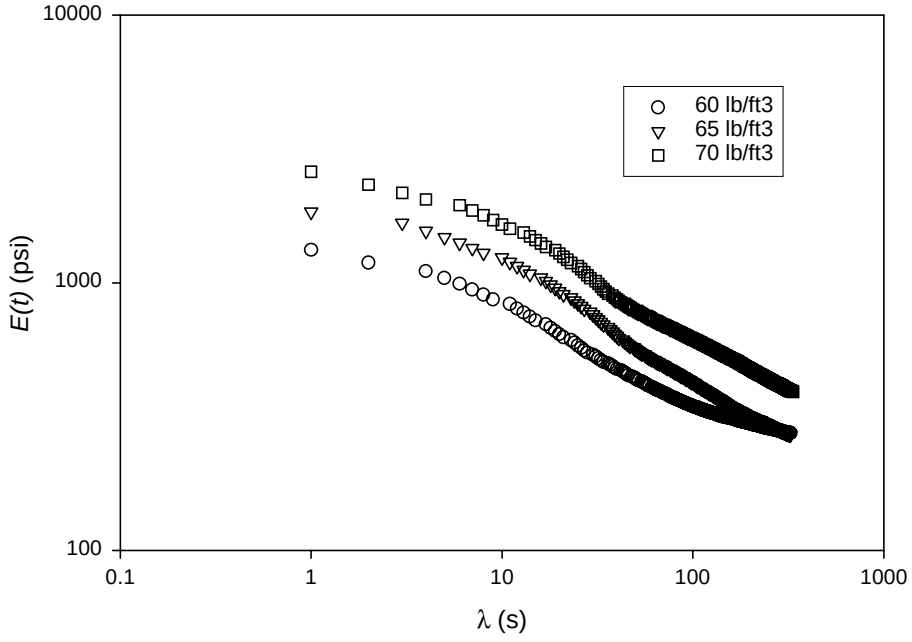

Figure 5.3. Log-log relationship for the relaxation moduli vs. time for varying densities of the 0%PP non-woven fiber mat at 180°C platen temperature.

$$\log E(t)_{\rho} = \log E(t)_{ref(\rho)} + c \qquad \text{Eq.5.9}$$

Where the relaxation moduli at any density within the range of study ($E(t)_{\rho}$) is related to a reference moduli ($E(t)_{ref(\rho)}$) by some constant (c). The calculation of $E(t)_{\rho}$ in Eq. 9 can then be simplified to the form in Eq. 10.

$$E(t)_{\rho} = E(t)_{ref(\rho)} 10^{c} \qquad \text{Eq. 5.10}$$

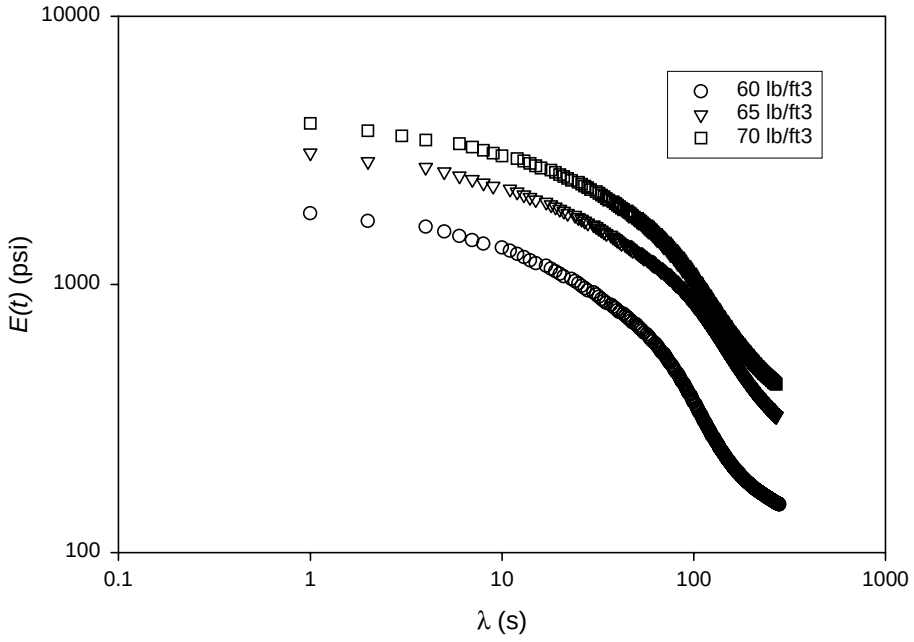

Figure 5.4. Log-log relationship for the relaxation moduli vs. time for varying densities of the 50%PP non-woven fiber mat at 180°C platen temperatures.

The constant *c*, was found through nonlinear regression techniques (Marquardt-Levenberg method) for the 60 and 70 lb/ft^3 density curves utilizing the moduli at the 65

lb/ft^3 density as the reference curve. A linear behavior was found for *c* at the three density levels and can be described through a linear regression as shown in Eq. 11, where *m* and *b* are the slope and y-intercept of the regression curve, respectively, and ρ denotes the density.

$$E(t)_{\rho} = E(t)_{ref(\rho)} 10^{m\rho+b} \qquad \text{Eq. 5.10}$$

The fit of Eq. 10 can be shown in Figures 5 and 6 on a linear scale for the 0 and 50%PP composites at the 180°C platen temperature. Similar fits were found with the 170 and 190°C platen temperatures and the 30 and 40% PP levels (Appendix F).

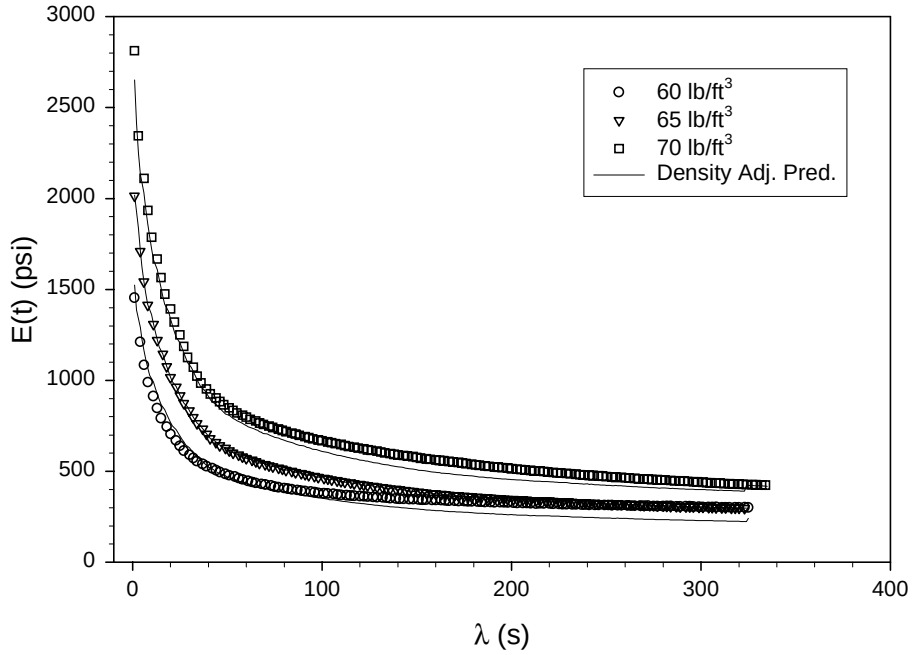

Figure 5.5. Density adjustment curve fit for the 0%PP panel at the experimental densities and a 180°C platen temperature.

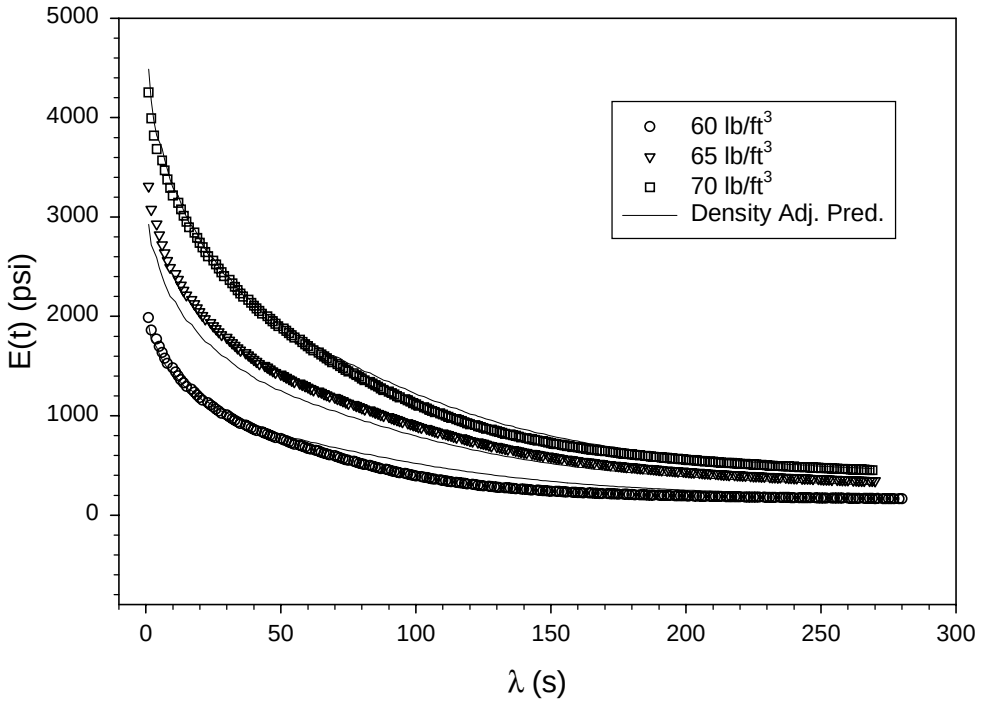

Figure 6. Density adjustment curve fit for the 50%PP panel at the experimental densities and a 180°C platen temperature.

Results and Discussion

The model developed to determine the pulling load of a wood and wood/PP fibrous mat was developed from a solid mechanics approach. The contribution to the pulling load can be classified into two separate behaviors, consolidation and friction. The horizontal component of consolidation forces occurs only in the entrance region, while the frictional resistance can be found throughout the entire die. The densities were targeted between 60-70 lb/ft^3 as to coincide with the results from the consolidation of fibrous mats in Chapter 2. The results of the pulling force model can be found in Table 5.1.

Table 5.1. Load values from experimental and modeled results.

%PP-Temp (°C)	Model Pulling Load (lbs)				Actual Load (Pa)	Average Density (lb/ft^3)*
	Consolidation	Friction		Total (Pp)		
		Entrance	CG			
0-170	709.7	397.1	1832.4	2939.2	3181.7	67.6 (2.68)
0-180	767.6	514.4	2103.9	3385.9	2974.5	69.4 (2.13)
0-190	757.3	595.7	2320.7	3673.6	2604.6	69.1 (3.54)
30-170	551.3	292.1	1671.9	2515.3	2606.4	64.5 (1.48)
30-180	491.2	307.0	1270.5	2068.7	1650.1	62.4 (2.39)
30-190	540.8	367.0	1274.6	2182.4	1539.0	64.1 (1.32)
40-170	775.1	362.2	2340.8	3478.2	2760.1	65.1 (1.99)
40-180	511.3	266.2	1346.2	2123.7	1410.6	61.7 (1.47)
40-190	532.6	325.2	1439.0	2296.9	1000.1	60.7 (3.06)
50-170	413.0	222.3	1178.5	1813.8	1953.8	55.8 (3.74)
50-180	358.3	225.7	1046.4	1630.4	1147.4	53.7 (2.97)
50-190	376.0	261.0	1130.8	1767.9	929.3	54.4 (1.5)

*Coefficient of variation in ().

The model results provide a good approximation for the pulling force required for mats containing 0%PP at all temperatures and the 30, 40 and 50% PP at the lowest temperature of 170°C. However, the increased temperature caused a much lower experimental load (Pa) as compared to the predicted load (Pp). In Figure 5.7, the ratio of Pp/Pa clearly identifies a deviation from the pulling force model as the temperature is increased. The effect is accentuated at the higher PP levels.

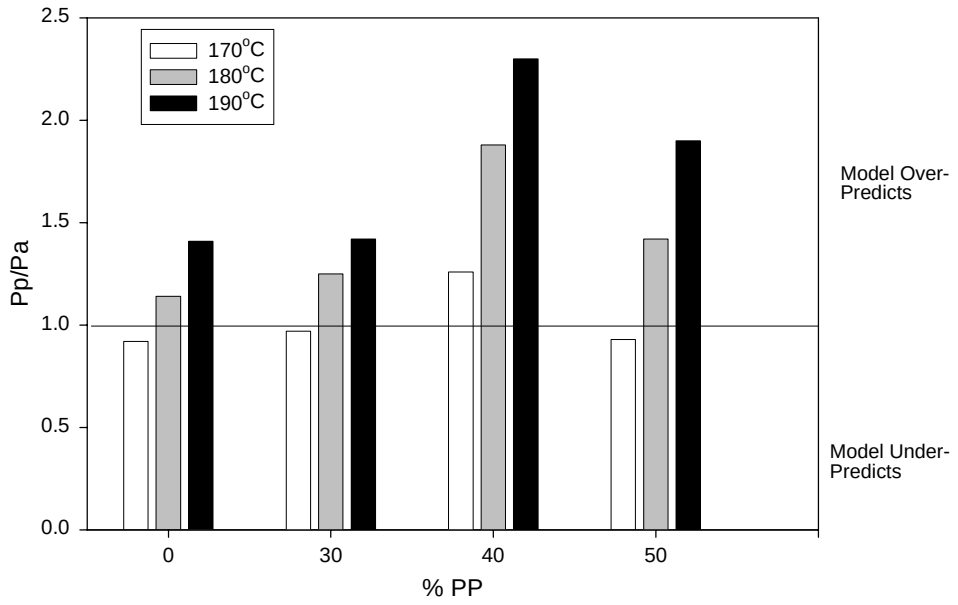

Figure 5.7. Ratio of the modeled load (Pp) to the experimental pulling load (Pa).

The deviation of the model at the higher temperatures may have been caused by the lateral contraction of the composite resulting from the applied tensile load. This Poisson effect would cause a lower normal stress against the die surface as the applied tensile load increases. As the pulling load is increased throughout the length of the die to a final load at the out-feed, the tensile stiffness of the composite is reduced as the composite temperature increases. At higher die temperatures, the Poisson effect is accentuated and can cause it to occur sooner within the die, resulting in lower pulling loads.

The viscous drag that is commonly associated with the pulling force modeling of thermoplastic composites (Bibbo and Gutowski 1986, Tso et al. 1993, Astrom and Pipes 1993a, Lee et al. 1991, and Blaurock and Mitchell 1997) may have also contributed to the lower than expected pulling loads, however, a contradiction exists with the similar trend exhibited with the 0% PP mats. Also, the sliding frictional response (Eq. 5.8) of the non-

woven mats were developed with similar temperatures, dwell time, and pressures exhibited through the pultrusion process.

Model Sensitivity

Density, temperature and friction are input variables to the pulling force model. The sensitivity of the model to the change in these variables can help assess the important mechanisms of pulling resistance and account for deviations within the model and experimental results. Highly sensitive variables can then be identified and future research can describe their behavior more efficiently.

The influence of density can be seen in the maximum σ_c of the composite, which influences the σ_r and friction of the composite. With an increase in the density, the values of σ_c and σ_r increase, while the μ_k experiences a decrease in value. The influence the change in density on the pulling force model is shown in Figure 5.8. Although a substantial difference is observed within the density range observed, the variability of density in the experimental data (Table 5.1) is quite minimal.

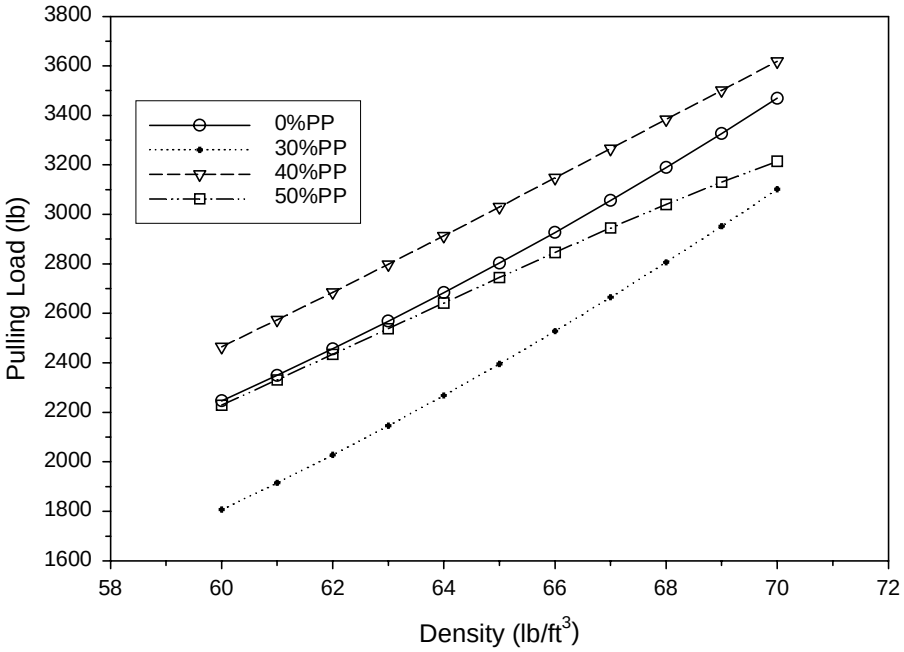

Figure 5.8. Influence of density on the modeled pulling load at a die temperature of 180°C.

With an increase in the temperature of the die, the non-woven mats with PP exhibited a decrease in the pulling load, while the 0%PP showed an increase in the pulling resistance (Figure 5.9). The load increase for the 0%PP composite is a result of the higher friction values associated with increasing temperature found in Chapter 4. An increase in μ_k was also observed for the mats with PP, however, the dramatic decrease in stress observed with the increase in temperature (Chapter 2), governed the model behavior.

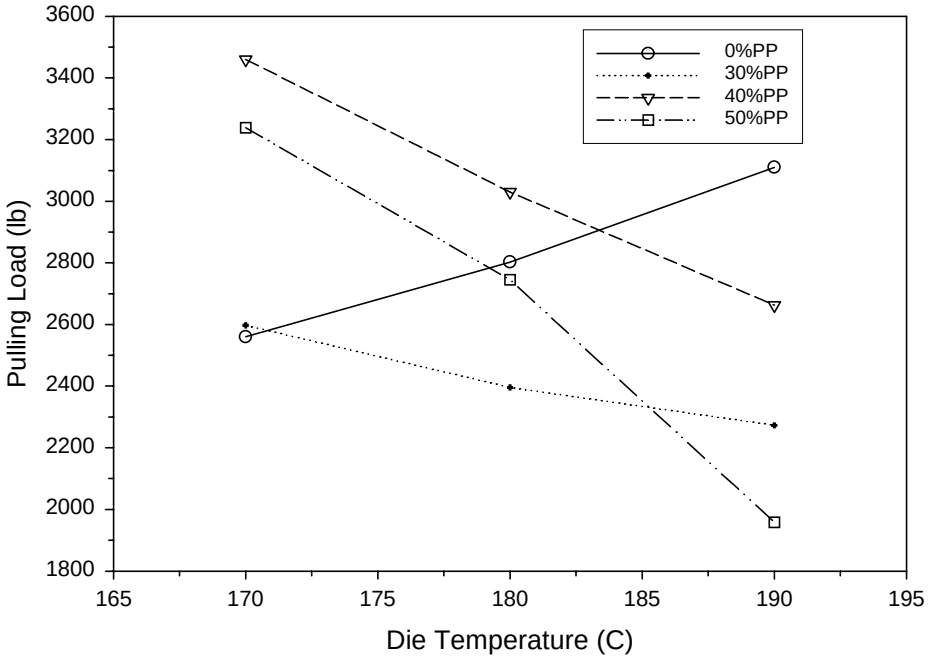

Figure 5.9. Influence of die temperature on the modeled pulling load at a density of 65 lb/ft^3.

As seen from the model results in Table 5.1., the contribution of friction is the primary mechanism of resistance in the pulling force model. The effect of friction is more pronounced with the higher PP composite (Figure 5.10). The data in Figure 10 was calculated by the addition of a constant change in μ_k ($\delta\mu_k$) to the friction model in Eq. 5.8. The results indicate the higher PP level mats were more significantly influenced by friction. Data for the 40 and 50% PP mats at the low $\delta\mu_k$ (-0.015 and –0.020) levels was discarded due to the μ_k falling below 0 at the higher loads.

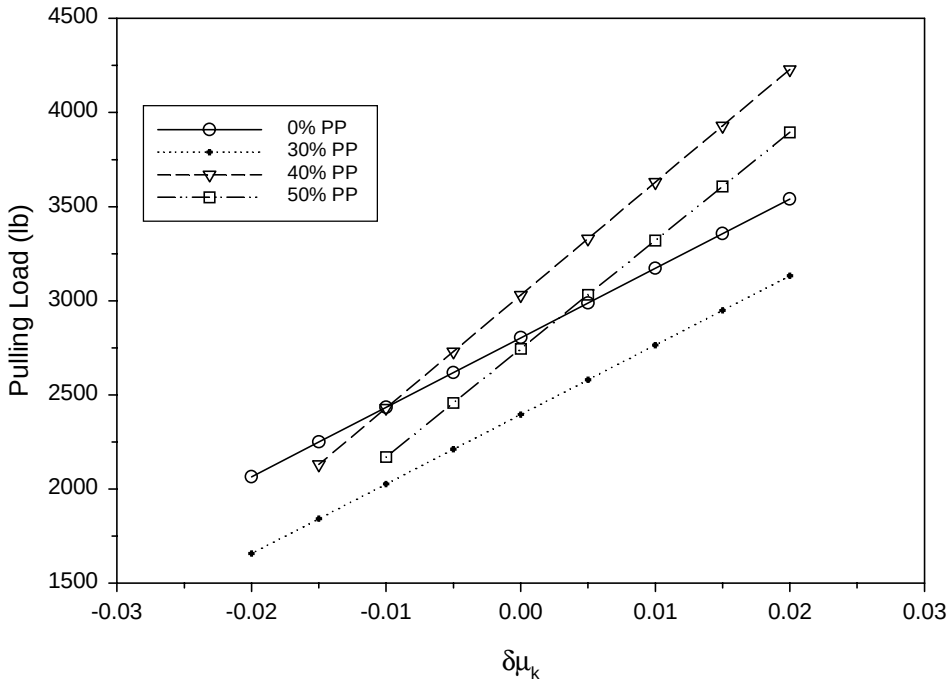

Figure 5.10. Influence of friction on the modeled pulling load at 180°C and at a density of 65 lb/ft^3.

Conclusion

The flow of a wood/thermoplastic composite in many polymer manufacturing techniques govern many of the processing parameters. Within a pultrusion process, the resistance attributed to the consolidation and frictional response of the wood material, may result in a tensile failure from high loads. Traditional polymer models utilize a fluid mechanics approach, which is incompatible with wood-based pultrusion. Therefore, a model was developed from a solid mechanics approach to determine the pulling load developed with a wood and wood/PP fiber composite.

Based upon the geometry of a thermoplastic pultrusion die, the total pulling force can be described through the consolidation and frictional behavior of the wood and wood/PP fiber mats. Models of the consolidation and relaxation behavior along with a

regression model of the frictional response were used to provide numerical descriptions of the pulling load. The consolidation and relaxation responses were adjusted to the density of the composite.

The results of the experimental pultrusion runs indicate the model provides good agreement with the 170°C data, however, the model over-predicted the pulling load as the temperature of the die increased. The sensitivity analysis showed the model to be strongly influenced by the density, temperature, and friction. As the density increased, a higher compressive load developed increased pulling loads from both consolidation and frictional forces. The temperature reduced the pulling loads of the composites containing PP fibers from the increased amount of relaxation. However, the 0% PP mats saw an increase in pulling load with temperature, which can be attributed from the increased contribution of friction at higher temperatures. The friction parameter of the model was more influential with higher PP content panels.

Some of the deviation in the model may have developed from the variability of the input parameters of friction and stress. However, the large discrepancy found within the model and experimental results at the higher PP and temperature levels can not be completely explained by the sensitivity of the model. The applied tensile load may have reduced the normal load against the die surface through a Poisson effect. With increased temperatures, the Poisson effect was accentuated as the stiffness of the material was reduced.

References

Astrom B.T., Larsson, P.H., and R.B. Pipes. 1991. Experimental investigation of a thermoplastic pultrusion process. 36th International SAMPE Symposium. 36:1319-1330.

Astrom, B.T. and R.B. Pipes. 1993a. A modeling approach to thermoplastic pultrusion. I: formulation of models. Polymer Composites 14(3):173-183.

Astrom, B.T. and R.B. Pipes. 1993b. A modeling approach to thermoplastic pultrusion. II: verification of models. Polymer Composites 14(3):184-194.

Batch, G.L. and C.W. Macosko. 1987. A computer analysis of temperature and pressure distributions in a pultrusion die. 42nd Annual Conference, Composites Institute, The Society of the Plastics Industry. Session 12B1-B7.

Bibbo, M.A. and T.G. Gutowski. 1986. An analysis of the pulling force in pultrusion. ANTEC:1430-1432.

Blaurock J. and W. Michaeli. 1997. Calculation of the pulling force in the thermoplastics pultrusion process. 42nd International SAMPE Symposium 42:1414-1425.

Kim, D.H., Han, P.G., Jin, G.H. and W.I.Lee. 1997. A model for thermosetting composite pultrusion process. Journal of Composite Materials. 31(20):2105-2122.

Lee, W.I, Springer, G.S., and F.N. Smith. 1991. Pultrusion of thermoplastics – a model. Journal of Composite Materials. 25:1632-1652.

Moschiar, S.M., Reforedo, M.M., Larrondo, H., and A.Vasquez. 1996. Polymer Composites. 17(6):850-858.

Parker, D.J and R.L. Pike. 1987. Parallam PSL: an evolution. Proceedings 21st International Particleboard/Composite Materials Symposium. 21:51-68.

Tso, W., Hou, T.H. and S.N. Tiwari. 1993. Analysis of pultrusion processing for long fiber reinforced thermoplastic composite system. Institute for Computational and Applied Mechanics. Report 93-103.

U.S. Patent #4,983,453. 1991. Hybrid pultruded products and method for their manufacture. U.S. Government Printing Office.

Chapter 6

Project Summary/Conclusion

Incorporating wood-based composites into a pultrusion or similar polymer processes requires an understanding of the material movement or flow through a stationary die. With polymer systems, a fluid mechanics approach can be utilized to model the influence processing parameters and composite design impart on material flow, however, with wood-based composites, a solid mechanics model is needed for assessing the material flow. Modeling the movement or flow of a wood and wood/PP fibrous mat through a forming die, typically utilized in the polymer industry, requires a description of the consolidation and frictional behavior of the composite. The resistance developed in a pultrusion die was modeled utilizing the described consolidation and friction mechanisms and the geometry of the pultrusion die.

The consolidation of a fibrous wood and wood/PP mat was separated into two separate time domains: stress-strain and stress-time. The stress-strain behavior did not follow traditional wood strand consolidation models, due to the high amount of fiber movement. However, a relationship was postulated, based upon published research on powder materials, utilizing the instantaneous modulus ($E(\varepsilon)$) and the true strain or relative density of the mat during closure. The experimental data showed good agreement with the model at all PP levels, temperatures, and density. The stress-time region of the consolidation curve was modeled utilizing a traditional viscoelastic

mechanical analogies. A 4-parameter Maxwell model was found to accurately describe the relaxation of stress.

The stress-strain behavior of the non-woven mats was found to be controlled by the viscoelastic nature of the composite materials and the mat structure and design . Both increased strain rate and density caused a higher ultimate stress, however, the trend of the compression curve remained the same. The addition of PP to the fiber network caused an increase in the ultimate stress and also showed a difference in the behavior of the curve. The higher flexural stiffness of the wood fibers increased the contribution of stress associated with the fiber bending stage of consolidation. Stress developed during the final stage of consolidation results from transverse fiber compression. Assuming the majority of the fibers lie within the plane of the platens, the greater transverse strength of the PP fibers, compared to the cellular wood fibers, increased the ultimate compressive stress of the PP mats.

Utilizing a relaxation spectrum, two distinct mechanisms of behavior were identified in the stress-time region of the curve. The initial stages of relaxation saw a contributive effect of interparticle movement. As heat transferred further into the center of the composite, the relaxation behavior was observed to be primarily material deformation of the amorphous wood constituents and PP fibers.

The results of the friction test procedure were related to the adhesion theory of friction, which is commonly associated with polymer tribiology. Based upon adhesion theory, the frictional force is developed through bonding of the two surfaces and the interfacial shear stress. The bonding is enhanced with a higher surface area and an increased shear stress. The dynamic coefficient of friction (μ_k) of the non-woven mats

was found to be altered with die temperature, dwell time, normal load, and PP content. The temperature range of study showed a slight increase in μ_k as temperature increased, which can be attributed to an increased contact area. A decrease in μ_k with dwell time and PP level was also observed, while the most dramatic effect was exhibited with a decrease in μ_k with the higher applied normal load, where a semi-logarithmic relationship was observed. The decrease in μ_k with the normal load results from the nonlinear behavior with the shear stress of the interface.

Theoretical models describing the behavior of μ_k can be difficult to apply to a composite systems, so an empirical multiple linear regression was utilized. The prediction of μ_k was based upon the temperature, dwell time, PP content, and normal stress and was found to fit the data with a $r^2 = 0.67$.

A pulling force model was developed from the consolidation and frictional resistance of the wood-based composite. The description of the compressive stress and the frictional response were utilized with the geometry of the pultrusion die to provide a pulling force model. With this model, the influence of processing conditions and composite design can be evaluated for their contribution to the applied tensile stress on the composite.

The pulling force model differed from traditional polymer pultrusion models in that a solid, not fluid, mechanics approach was utilized. The Maxwell model, which described the relaxation response, was adjusted to the experimental density through a linear transformation from a reference curve. The pulling force model predicted the accumulated load with reasonable accuracy for the lower temperature (170°C) pultrusion

runs. However, at the higher temperatures, the model overestimated the pulling load, this error increased with increased PP content. The model sensitivity can account for slight deviations in predicted loads, however the significant over-predictions may have been a result of the lateral contraction of the composite under the applied load. As the temperature was increased, the Poisson effect from the tensile load was more prevalent, due to the reduced stiffness of the composite. Both the model and experimental results showed a decrease in pulling load with lower densities and higher amounts of PP. With PP in the composite, the load was reduced further through an increase in temperature, which allowed more relaxation to occur.

The significance of modeling the pulling load of a wood-based composite does not lie solely on a numerical prediction of pulling resistance. The knowledge obtained through pultrusion modeling, allows for a more comprehensive understanding of the mechanisms associated in material movement or flow through a die. The response of the viscoelastic composite material to compression and sliding friction is important not only to a pultrusion process, but also to many other polymer and wood composite processing techniques.

Appendix A. Compression Curves

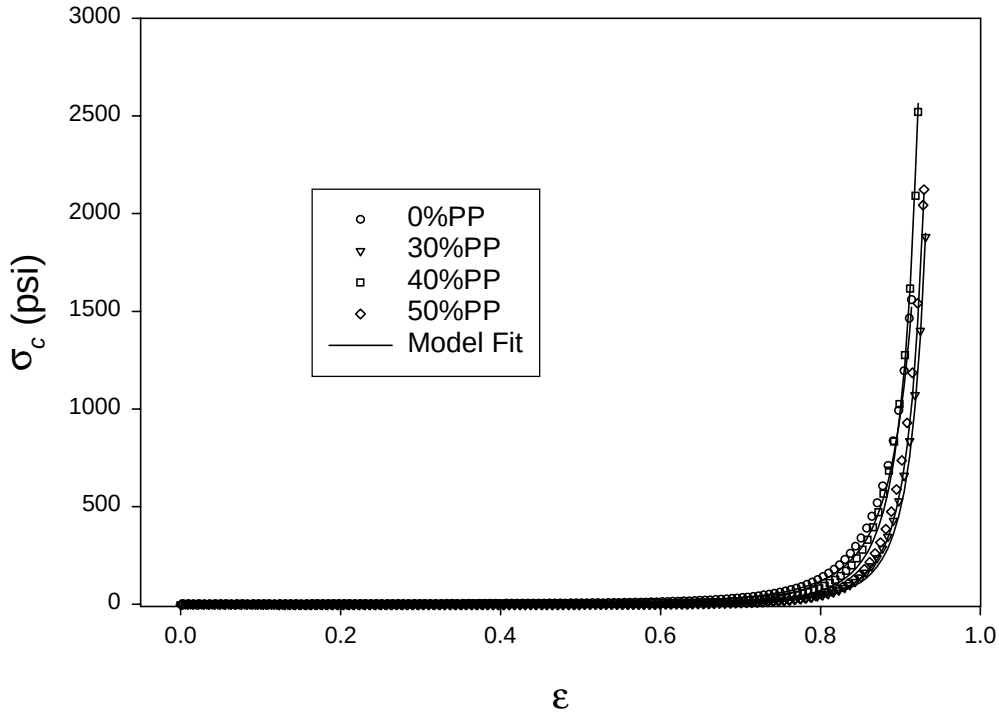

Figure A.1. Representative compression curves for non-woven mats at 170°C pressed to a 60 lb/ft^3.

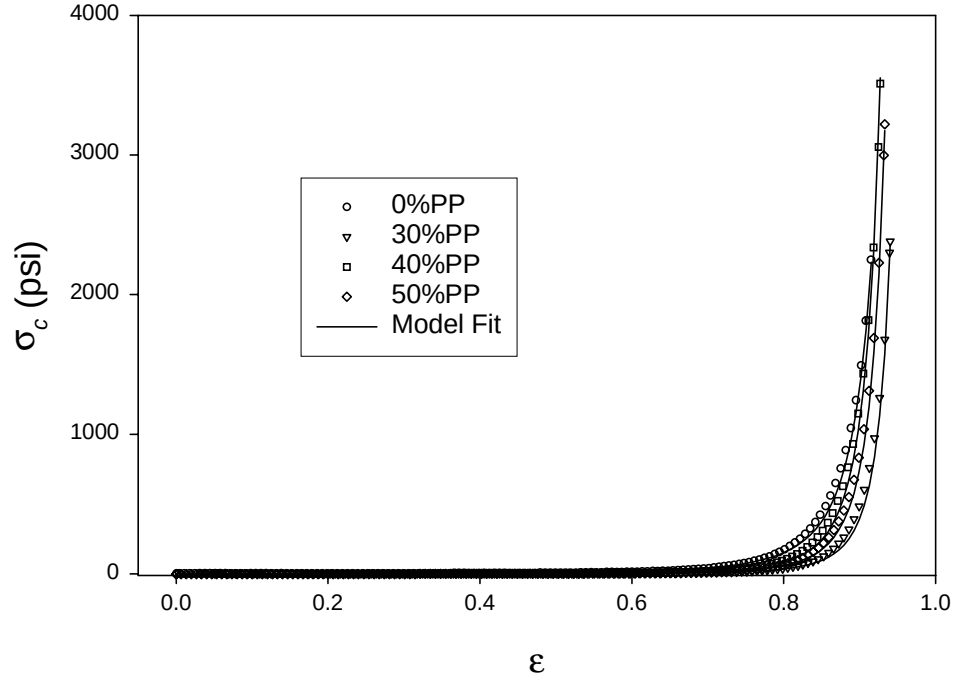

Figure A.2. Representative compression curves for non-woven mats at 170°C pressed to a 65 lb/ft^3.

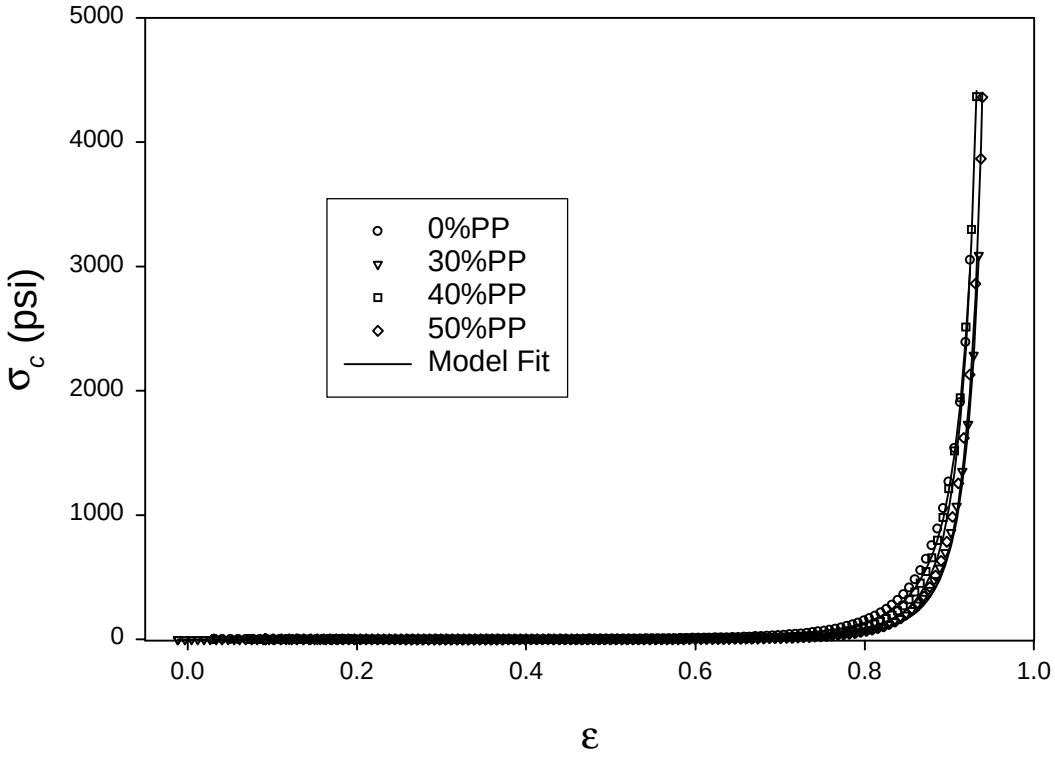

Figure A.3. Representative compression curves for non-woven mats at 170°C pressed to a 70 lb/ft^3.

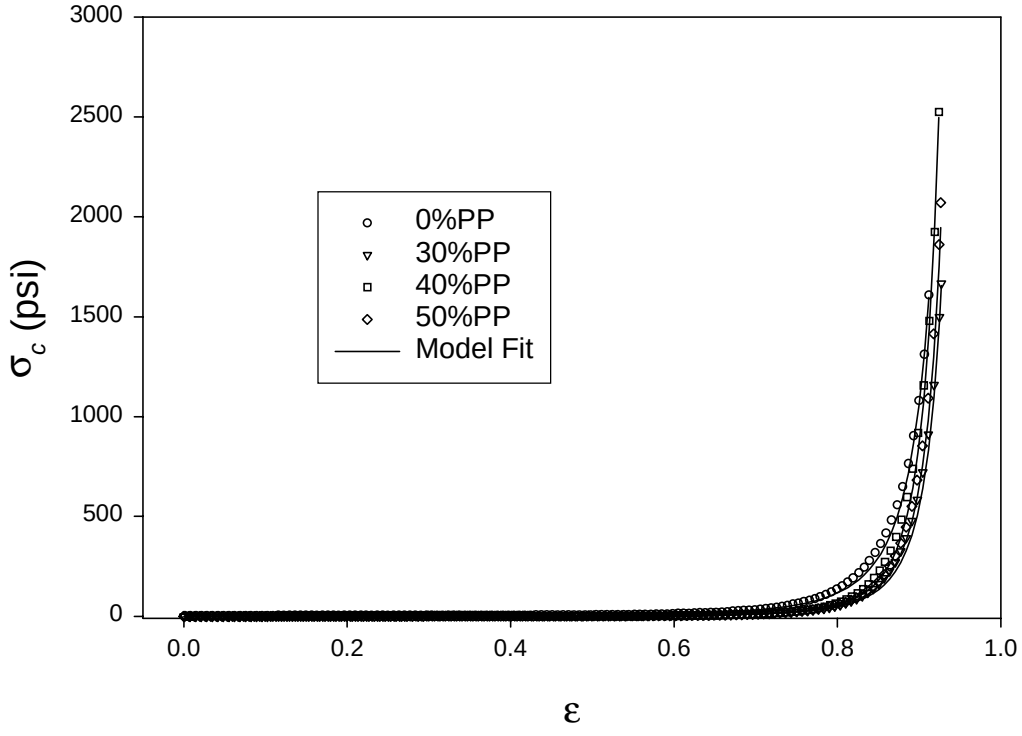

Figure A.4. Representative compression curves for non-woven mats at 180°C pressed to a 60 lb/ft^3.

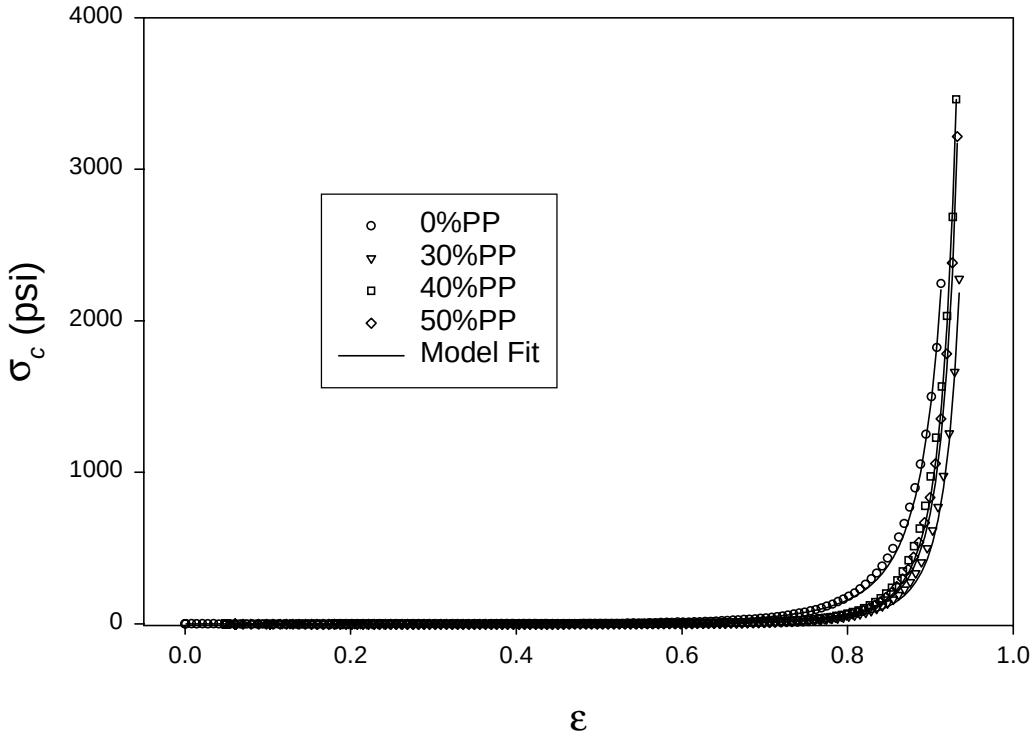

Figure A.5. Representative compression curves for non-woven mats at 180°C pressed to a 65 lb/ft^3.

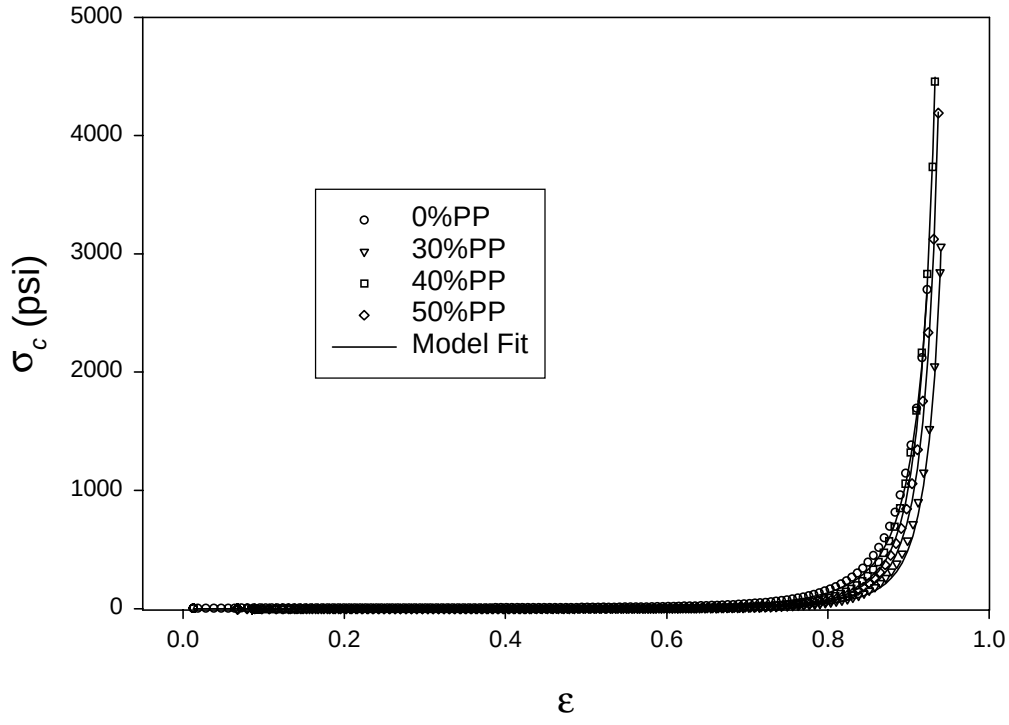

Figure A.6. Representative compression curves for non-woven mats at 180°C pressed to a 70 lb/ft^3.

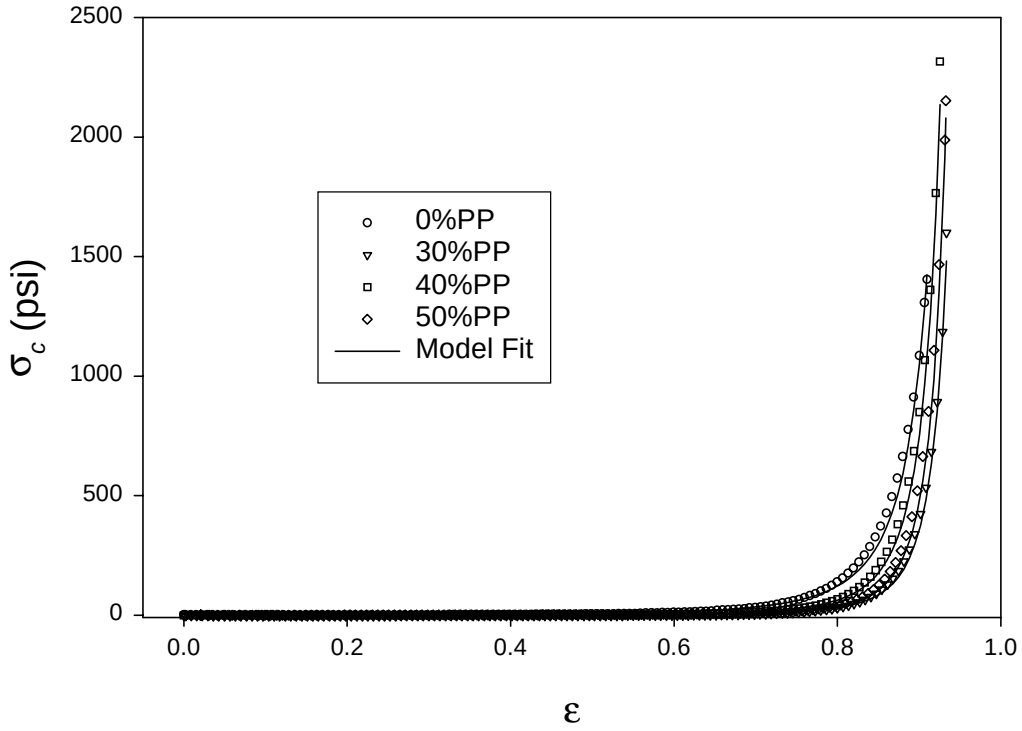

Figure A.7. Representative compression curves for non-woven mats at 190°C pressed to a 60 lb/ft^3.

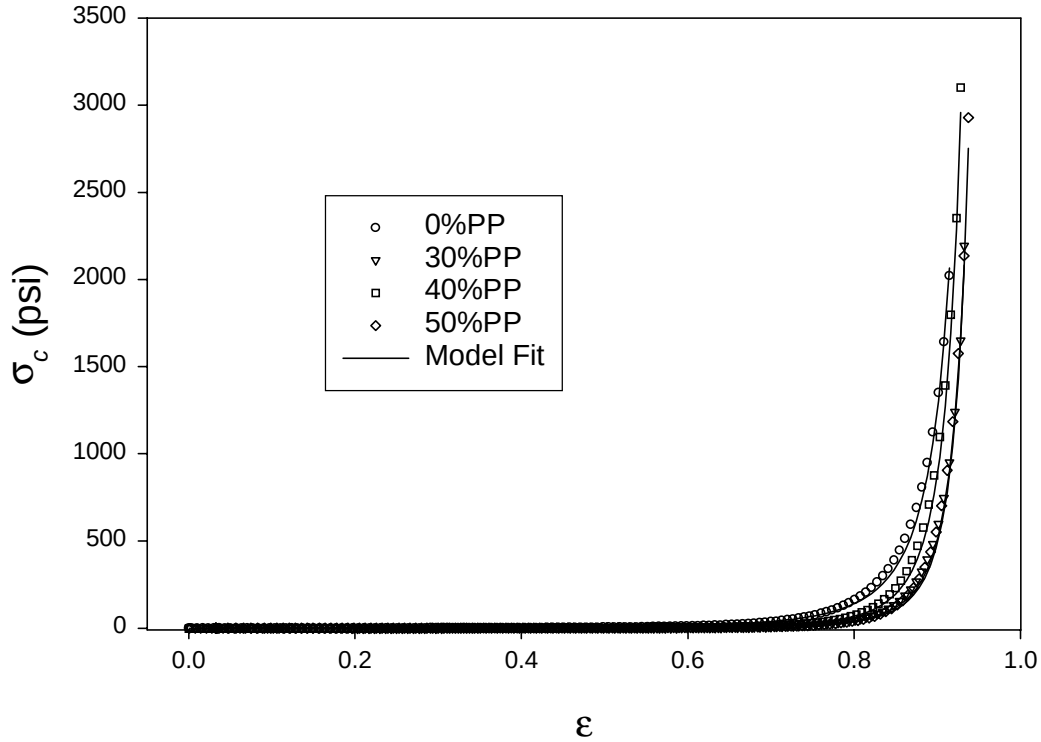

Figure A.8. Representative compression curves for non-woven mats at 190°C pressed to a 65 lb/ft^3.

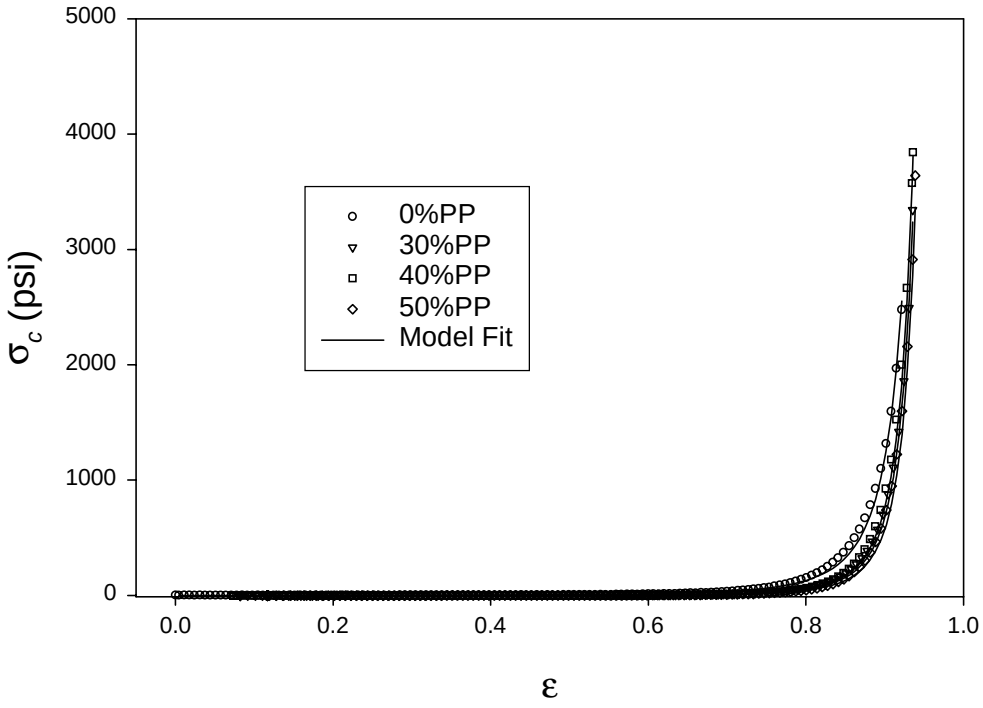

Figure A.9. Representative compression curves for non-woven mats at 190°C pressed to a 70 lb/ft^3.

Appendix B. Relaxation Curves

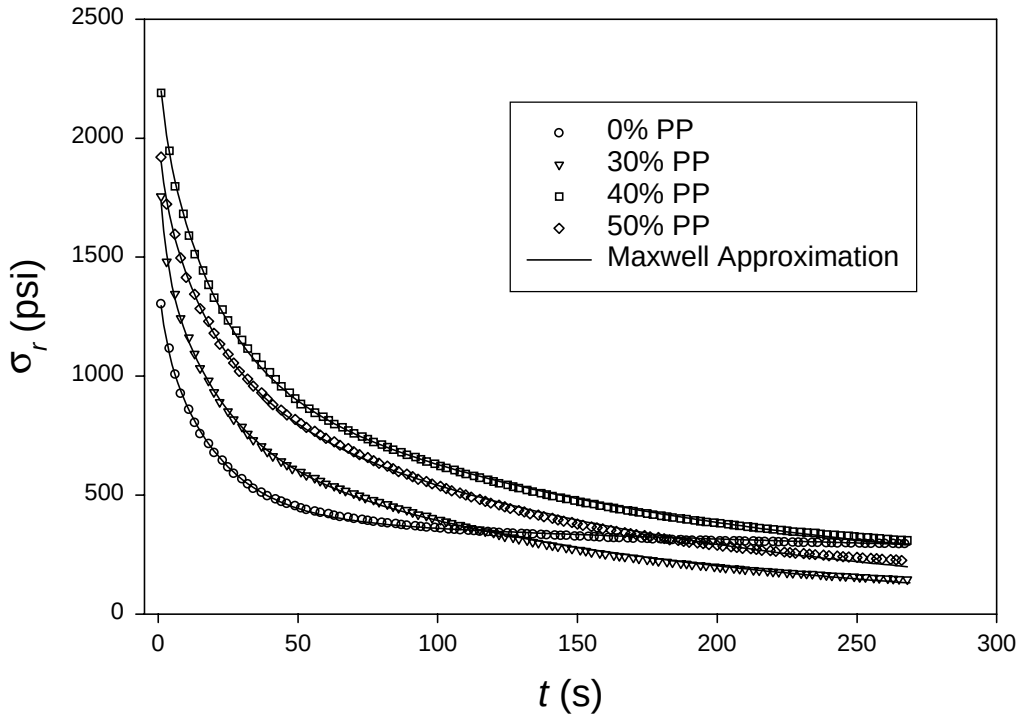

Figure B.1. Representative relaxation curves for non-woven mats at 170°C pressed to a 60 lb/ft^3.

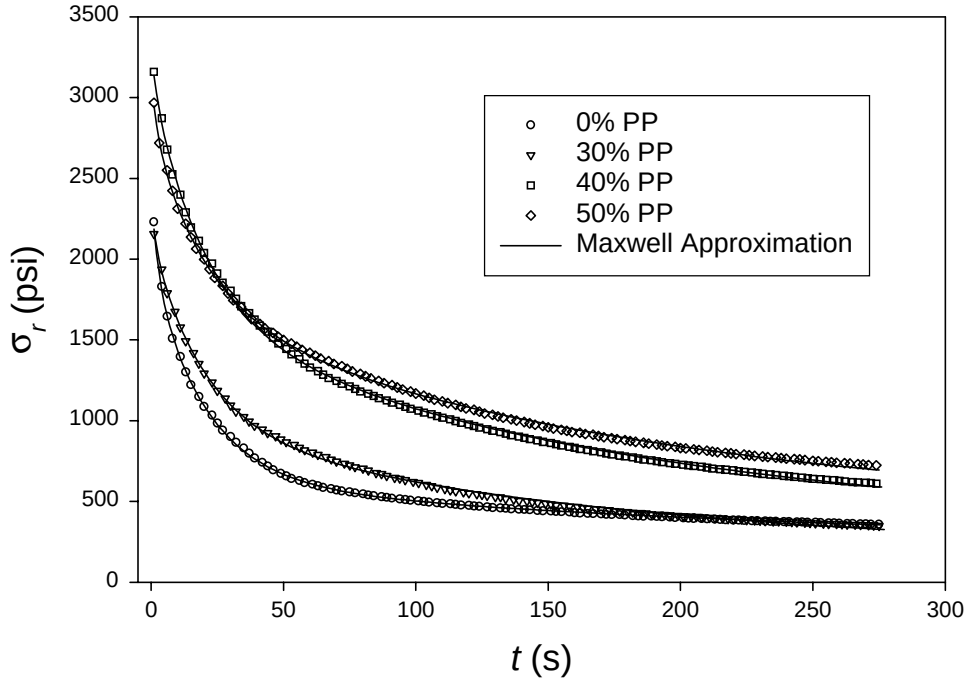

Figure B.2. Representative relaxation curves for non-woven mats at 170°C pressed to a 65 lb/ft^3.

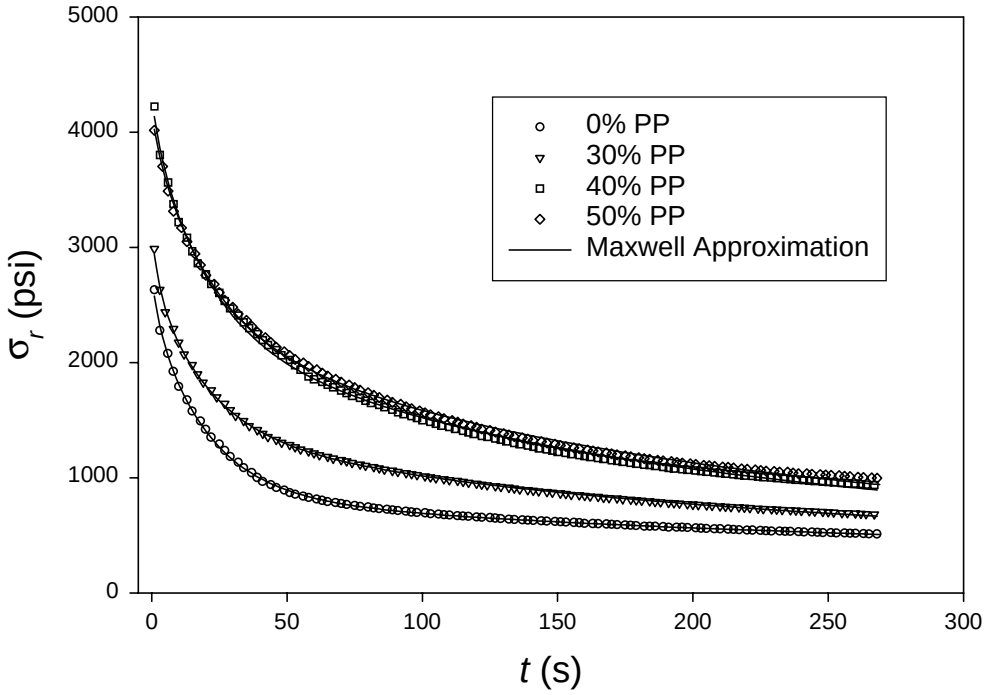

Figure B.3. Representative relaxation curves for non-woven mats at 170°C pressed to a 70 lb/ft^3.

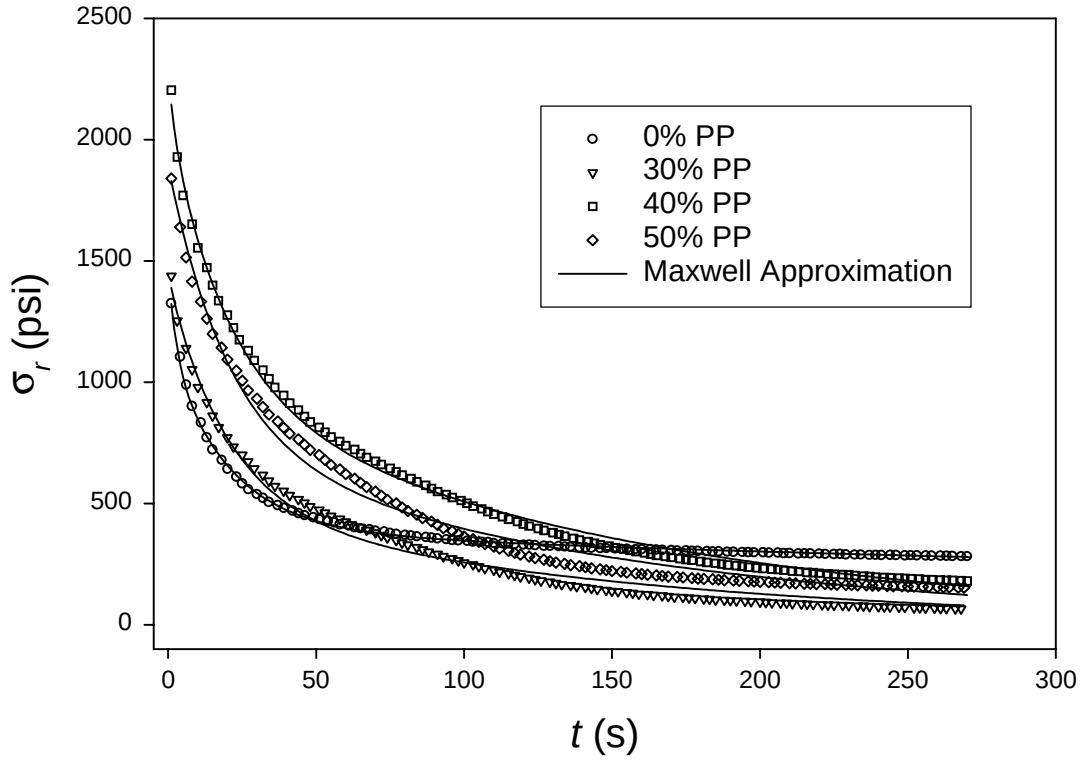

Figure B.4. Representative relaxation curves for non-woven mats at 180°C pressed to a 60 lb/ft^3.

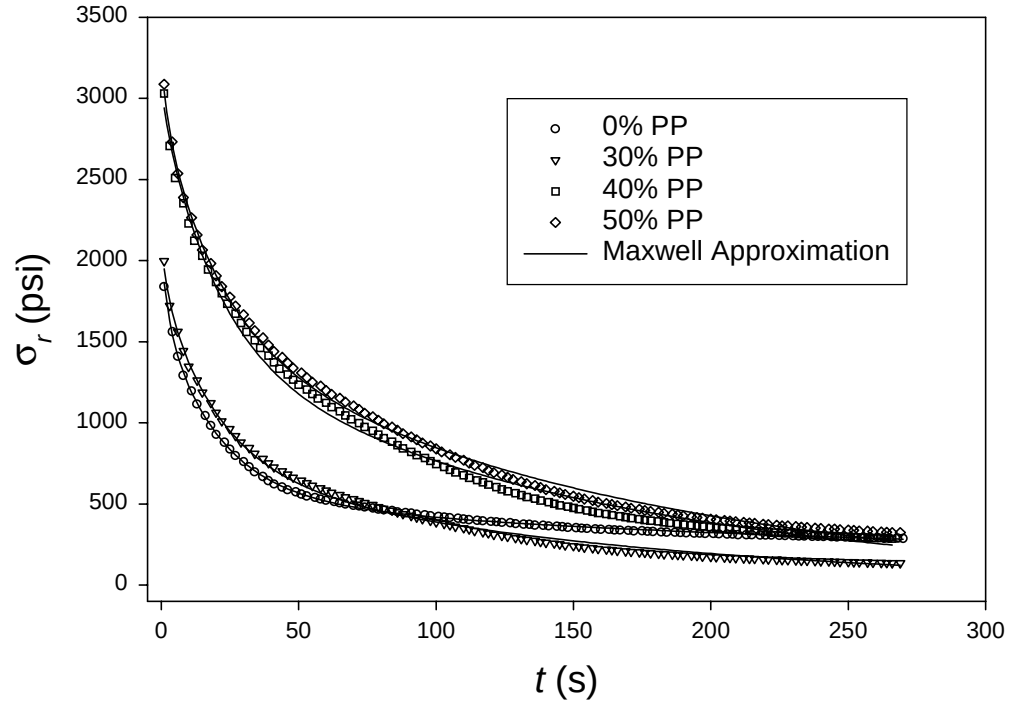

Figure B.5. Representative relaxation curves for non-woven mats at 180°C pressed to a 65 lb/ft^3.

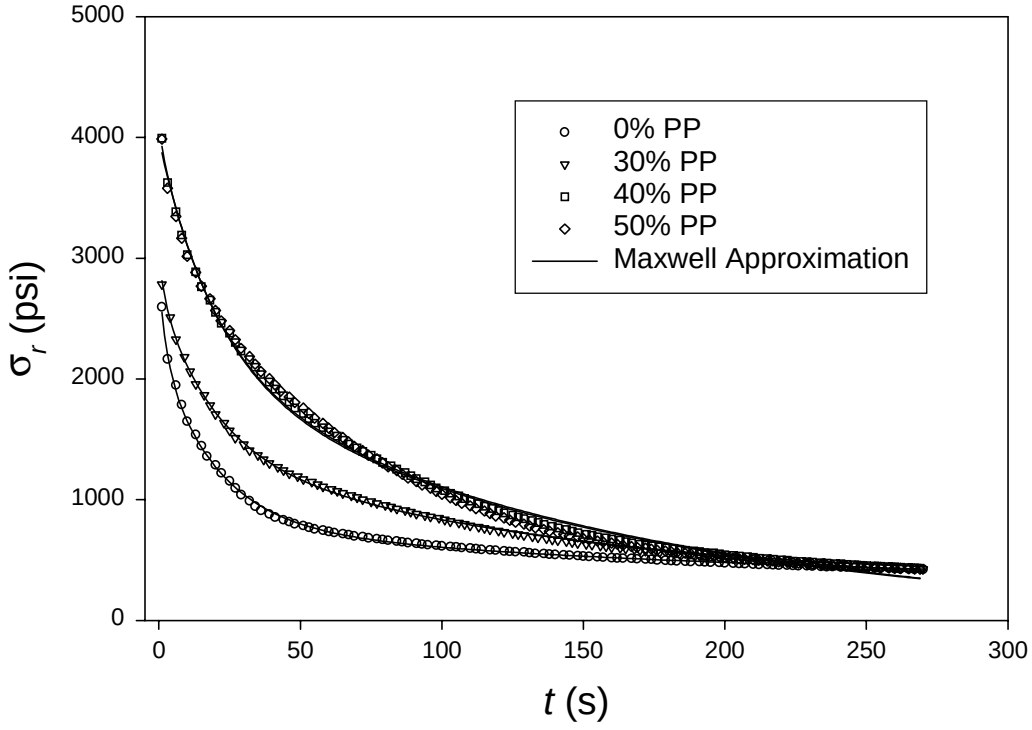

Figure B.6. Representative relaxation curves for non-woven mats at 180°C pressed to a 70 lb/ft^3.

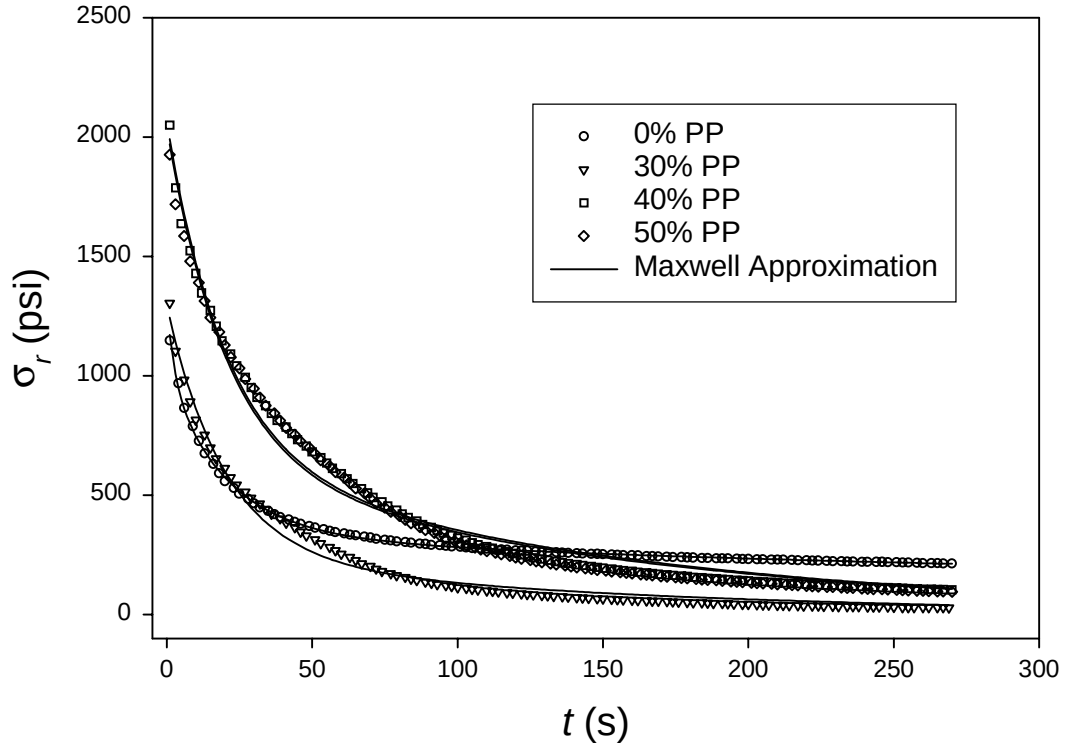

Figure B.7. Representative relaxation curves for non-woven mats at 190°C pressed to a 60 lb/ft^3.

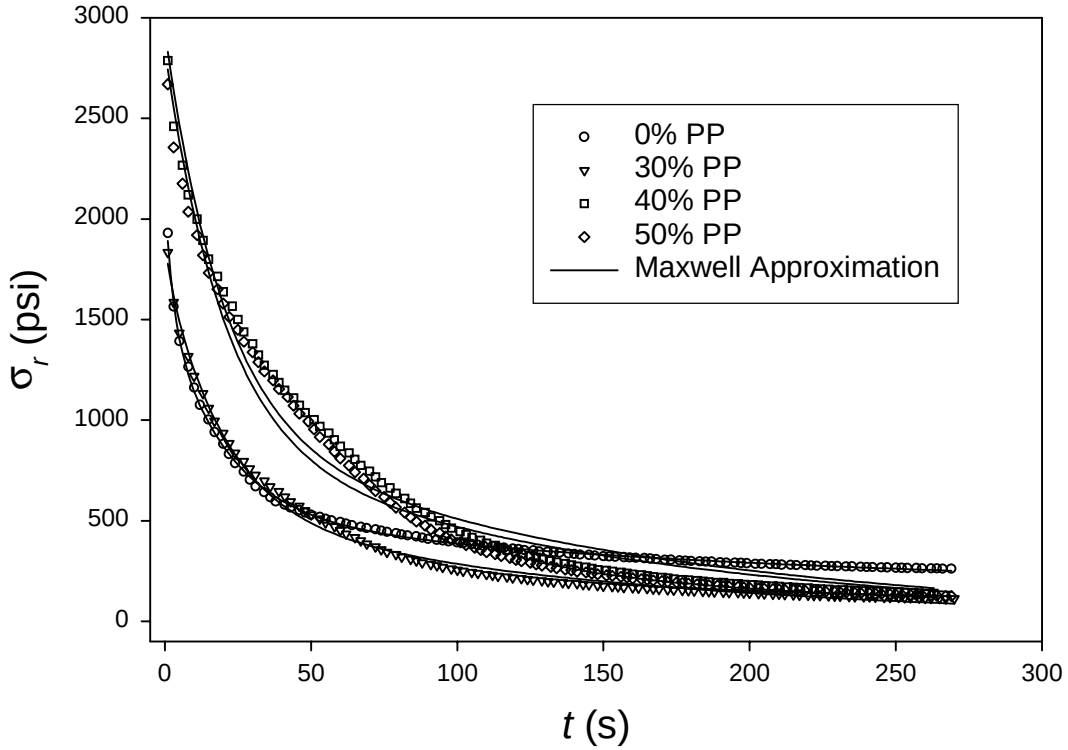

Figure B.8. Representative relaxation curves for non-woven mats at 190°C pressed to a 65 lb/ft^3.

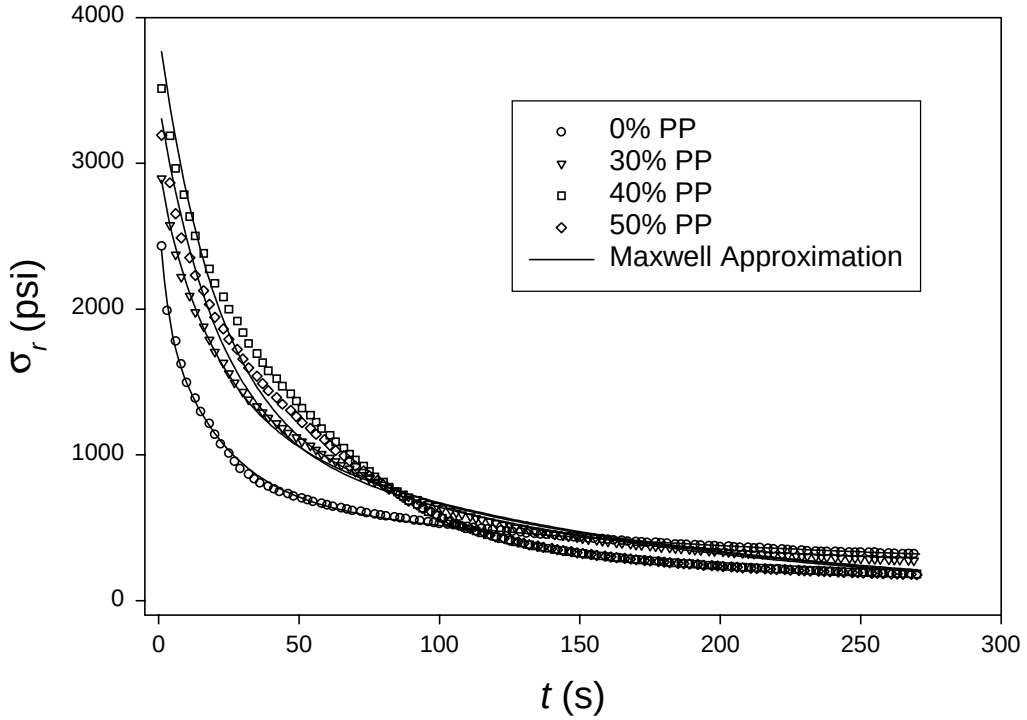

Figure B.9. Representative relaxation curves for non-woven mats at 190°C pressed to a 70 lb/ft^3.

Appendix C. Friction Data – Influence of Normal σ

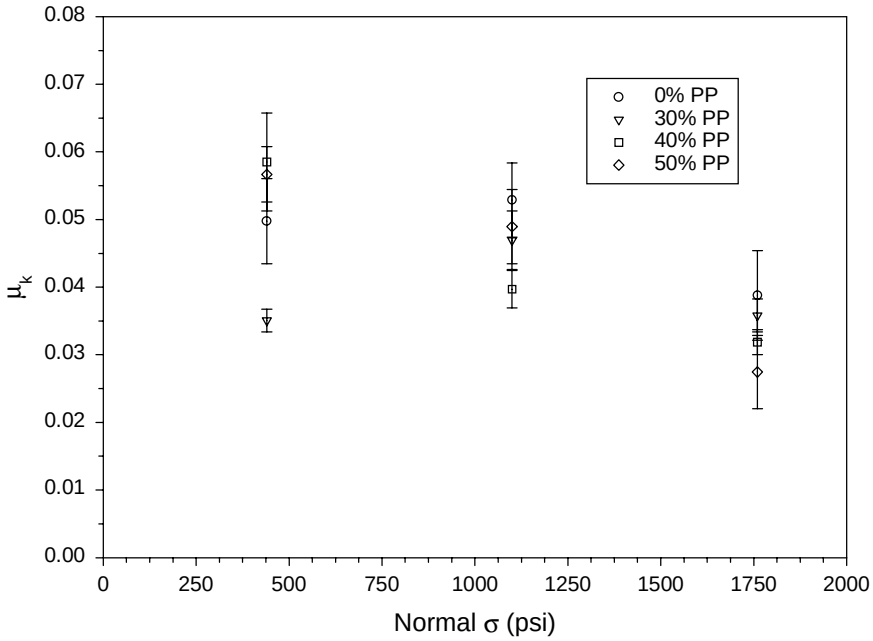

Figure C.1. Influence of normal σ on μ_k, at 170°C and a 1 s dwell time.

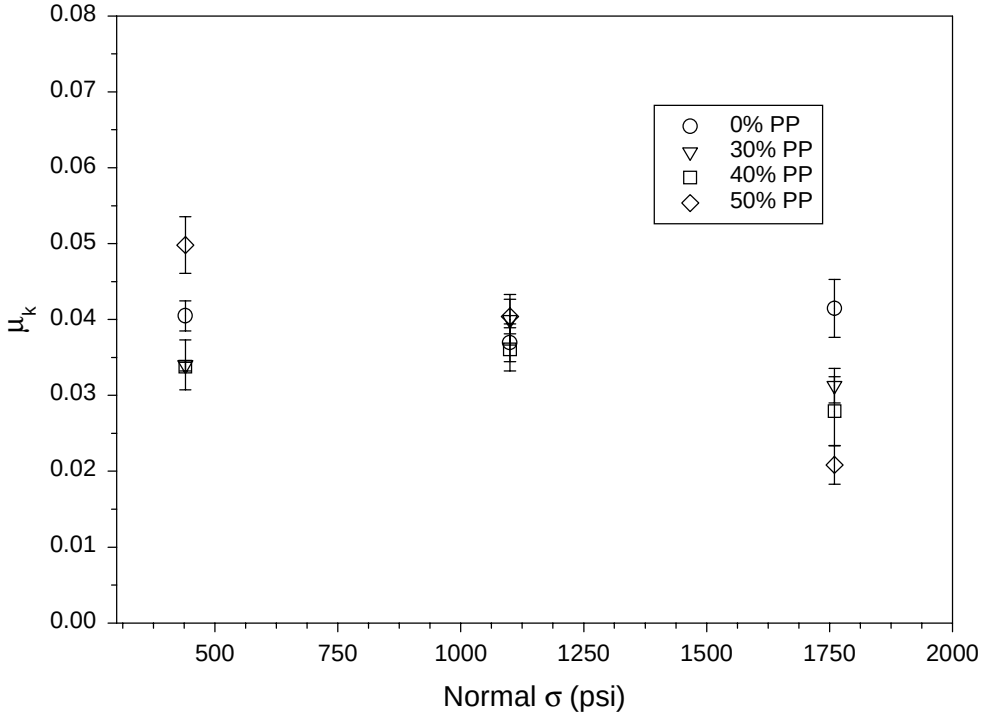

Figure C.2. Influence of normal σ on μ_k, at 170°C and a 60 s dwell time.

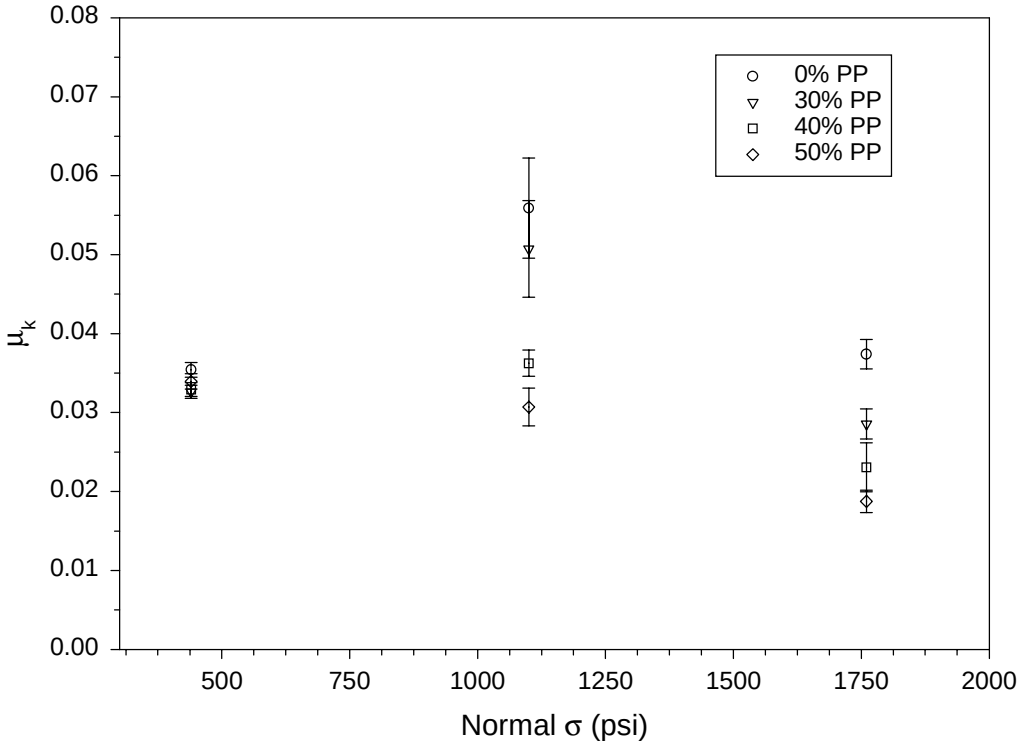

Figure C.3. Influence of normal σ on μ_k, at 170°C and a 180 s dwell time.

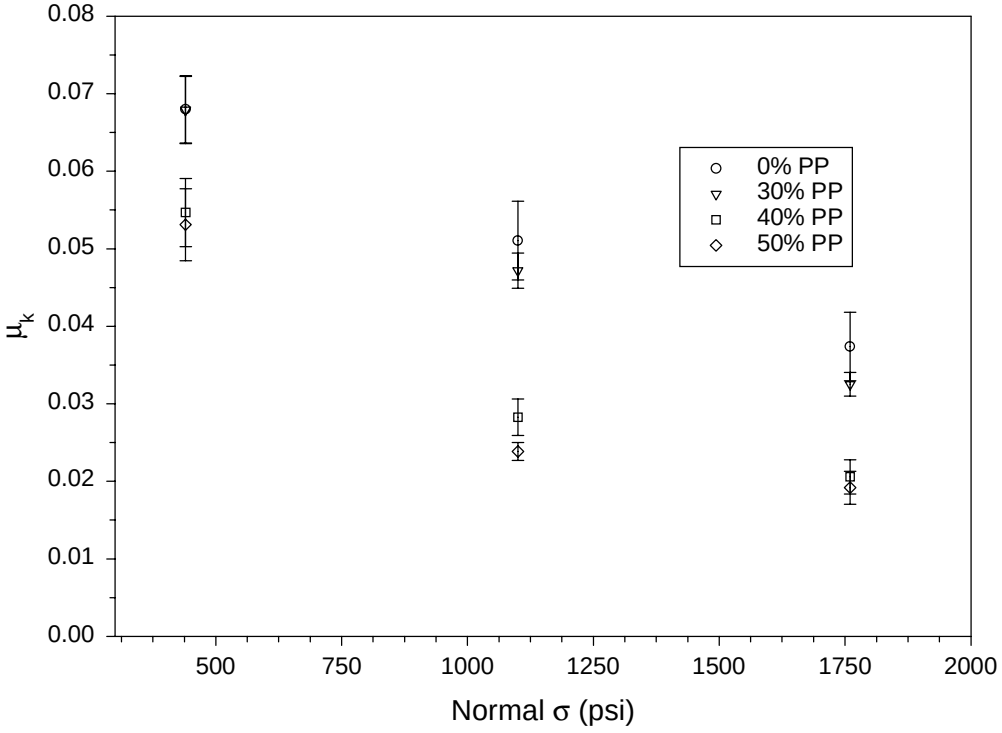

Figure C.4. Influence of normal σ on μ_k, at 180°C and a 1 s dwell time.

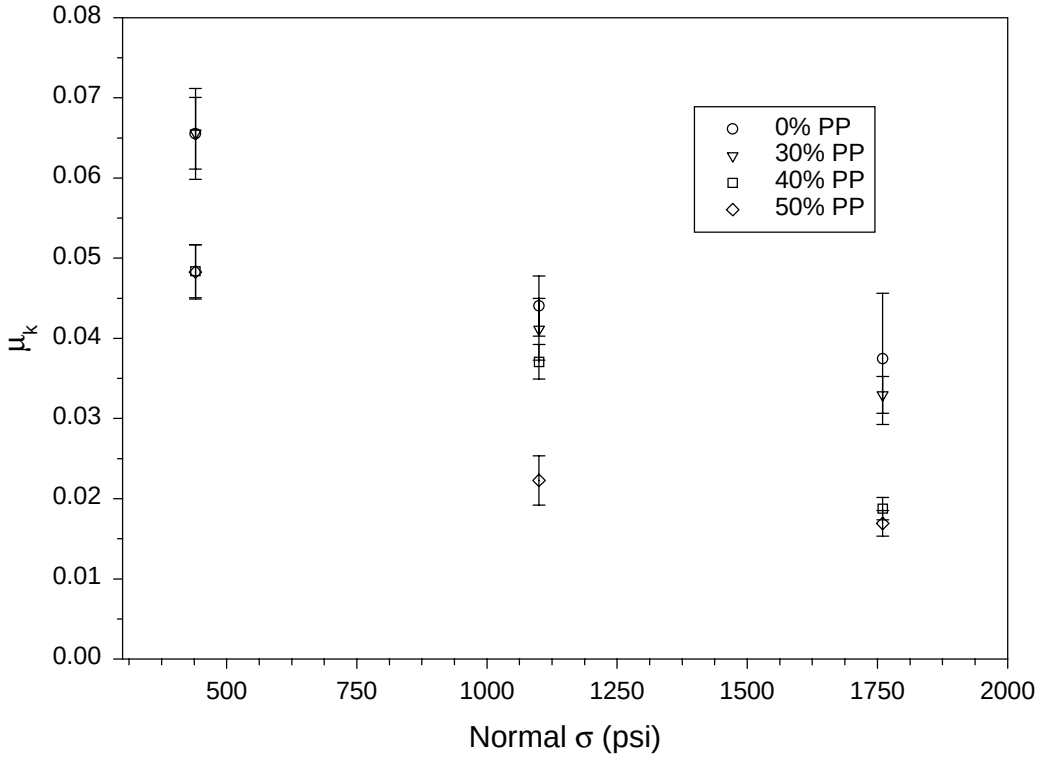

Figure C.5. Influence of normal σ on μ_k, at 180°C and a 60 s dwell time.

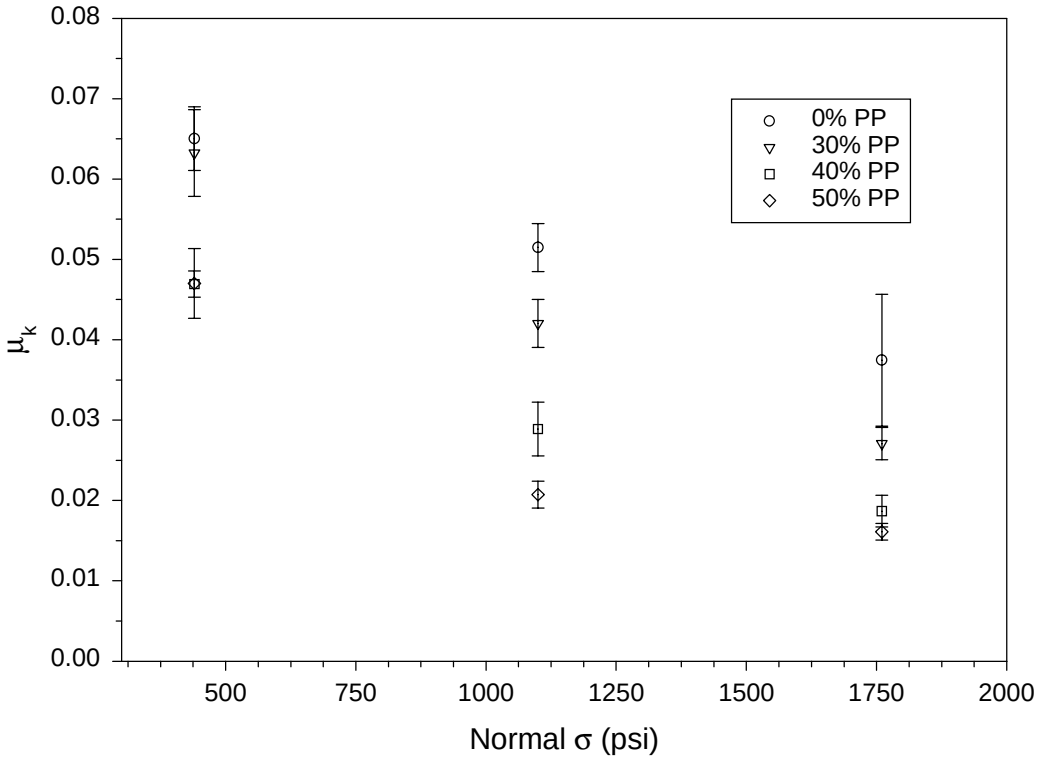

Figure C.6. Influence of normal σ on μ_k, at 180°C and a 180 s dwell time.

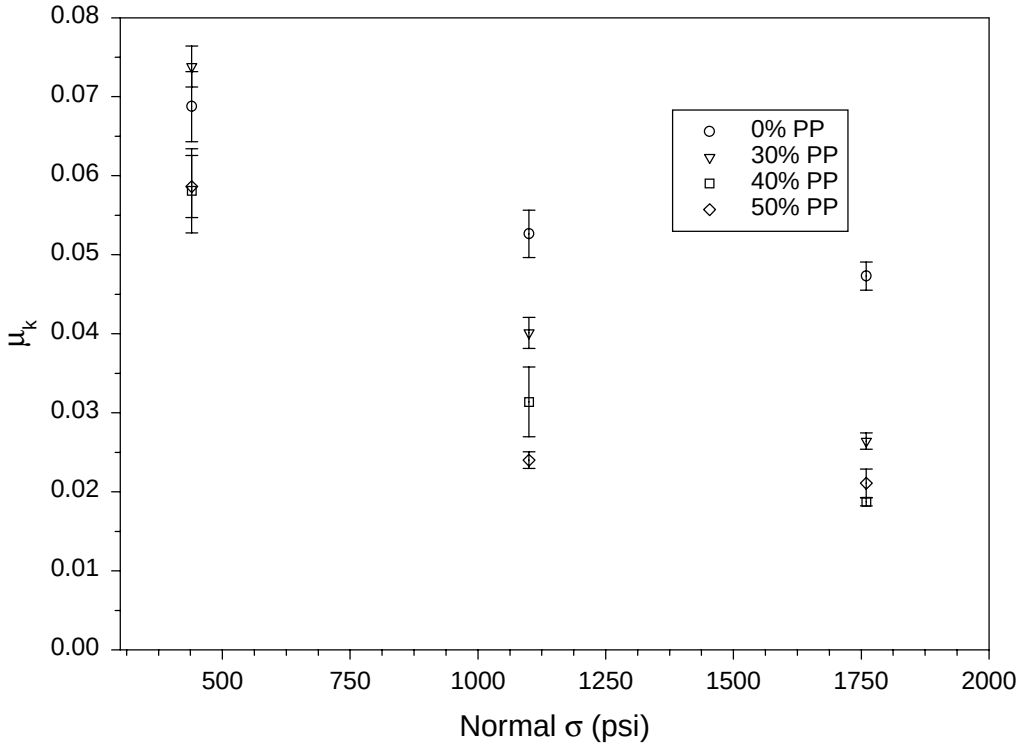

Figure C.7. Influence of normal σ on μ_k, at 190°C and a 1 s dwell time.

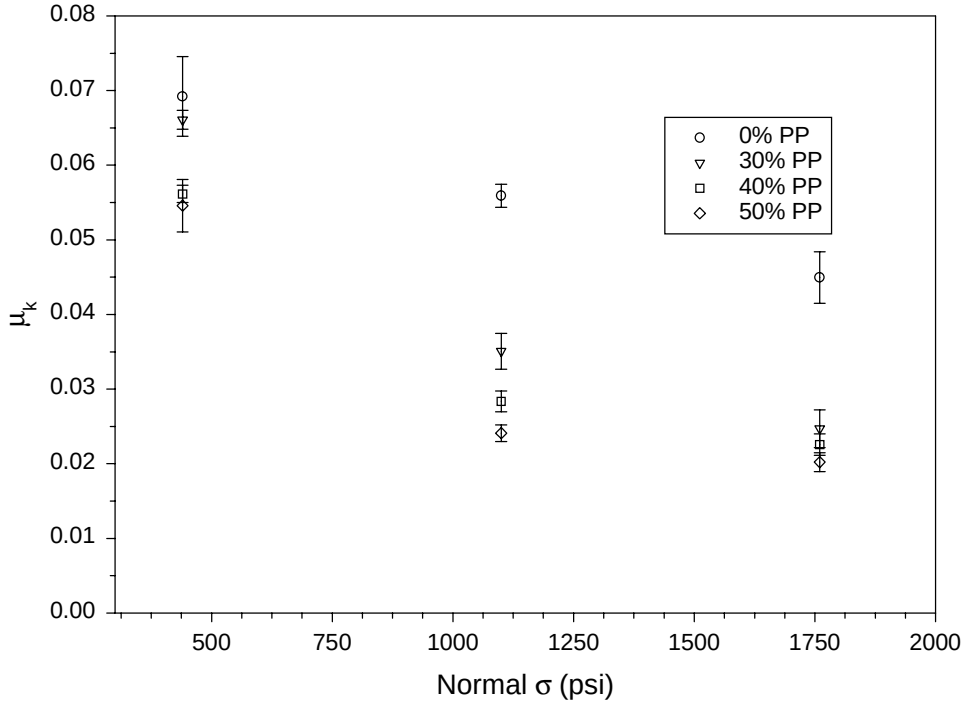

Figure C.8. Influence of normal σ on μ_k, at 190°C and a 60 s dwell time.

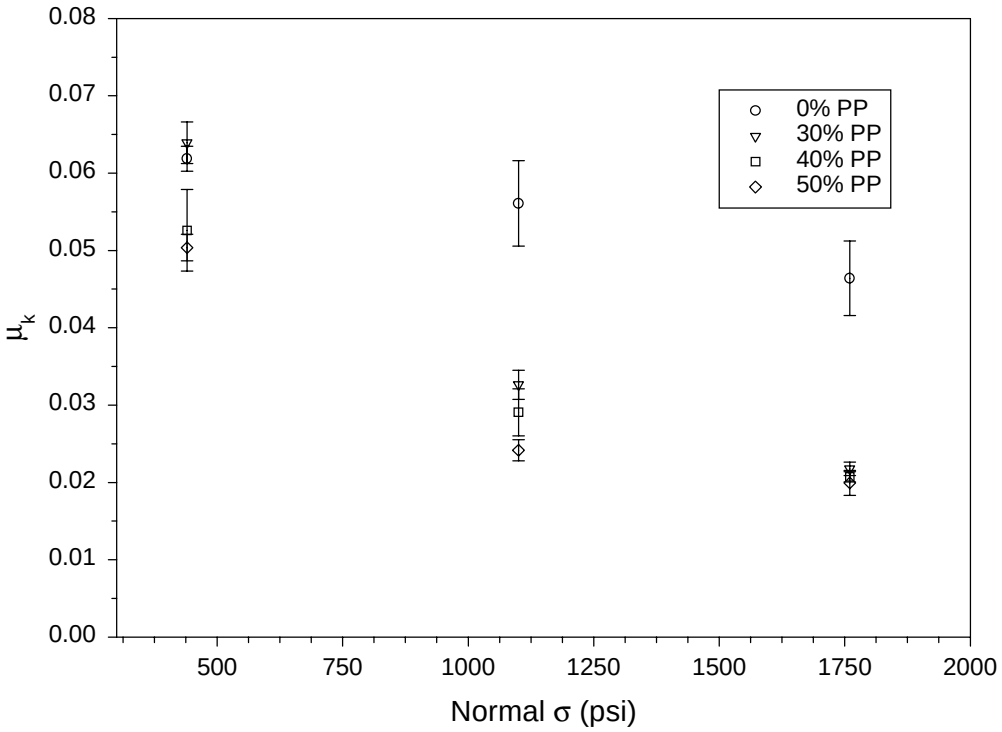

Figure C.9. Influence of normal σ on μ_k, at 190°C and a 180 s dwell time.

Appendix D. Friction Data – Influence of Dwell Time

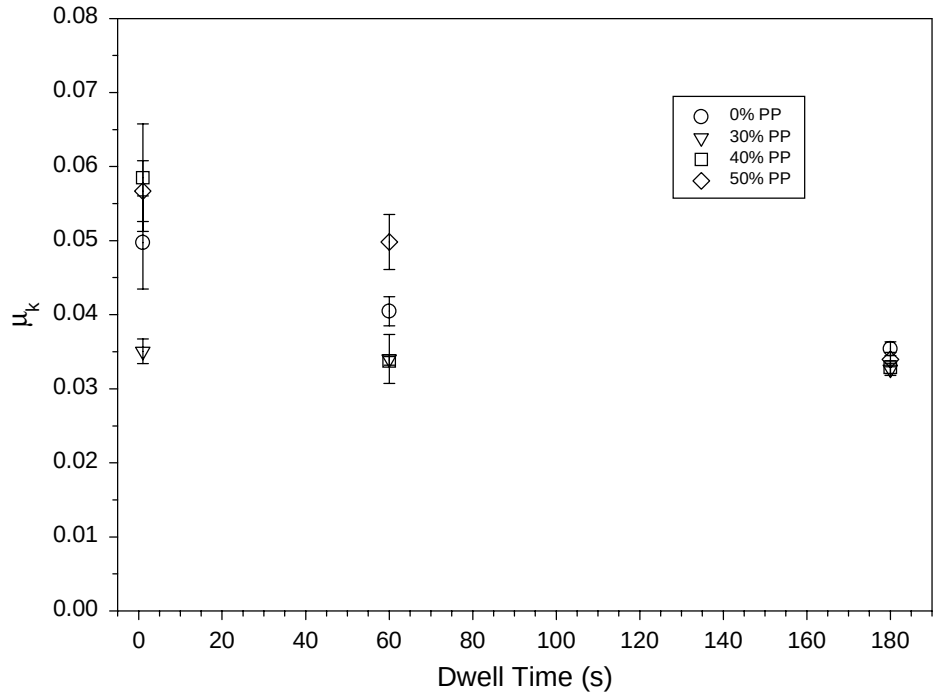

Figure D.1. Influence of dwell time on μ_k, at 170°C and 440 psi.

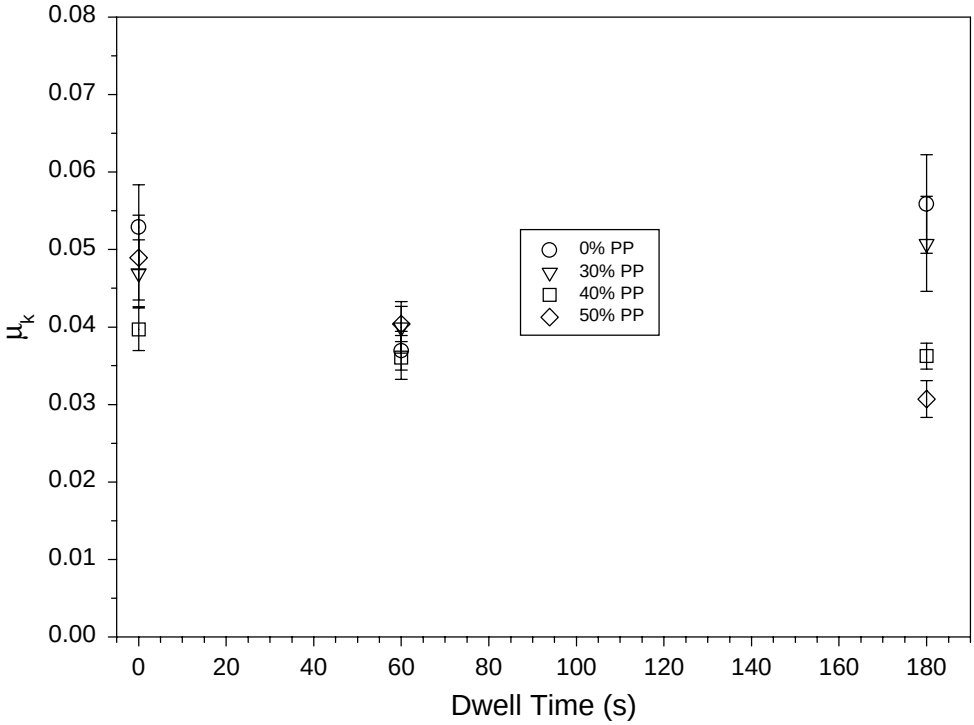

Figure D.2. Influence of dwell time on μ_k, at 170°C and 1,100 psi.

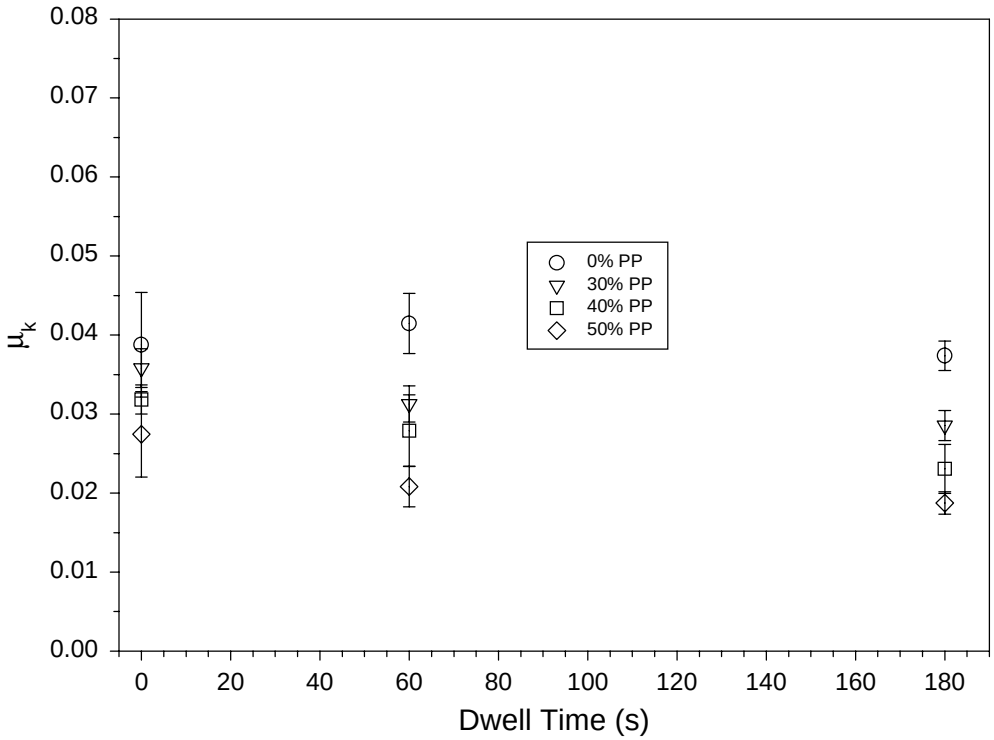

Figure D.3. Influence of dwell time on μ_k, at 170°C and 1,760 psi.

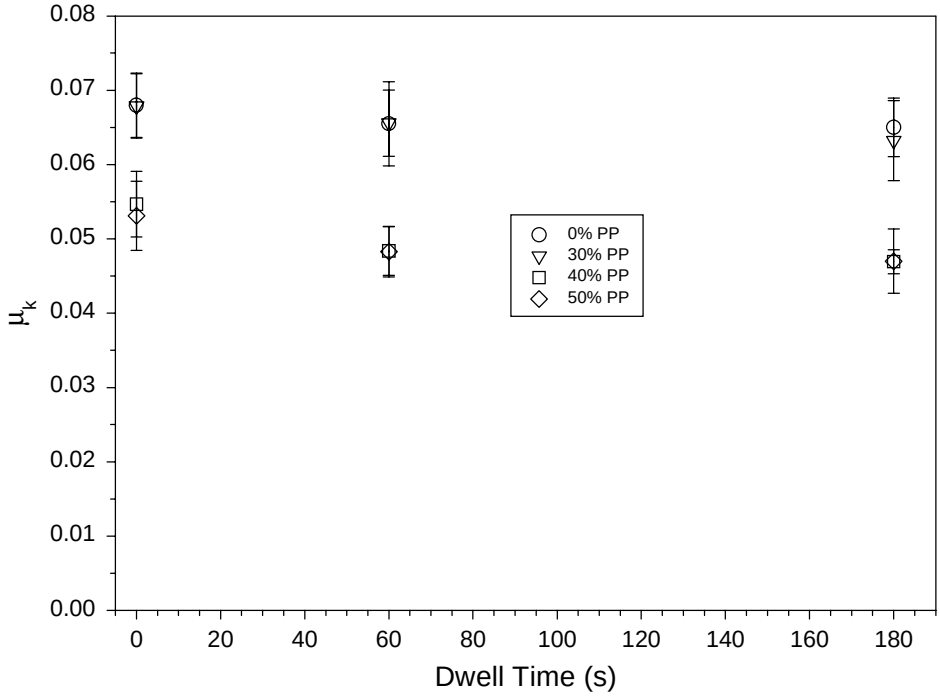

Figure D.4. Influence of dwell time on μ_k, at 180°C and 440 psi.

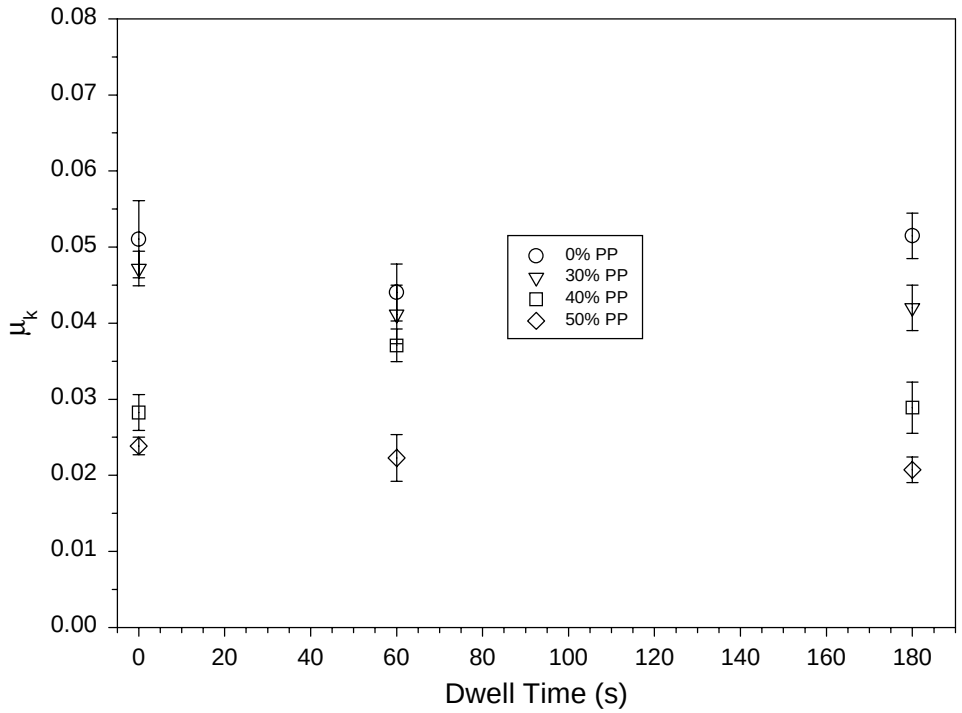

Figure D.5. Influence of dwell time on μ_k, at 180°C and 1,100 psi.

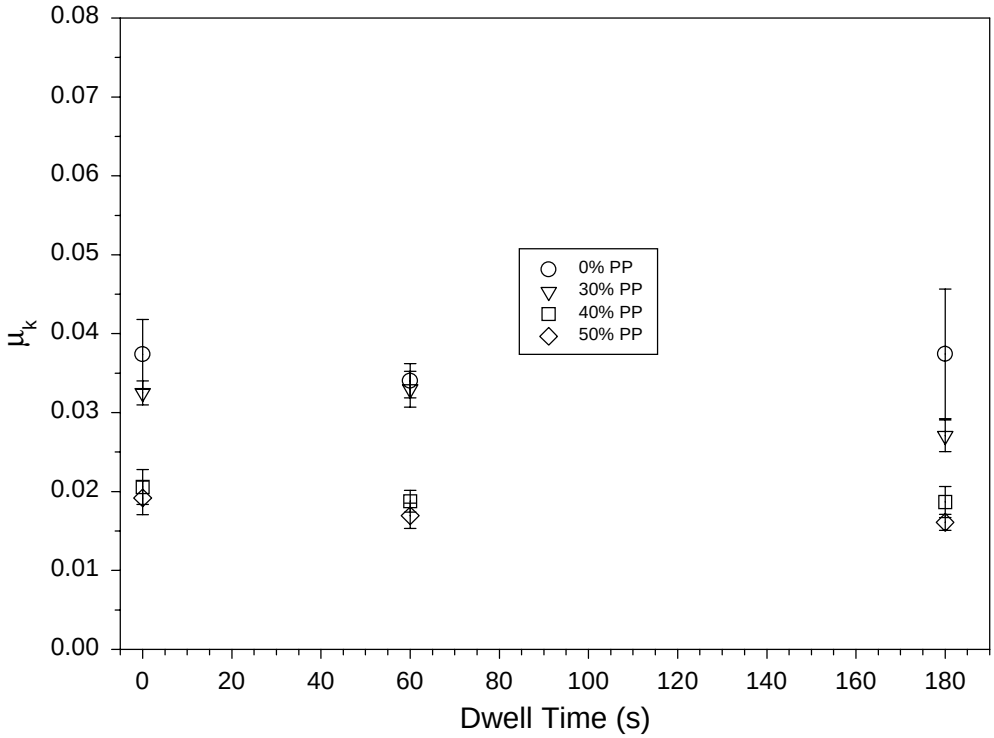

Figure D.6. Influence of dwell time on μ_k, at 180°C and 1,760 psi.

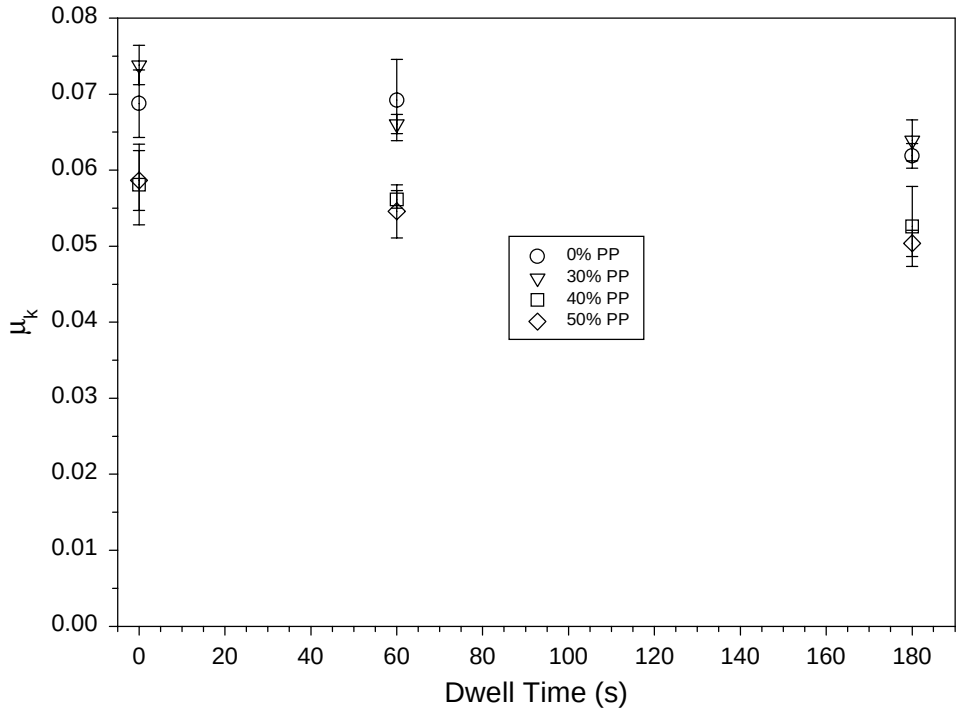

Figure D.7. Influence of dwell time on μ_k, at 190°C and 440 psi.

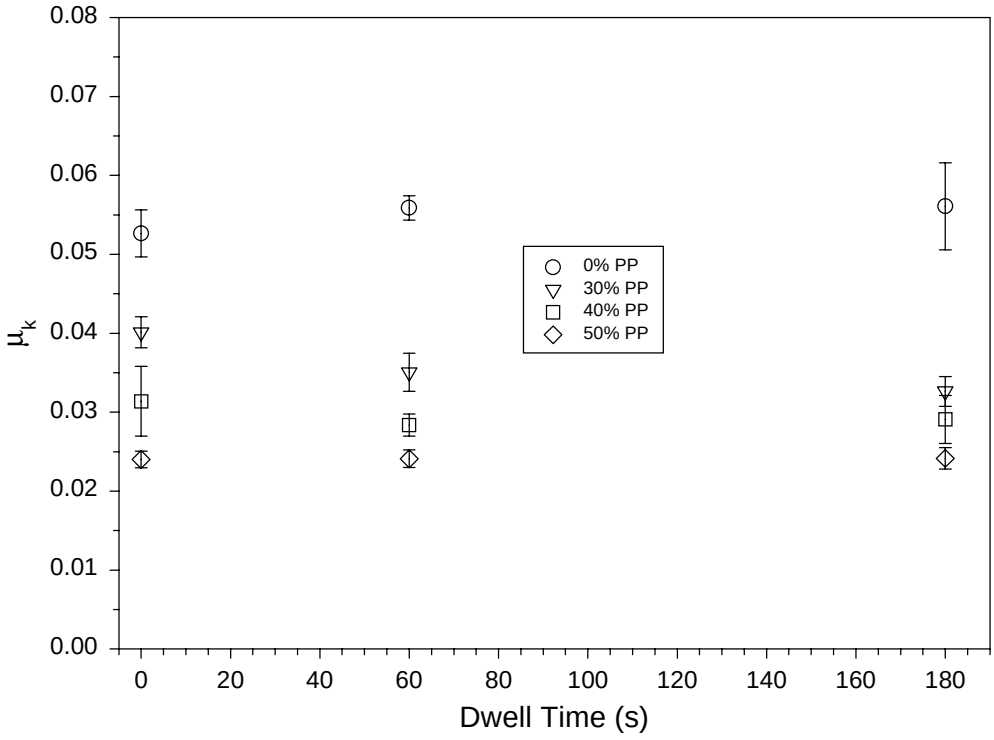

Figure D.8. Influence of dwell time on μ_k, at 190°C and 1,100 psi.

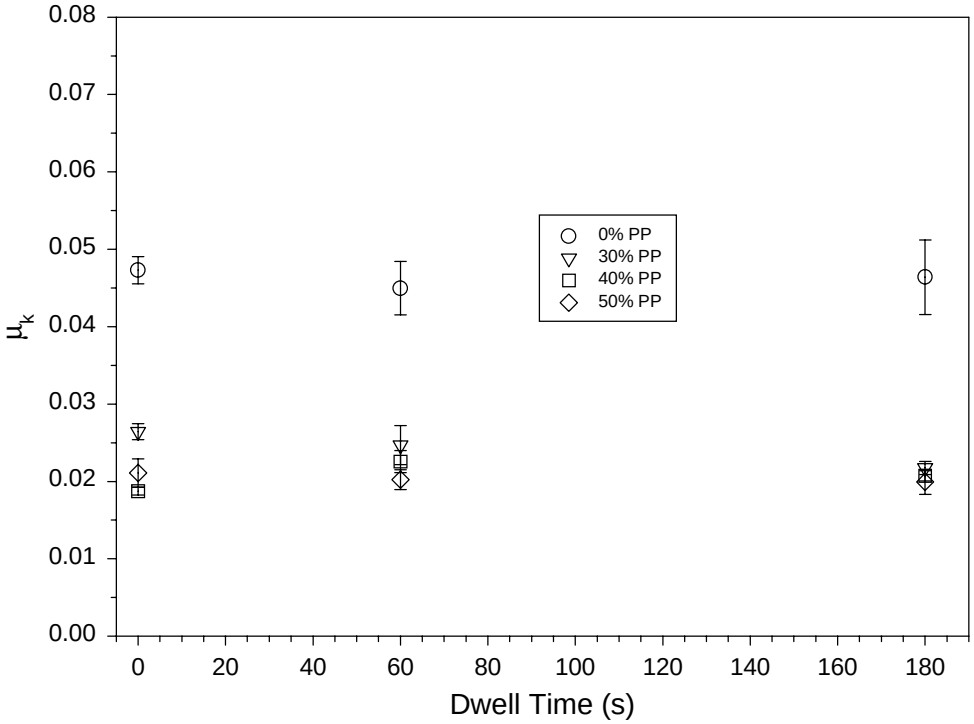

Figure D.9. Influence of dwell time on μ_k, at 190°C and 1,760 psi.

Appendix E. Friction Data – Influence of Temperature

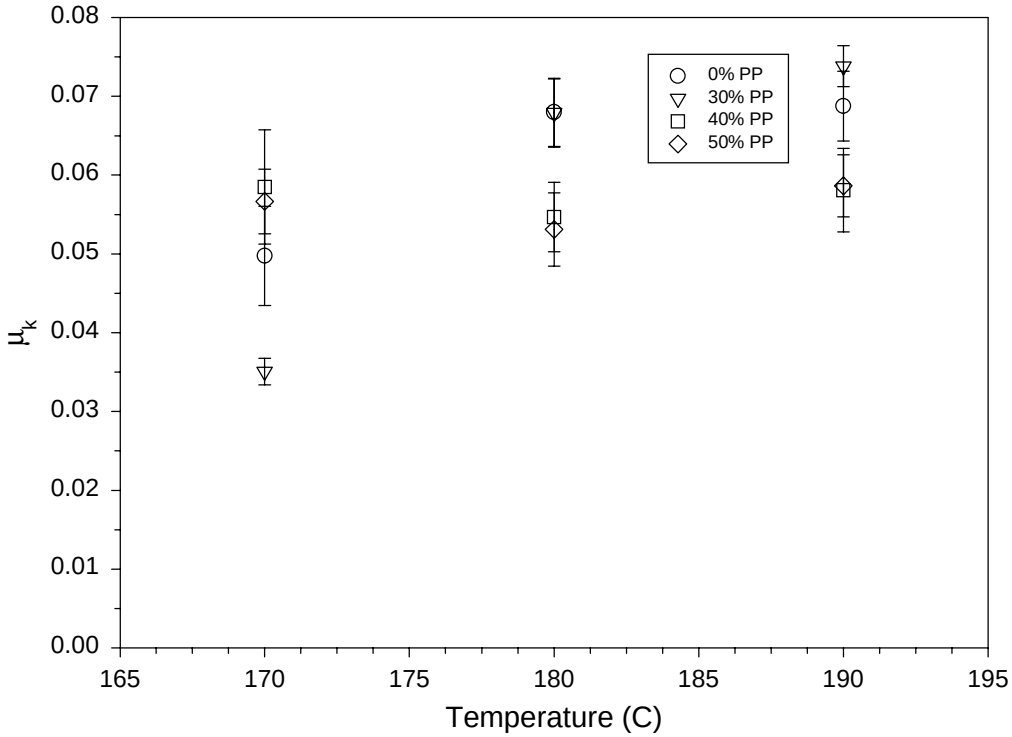

Figure E.1. Influence of temperature on μ_k, at a normal s of 440 psi and a 1 s dwell time.

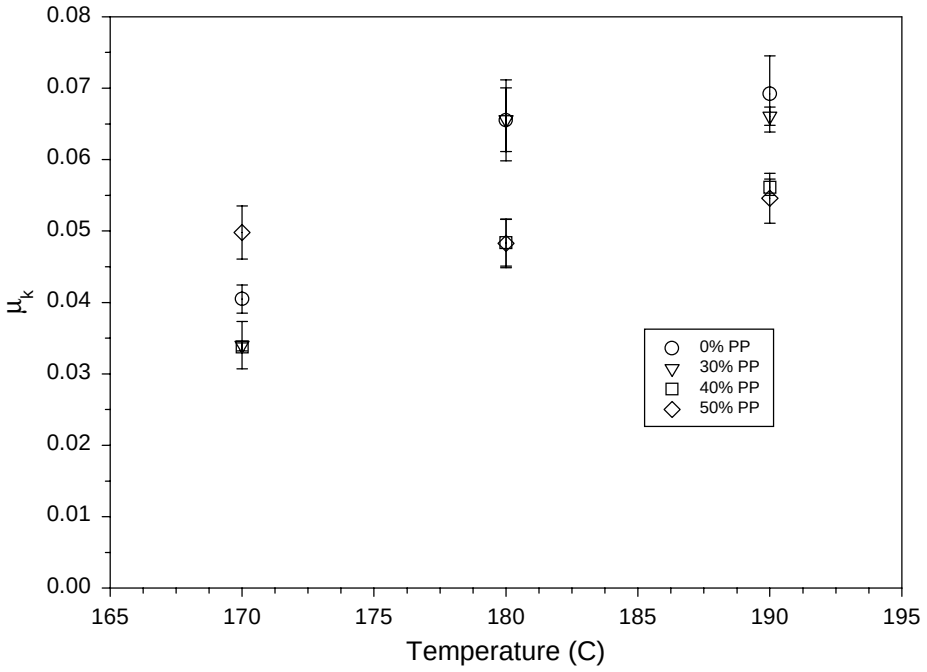

Figure E.2. Influence of temperature on μ_k, at a normal s of 440 psi and a 60 s dwell time.

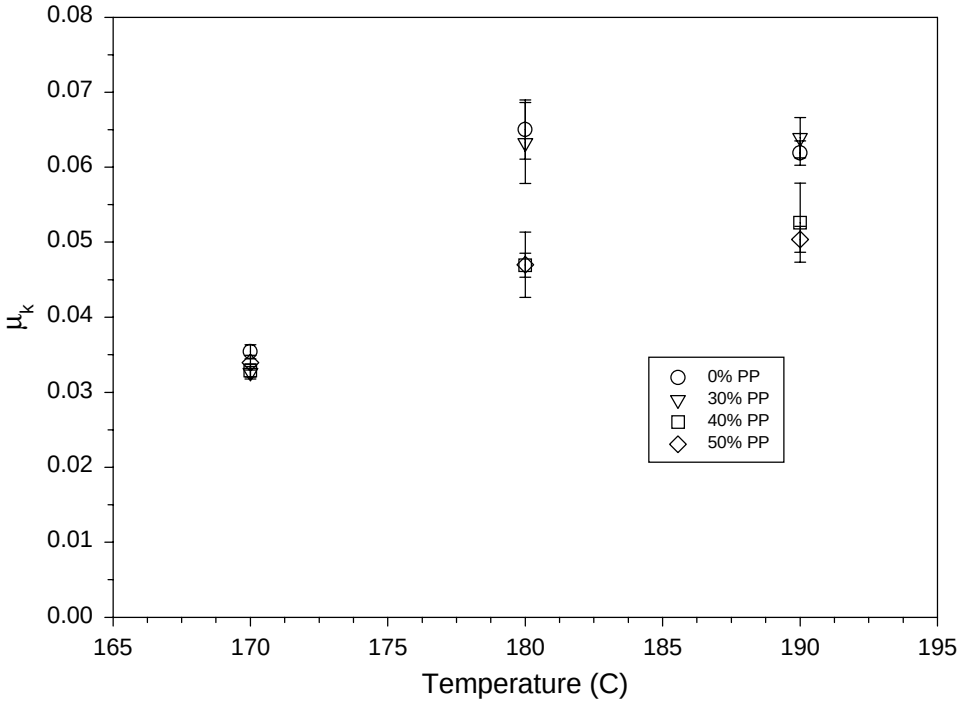

Figure E.3. Influence of temperature on μ_k, at a normal s of 440 psi and a 180 s dwell time.

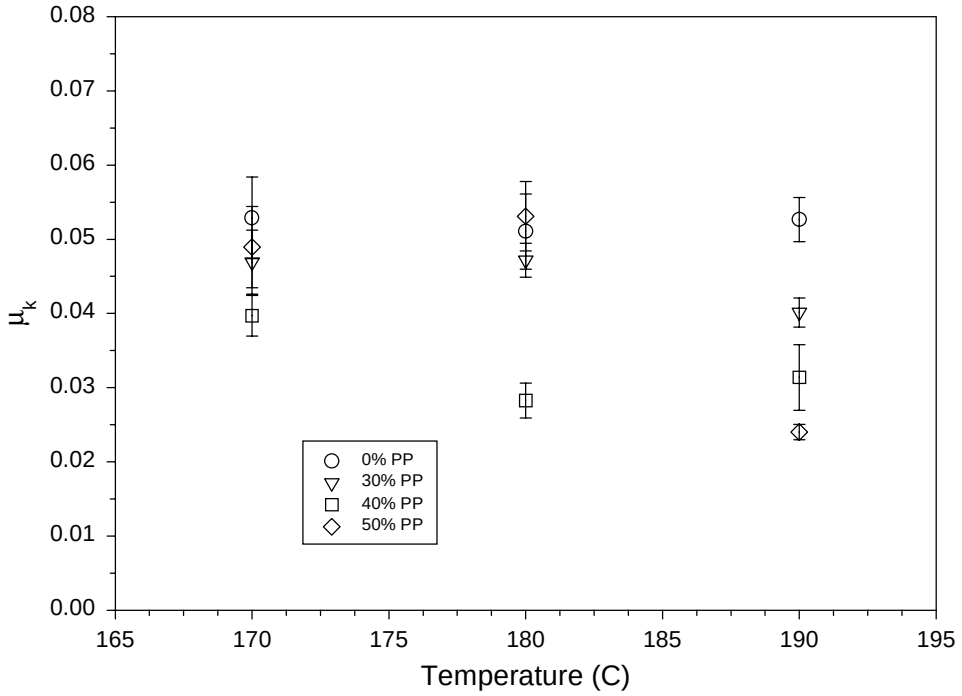

Figure E.4. Influence of temperature on μ_k, at a normal s of 1,100 psi and a 1 s dwell time.

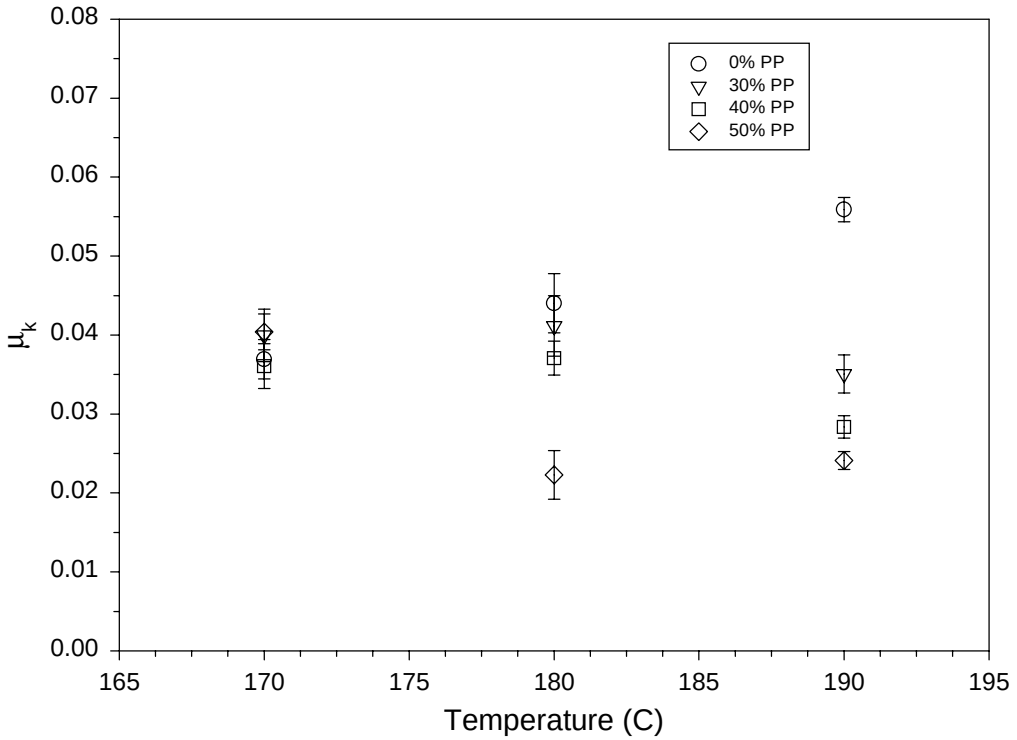

Figure E.5. Influence of temperature on μ_k, at a normal s of 1,100 psi and a 60 s dwell time.

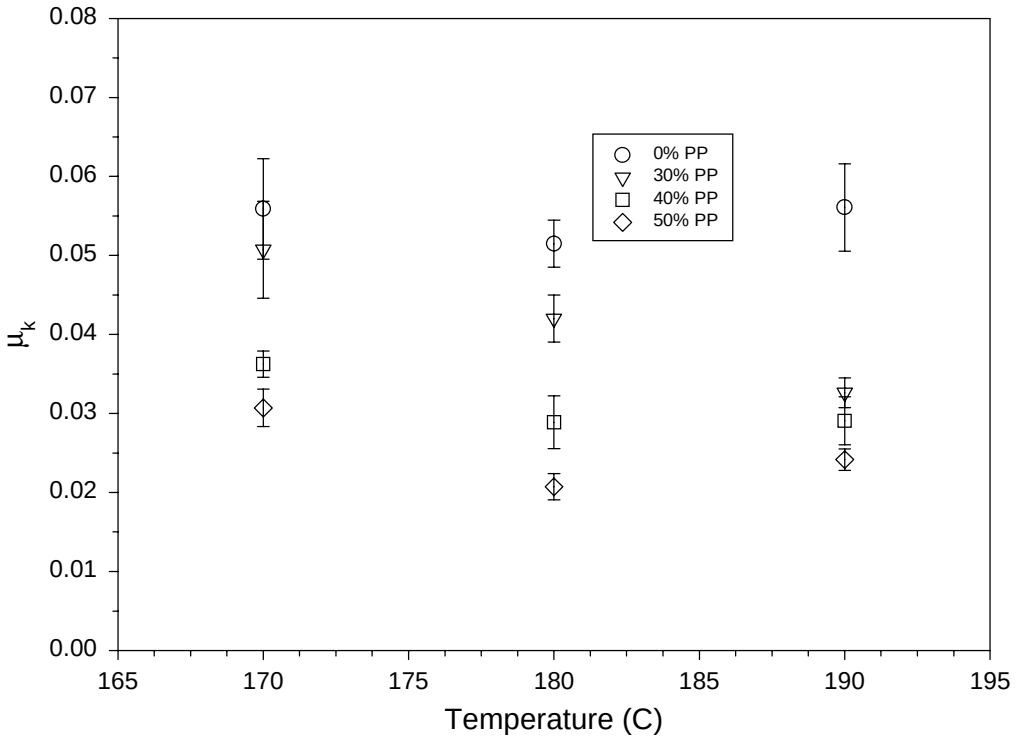

Figure E.6. Influence of temperature on μ_k, at a normal s of 1,100 psi and a 180 s dwell time.

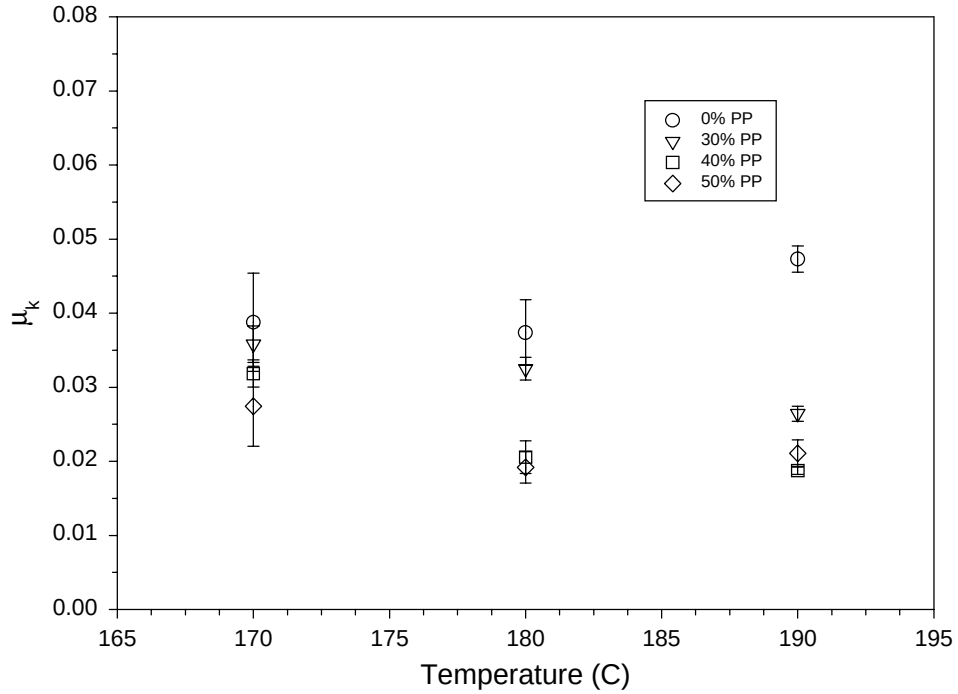

Figure E.7. Influence of temperature on μ_k, at a normal s of 1,760 psi and a 1 s dwell time.

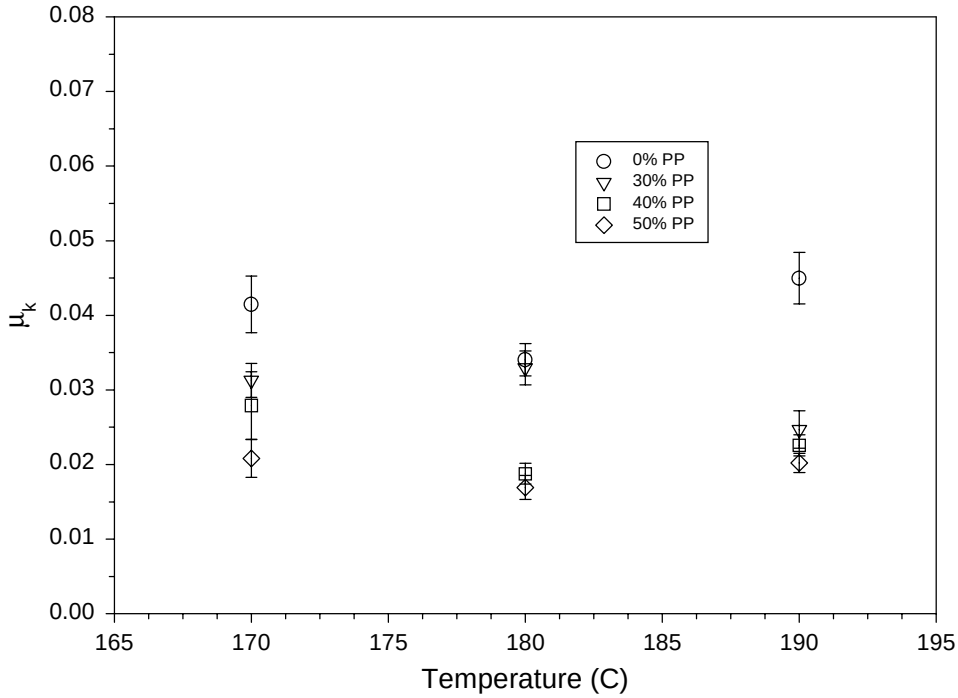

Figure E.8. Influence of temperature on μ_k, at a normal s of 1,760 psi and a 60 s dwell time.

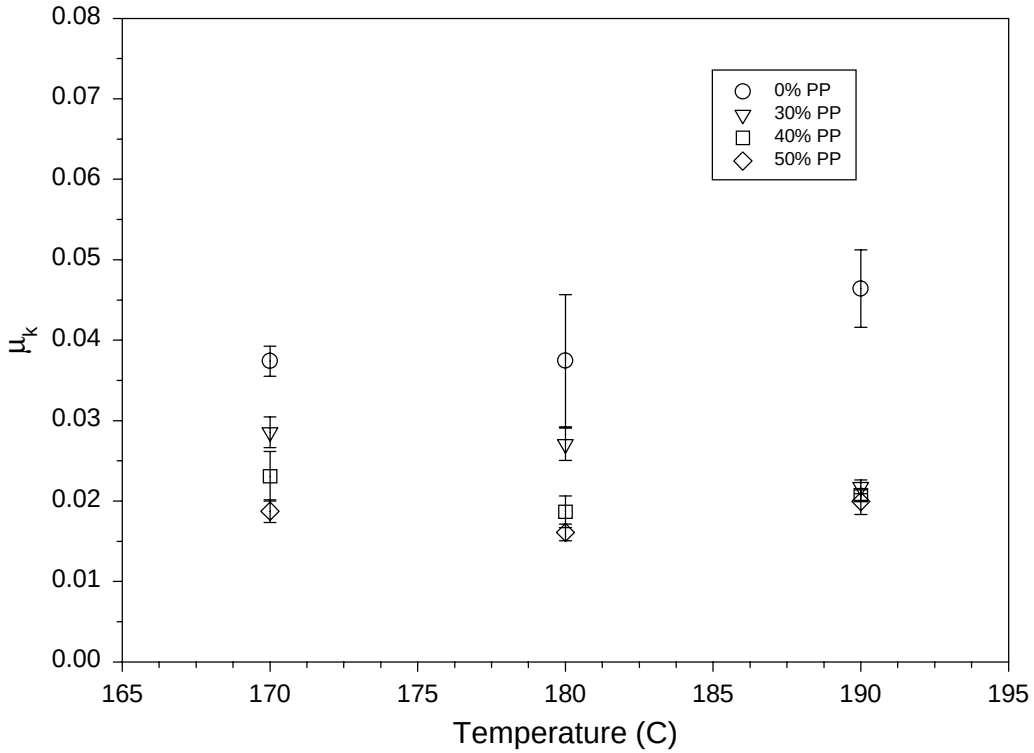

Figure E.9. Influence of temperature on μ_k, at a normal s of 1,760 psi and a 180 s dwell time.

Appendix F. Density Adjustment Data

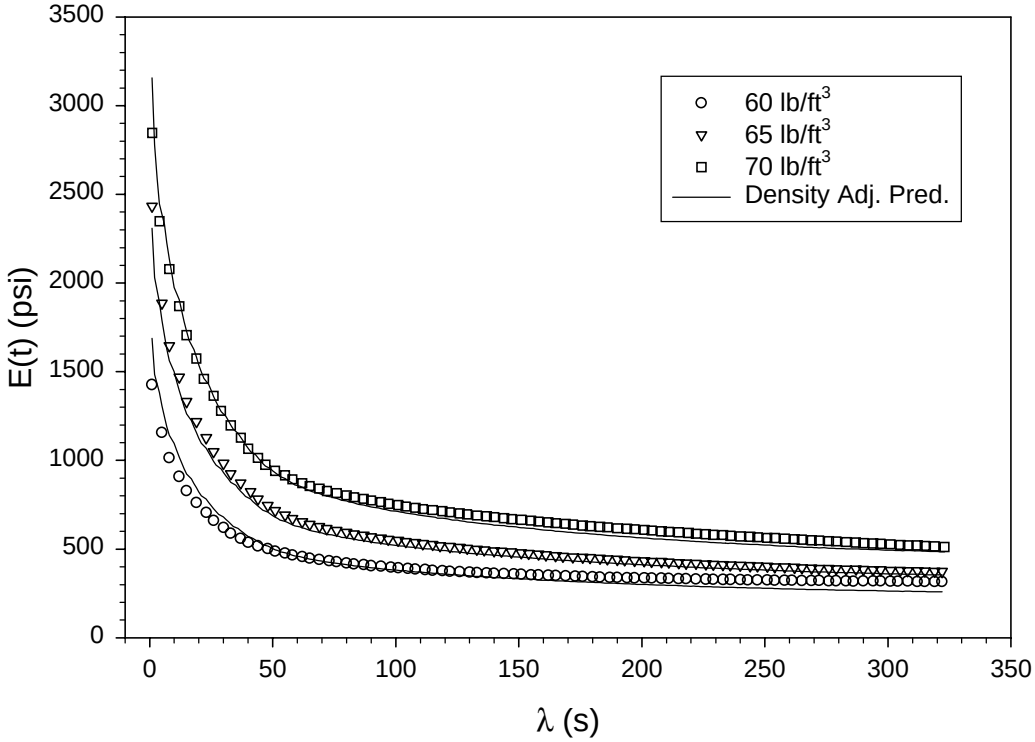

Figure F.1. Density adjustment for 0%PP mats at 170°C.

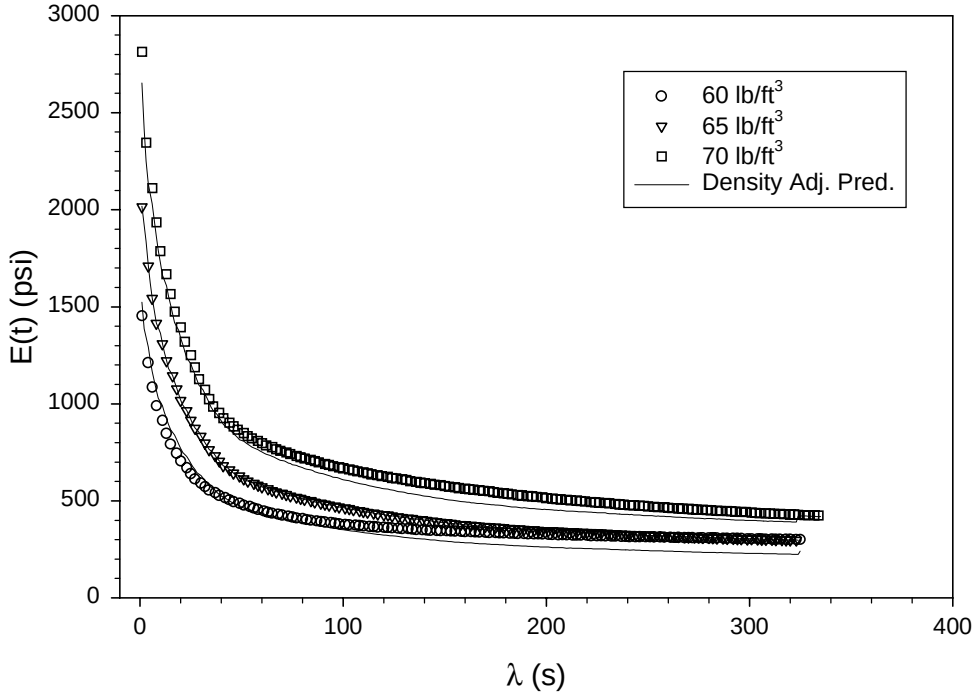

Figure F.2. Density adjustment for 0%PP mats at 180°C.

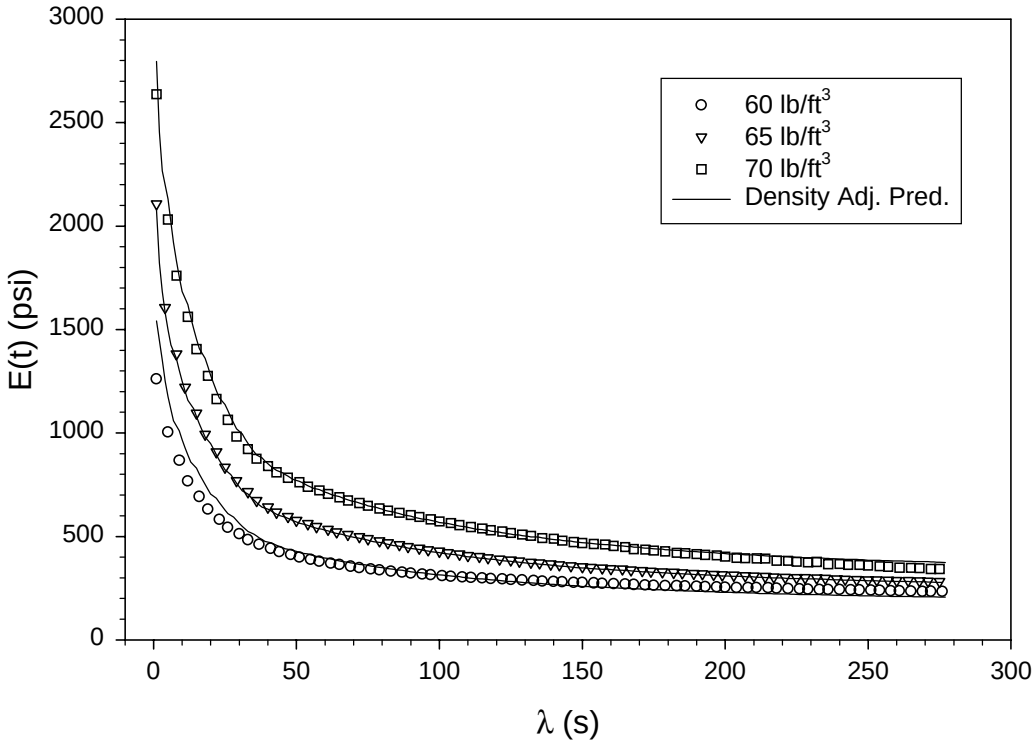

Figure F.3. Density adjustment for 0%PP mats at 190°C.

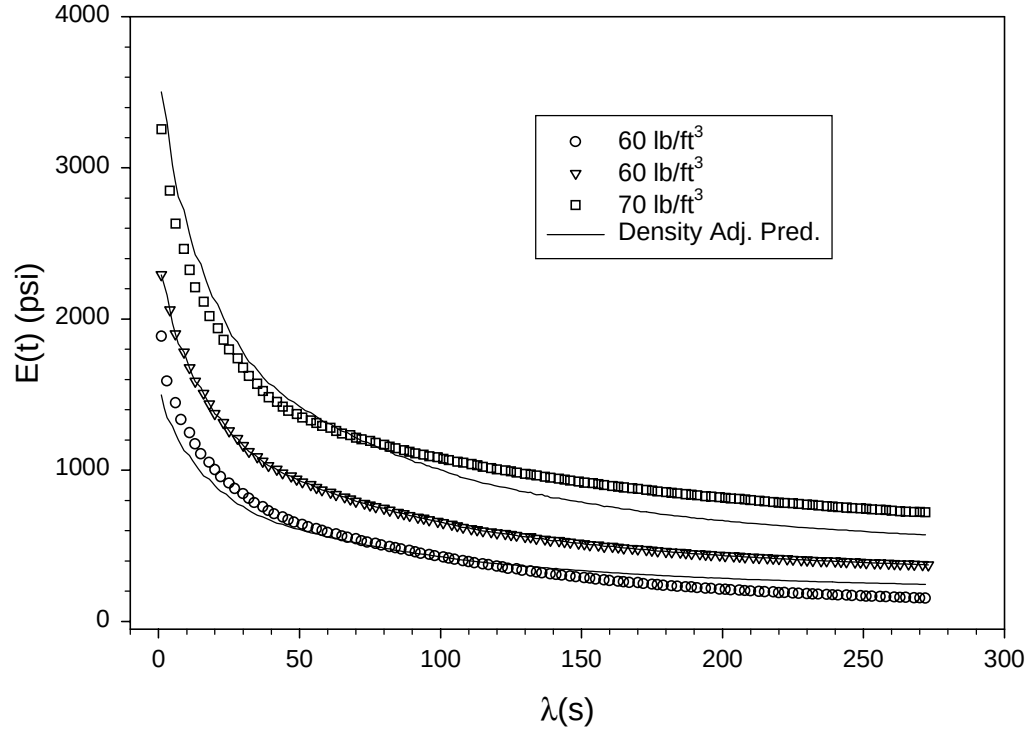

Figure F.4. Density adjustment for 30%PP mats at 170°C.

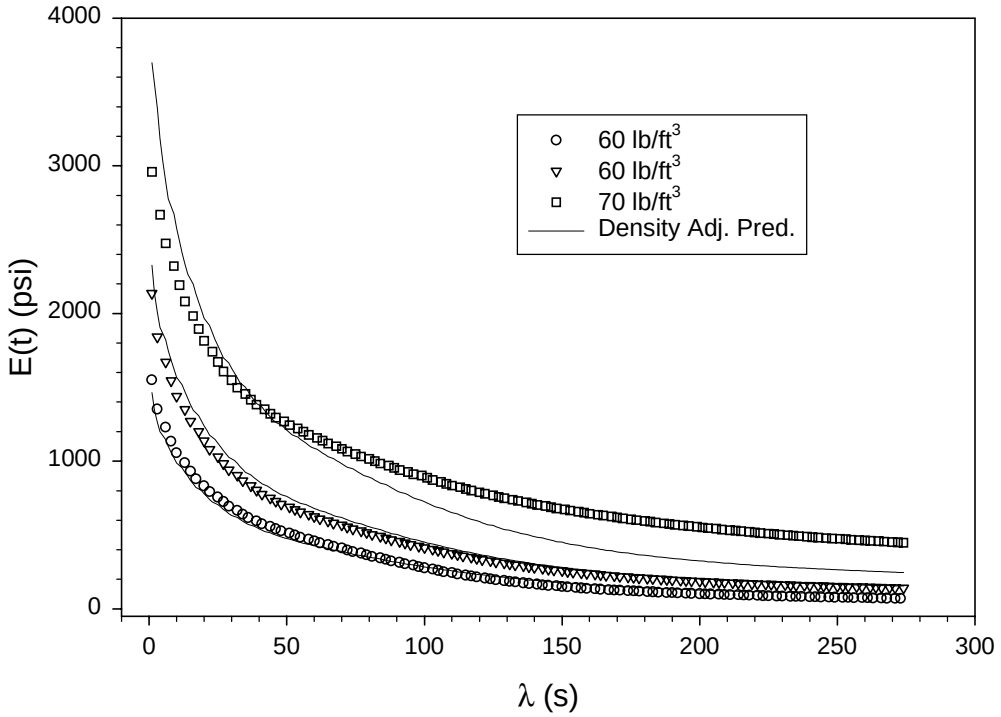

Figure F.5. Density adjustment for 30%PP mats at 180°C.

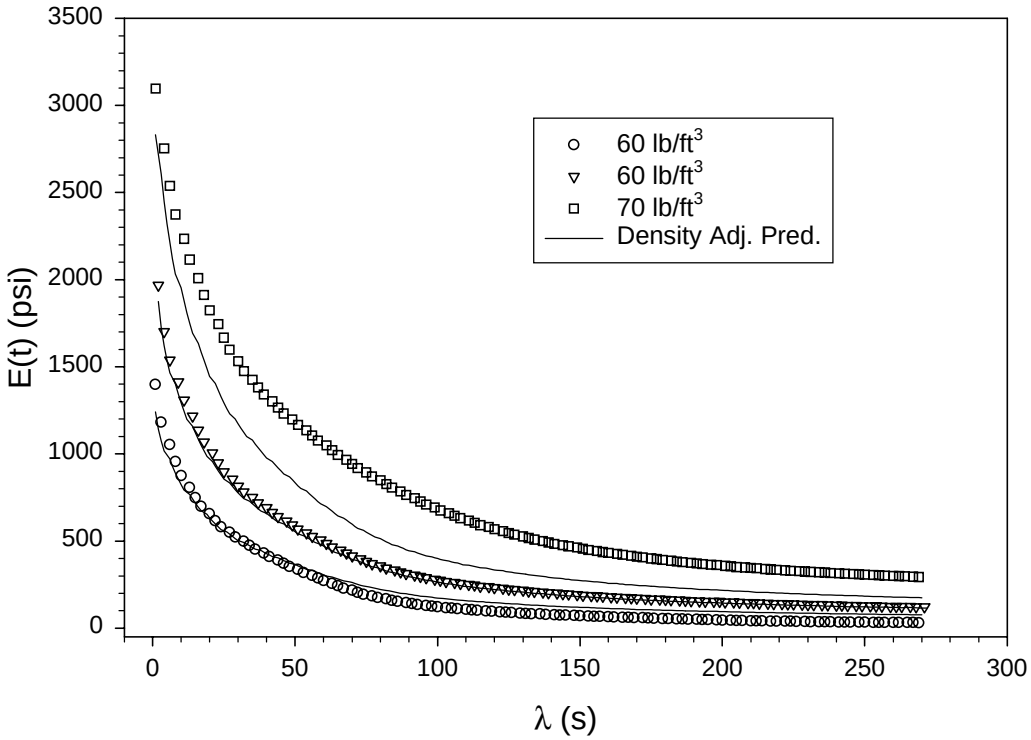

Figure F.6. Density adjustment for 30%PP mats at 190°C.

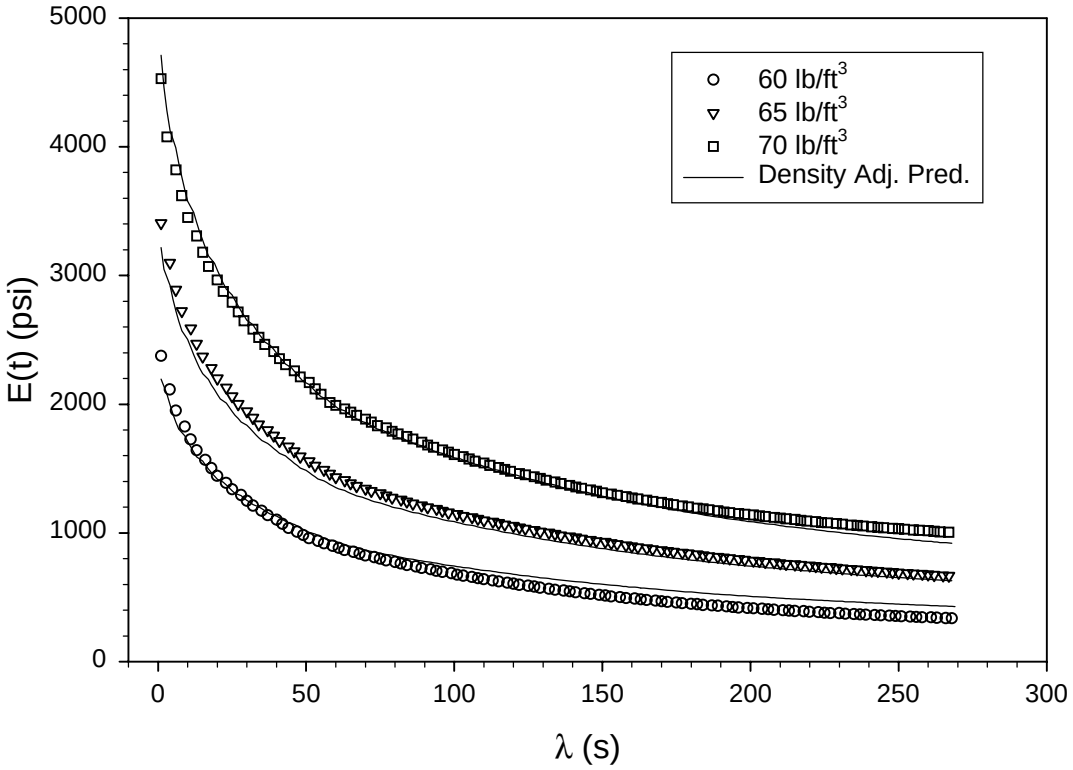

Figure F.7. Density adjustment for 40%PP mats at 170°C.

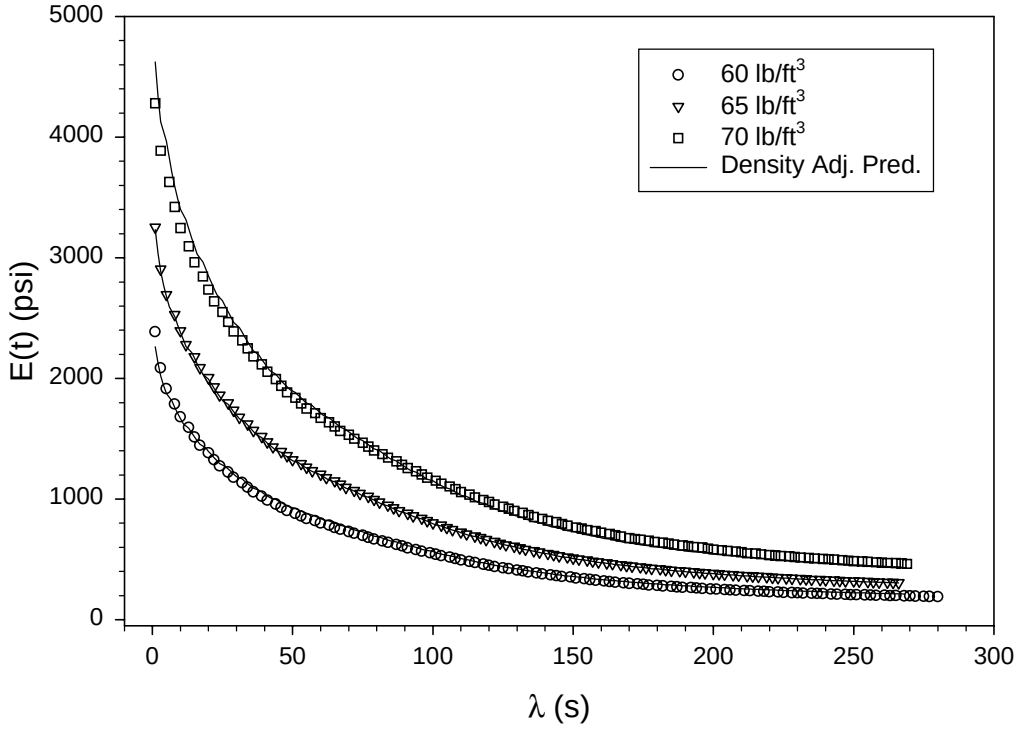

Figure F.8. Density adjustment for 40%PP mats at 180°C.

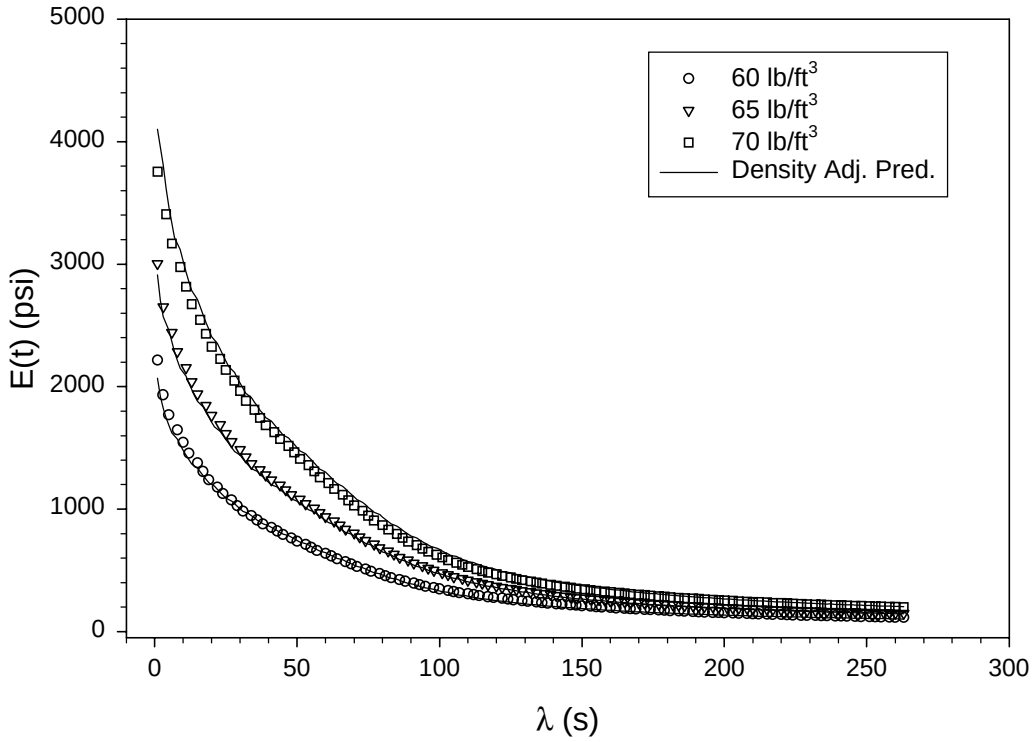

Figure F.9. Density adjustment for 40%PP mats at 190°C.

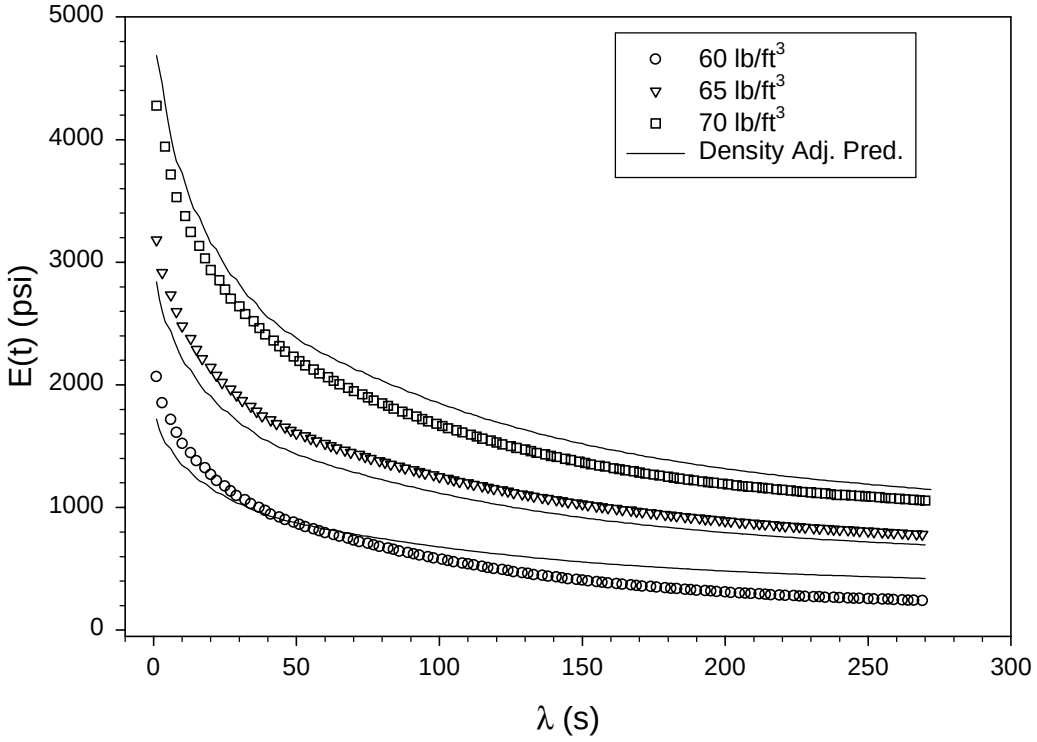

Figure F.10. Density adjustment for 50%PP mats at 170°C.

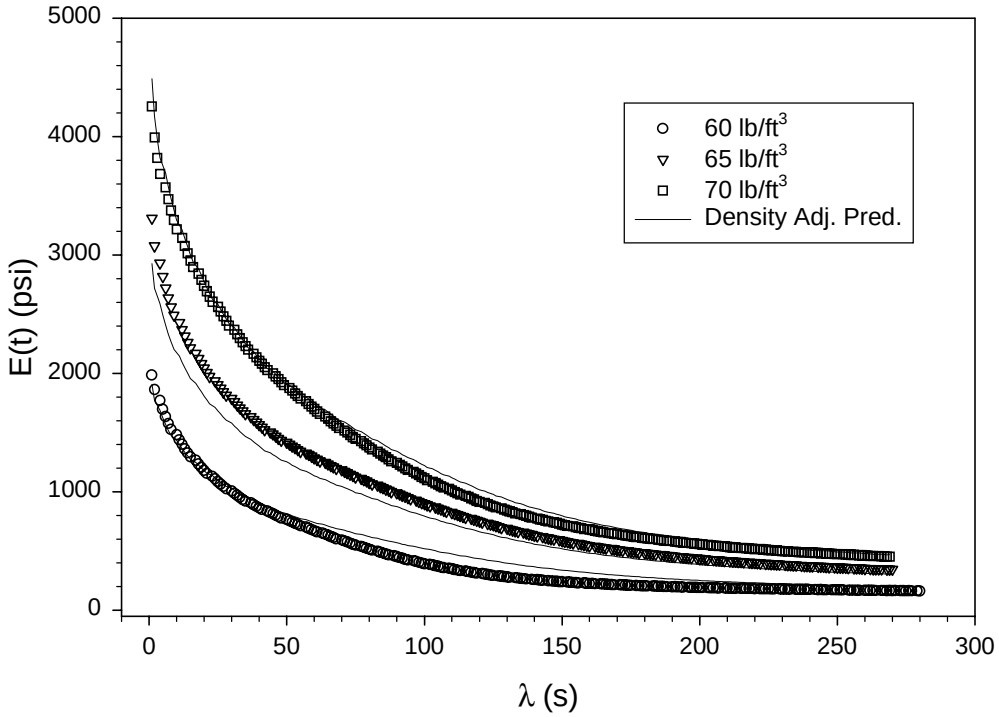

Figure F.11. Density adjustment for 50%PP mats at 180°C.

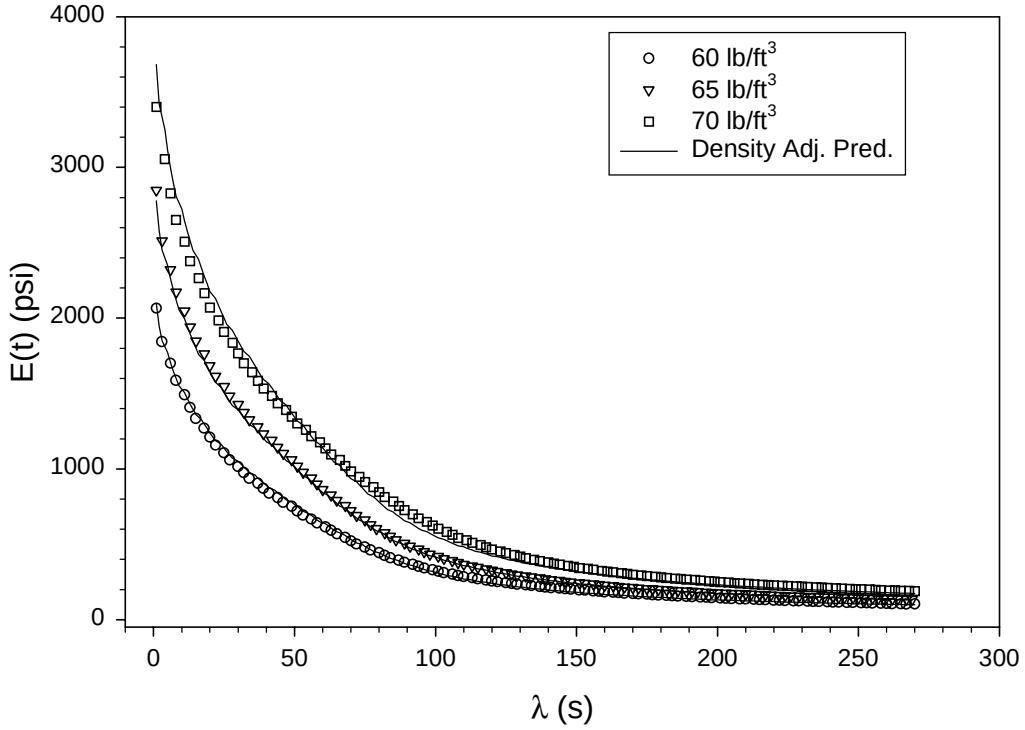

Figure F.12. Density adjustment for 50%PP mats at 190°C.